Funded by the European Union

This project has received funding from the European Union's Horizon Europe research and innovation programme under grant agreement No. 101136257

AUTOFLEX

[D3.3] SAFE, SECURE, AND RESILIENT TRANSPORT

Workpackage	WP3	Developing automated multimodal zero-emission Transport System
Lead Author	NTUA	Lianna Serafeim (NTUA), Marios Koimtzoglou (NTUA), Konstantinos Louzis (NTUA)
Co-Author(s)	-	-
Reviewer	SO	Renan Guedes Maidana (SO)
Dissemination Level	PU	R
Date / Project Month		17/09/2026 - PM33

DELIVERABLE INFORMATION

This publication has been provided by members of the AUTOFLEX consortium and is intended as input to the development of autonomous and flexible inland waterway vessels and respective business models. The content of this publication has been reviewed and accepted by the members of the AUTOFLEX participants. However, not necessarily every aspect of it represents the view of each individual member of the AUTOFLEX consortium.

While the information contained in the document is believed to be accurate, AUTOFLEX participants make no warranty of any kind with regard to this material including, but not limited to the implied warranties of merchantability and fitness for a particular purpose. None of the AUTOFLEX participants, their officers, employees, or agents shall be responsible for, liable in negligence, or otherwise howsoever in respect of any inaccuracy or omission herein. Without derogating from the generality of the foregoing, neither AUTOFLEX participants, their officers, employees or agents shall be liable for any direct, indirect, or consequential loss or damage caused by or arising from any information advice or inaccuracy or omission herein.

The material in this publication can be reproduced provided that a proper reference is made to the title of this publication and the AUTOFLEX project.

An example for reference is given here:

Serafeim, Lianna; Koimtzoglou, Marios; Louzis, Konstantinos; 'AUTOFLEX Deliverable D3.3 – Safe, secure, and resilient transport; Revision 1.0; July 2026

Document History		
10.01.2026	Version 0.1	First draft
04.06.2026	Version 0.2	Review by Marios Koimtzoglou (NTUA)
15.07.2026	Version 0.3	Second round of internal review, cross-checking of data provided by SINTEF
27.07.2026	Version 0.4	Shared for internal review by Renan Guedes Maidana (SO)
16.09.2026	Version 0.5	Final updates after review comment
17.09.2026	Version 1.0	Final version - Submitted to the European Commission

Funded by the European Union
Grant Agreement: 101136257

EXECUTIVE SUMMARY

This deliverable presents the work carried out within Task 3.6 – Safety, security, and resilience of transport systems. Task 3.6 was led by NTUA[1]. The task focuses on safety, cybersecurity, and resilience aspects related to the design and operation of the AUTOFLEX inland waterway (IWW) transport system and its innovations. Its overall goal is to develop a risk-based approach that systematically supports hazard identification, risk assessment, and risk mitigation, enabling structured detection, evaluation, and reduction of risks that may disrupt the normal operation of the AUTOFLEX transport and logistics system. The scope includes hazardous scenarios associated with: (i) interactions between AUTOFLEX solutions and existing IWW transport infrastructure, (ii) interactions with recreational and non-professional waterway users, (iii) potential safety and security related threats, and (iv) the proposed transport system concept (as developed in Task 3.4 per the feedback received from Task T3.1-T3.3) as well as inputs from related activities (e.g., feed from Task 3.5). The method is designed to address both operational and cybersecurity failures related to supply chain delay, capturing their implications on safe and resilient system performance.

The development of the Task 3.6 methodology is structured around three main pillars:

1. Hazard Identification, targeting the systematic documentation of hazards and hazardous events relevant to safety, cybersecurity, and resilience of each AUTOFLEX Innovation related to the supply chain delay.
2. Risk Assessment, through Graph and Percolation Theory, to quantify system resilience and to analyse the propagation of supply chain related disruptions through interdependencies.
3. Risk Mitigation, resulting in risk control options, mitigation measures, and recommendations to reduce negative effects and prevent escalation to hazardous states.

[1] National Technical University of Athens

Funded by the European Union
Grant Agreement: 101136257

TABLE OF CONTENTS

Funded by the European Union
Grant Agreement: 101136257

Funded by the European Union

Grant Agreement: 101136257

TABLE OF FIGURES

Funded by the European Union
Grant Agreement: 101136257

TABLE OF TABLES

Funded by the European Union
Grant Agreement: 101136257

LIST OF ABBREVIATIONS

Abbreviation	Description
APL	Average Path Length
BC	Betweenness Centrality
CCTV	Closed-Circuit Television System
CEMT	Conférence Européenne des Ministres des Transports
CC	Clustering Coefficient
CDD	Cumulative Degree Distribution
FMEA	Failure Mode and Effects Analysis
GPS	Global Positioning System
HAZID	Hazard Identification
IT	Information Technology
IWW	Inland Waterway
IWT	Inland Waterway Transport
MDCs	Mobile Distribution Centres
NESC	NASA Engineering and Safety Center
NW	Node Weight
QR	Quick Response
RF	Reduction Factor
RCO	Risk Control Option
S&C	Stow & Charge
SIS	Susceptible–Infected–Susceptible
TPT	Temporary Port Terminal
TICs	Traffic-Intense Corridors
VS	Vertex Strength
WACs	Waterborne Alternative Corridors
ZES	Zero Emission Services

Funded by the European Union
Grant Agreement: 101136257

1 INTRODUCTION

Inland Waterway Transport (IWT) is an important component of the European freight transport system, enabling the movement of goods while offering an alternative that can relieve pressure on congested road networks. As inland transport is embedded in multimodal transportation systems, failures or disturbances in IWT can propagate further along the supply chain, affecting performance, reliability, and continuity across various logistics activities.

As the European transport sector increasingly adopts automation towards improving operational efficiency and sustainability, an aspect which the AUTOFLEX project and its outcomes also seek to improve, understanding and managing these risks becomes increasingly important.

AUTOFLEX project introduces a series of innovative transport system components, including autonomous inland vessels, Temporary Port Terminals (TPTs), Mobile Distribution Centres (MDCs), and Stow & Charge (S&C) hubs. While these innovations are expected to enhance the flexibility, efficiency, and environmental performance of inland waterway transport, they also introduce new safety, cybersecurity, and resilience challenges that require systematic assessment, capable of capturing interdependencies across system components and quantifying how local failures can expand into wider network-level degradation.

1.1 PURPOSE OF THE DOCUMENT

This deliverable presents an assessment framework based on network science to evaluate the robustness and resilience of an autonomous IWT system. The approach models the transport system as a graph, capturing ports, AUTOFLEX operational innovations, and locations, and analyses how connectivity and performance evolve as nodes and edges are progressively removed. Both random and targeted failures are considered to reflect both worst case and more realistic failure scenarios. The analysis aims to identify critical components, the loss of which could trigger fragmentation, reduce accessibility, or significantly impair network efficiency, thereby generating quantitative indicators of vulnerability and resilience. To better understand functional behaviour, the proposed framework integrates percolation theory with network analysis, enabling the investigation and analysis of failure propagation, the identification of critical thresholds, and the quantification of resilience under progressive degradation.

1.2 SCOPE OF T3.6 WITHIN WP3

Task 3.6 builds upon the obtained inputs from Task 3.1– Task 3.3 in order to systematically identify and assess risks associated with all innovations of the AUTOFLEX transport system, with particular emphasis on risks that may induce only supply chain delays. In coordination with Tasks 3.4 and 3.5, the work performed in the context of Task 3.6 supports the construction of a graph-based representation of the transport system, capturing where AUTOFLEX innovations are deployed to identify how the entire network behaves after supply chain failures. This network model is used to evaluate the system's resilience against

Funded by the European Union
Grant Agreement: 101136257

identified risks, assessing how disruptions may affect connectivity and operational performance. This network representation enables a structured assessment of whether the AUTOFLEX transport system remains robust and resilient when exposed to a variation of hazards.

1.3 RELATION TO OTHER TASKS

Task 3.6 serves as the safety and resilience assessment task within WP3, integrating the outcomes of the previous tasks into a system-level evaluation of the AUTOFLEX transport system. It builds upon the provided structure, technical and operational inputs from Tasks 3.1–3.3 (i.e., the AUTOFLEX innovations) and uses them to systematically identify and assess risks, especially those that can trigger supply chain delays. In parallel, it fits with Task 3.4, which defines the proposed transport system and routing network configuration, by translating the system description into a graph-based network representation to test resilience criticality and the effects of disruptions on connectivity and performance. The resulting outputs, including Risk Control Options (RCOs), prioritised critical nodes and edges, redundancy strategies, and physical or cybersecurity findings.

1.4 STRUCTURE OF THE DOCUMENT

The Deliverable is structured into six Sections. Section 1 introduces the context, objectives, and scope of the Deliverable. Section 2 provides background on risk-based approach methods applied to IWT and an overview of hazards in IWW. Section 3 presents the proposed AUTOFLEX risk-based approach and overall methodology, describing its main structure and workflow. Section 4 presents the results of the applied methodology, integrating the outputs of the risk identification, risk assessment, and risk mitigation stages. More specifically, it covers the Hazard Identification (HAZID)-based identification process and hazard catalogue which is described in detail in the Appendix, the use of percolation theory and graph-based indicators to evaluate resilience and vulnerability under supply chain disruption, and the mitigation measures and recommendations proposed to enhance safety, cybersecurity, and resilience. Section 5 discusses the key findings and their implications for the AUTOFLEX inland waterway transport system. Finally, Section 6 summarises the main conclusions and outlines next steps and directions for further work.

Funded by the European Union
Grant Agreement: 101136257

2 BACKGROUND OF RISK-BASED APPROACHES IN IWW

The identification and assessment of risks affecting inland waterway transport operations is not simply an auxiliary activity, but a prerequisite for maintaining the continuity, sustainability, and efficiency of wider logistics networks Addressing the various risks that may disrupt the broader supply chain and cause delays is particularly challenging, as such disruptions can propagate beyond their point of origin, triggering cascading effects across interconnected system components and operational activities, and ultimately reducing overall system performance. This potential for propagation highlights the need for analytical approaches capable of capturing systemic interdependencies and assessing how localized disturbances may affect the resilience of the whole network. Against this backdrop, the following literature review examines the principal methodological approaches to assessing risk, vulnerability, and resilience in interconnected transport and logistics systems, with particular emphasis on network-based perspectives., as the AUTOFLEX inland waterway transport system (IWTS) can be modelled as an integrated transport network. In Section 2.1, a comprehensive review of the literature on methodologies related to risk assessment and the resilience of inland navigation systems is presented, alongside an overview of the most common challenges encountered in inland waterway transport systems. Drawing on these insights, as well as the specific requirements set in Task 3.6 description, a risk-based methodological framework was developed.

2.1 OVERVIEW OF OTHER RISK-BASED APPROACHES IN IWW

Risk analysis of networked logistics and transport systems has increasingly shifted from isolated component-level assessments toward approaches that explicitly capture interdependence, propagation, and the formation of systemic consequences. For this reason, the relevant literature was reviewed to obtain a holistic understanding of the current state of the field, identify research gaps that could be addressed, and explore promising approaches that could be adopted with the necessary adaptations. Disruptions in such systems rarely remain localized, and instead spread through interconnected nodes, edges, and operational layers, ultimately producing network-wide or supply chain-level effects. This propagation logic is well captured by diffusion-based approaches and epidemic-style formulations, as shown by Chen et al. [1], who modelled risk propagation in emergency logistics networks through an improved Susceptible–Infected–Susceptible (SIS) framework. Similarly, Feng et al. [2] analysed accident spread and risk propagation in complex industrial system networks through an epidemiological model. Both studies support the view that risk should be understood as a dynamic process unfolding over the network rather than as a static property of isolated elements.

A second major stream of research focuses on structural vulnerability and criticality using graph theory and related network metrics. In this literature, vulnerability is associated with the structural role that nodes and edges play in preserving connectivity, performance, and robustness. Liu et al. [3], for example, examined maritime supply chains as complex networks and combine resilience analysis with centrality based metrics to identify vulnerable nodes and edges. Similarly, Wen et al. [4] approached vulnerability from an entropy-oriented

Funded by the European Union
Grant Agreement: 101136257

perspective, while Ongkowijoyo et al. [5] used network analysis tools to explore risk causality, interaction patterns, and intervention points through graph-based visualization. These studies demonstrate that topology-driven approaches can be highly effective in identifying structurally critical modules, influential nodes, and fragile pathways. A useful complementary perspective is provided by percolation-based approaches, which examine how network functionality degrades as nodes or edges are progressively removed and identify critical transition points beyond which large-scale fragmentation occurs. In this respect, Hamedmoghadam et al. [6] showed that, in transportation networks, percolation analysis enriched with heterogeneous flow demand can reveal functionally critical bottlenecks that may remain undetected under purely topological assessment; this methodological perspective is further explored in Task 3.6. At the same time, however, they remain largely centered on network structure and interaction topology and therefore do not always capture the heterogeneous hazard characteristics, exposure conditions, or operational attributes associated with specific nodes and edges of a real logistics system. This limitation has also been recognized more broadly in the critical infrastructure literature. LaRocca and Guikema [7] showed that network-theoretic approaches are highly valuable for understanding infrastructure vulnerability, especially in systems that are simultaneously physical, geographic, and logical networks. Still, they also imply that structural modelling alone is not always sufficient for full risk characterization. In a similar logic, Eusgeld et al. [8] argued that vulnerability analysis in interdependent critical infrastructures should go beyond conventional cause–consequence logic, because highly coupled infrastructures generate spillover failures and emergent vulnerabilities that cannot be adequately represented by decomposition-based methods alone. This argument is particularly relevant to transport and logistics systems. Therein, operational vulnerability is determined not only by the structure of the network, but also by hidden interdependencies, tightly coupled processes, and cascading effects that extend across subsequent stages of the supply chain. A related development in the literature concerns the distinction between structural vulnerability and service-oriented vulnerability. Meng et al. [9] criticized approaches that focus only on topological structure or simple performance loss. Instead, they propose a vulnerability distribution framework for interdependent critical infrastructures based on simulation and "vulnerability clouds." Their work showed that vulnerability may differ across topology, function, and service dimensions, and that interdependent infrastructures may exhibit nonlinear patterns of service degradation. For logistics systems, this perspective is particularly useful because the significance of disruption does not depend only on whether the network remains connected, but also on how effectively services, routing choices, and operational capacities are preserved after disruption.

From a resilience perspective, another important line of work moves beyond static robustness assessment and examines the system's ability to recover over time after disruption. Zhang et al. [10] defined resilience in networked systems through time-dependent restoration behaviour, explicitly considering remaining capacity, restoration capability, and recovery speed. This is a critical contribution for transport and logistics applications, because the severity of a disruption cannot be understood solely through the initial loss of function; it must also be evaluated in relation to how rapidly and effectively network performance can be restored. Consequently, resilience is not only a matter of resistance, but also a matter of recovery trajectory. At the same time, the literature has highlighted the limitations of conventional methodologies such as Failure Mode and Effects Analysis (FMEA) when they

Funded by the European Union
Grant Agreement: 101136257

are applied to highly interconnected socio-technical systems. X. Li et al. [11] argued that classical risk-analysis methods often struggle to capture the complexity of systems in which hardware, software, communication processes, human operators, and organizational decisions interact dynamically. In such contexts, risks are not simply isolated failure modes, they are embedded in a network of causal relations and may propagate through multiple interdependent pathways. This is particularly relevant for advanced logistics and transport environments, where automation, cyber-physical integration, and operational interdependence make causal structures more complex than those assumed in conventional tabular risk methods.

Alongside FMEA, Hazard and Operability Analysis (HAZOP) is a structured method for identifying deviations from intended system operation. Kurt et al. [12] applied HAZOP in combination with an extended Cognitive Reliability and Error Analysis Method to maritime autonomous surface ship operations. HAZOP was used to identify operational deviations, their causes, potential consequences, and corresponding safeguards, while the extended CREAM supported the estimation of occurrence probabilities and risk levels. From a system-theoretic perspective, Chaal et al. [13] proposed a framework for developing the hierarchical control structure of an autonomous ship as the basis for applying System-Theoretic Process Analysis (STPA). Their study demonstrates how STPA can support safety analysis during the early design stages of autonomous vessels by representing both technical functions and their integration into the wider organisational control structure. At a broader hazard-screening level, Spachtholz et al. [14] applied HAZID to compare conventional, remotely controlled, and autonomous inland vessels across three operational scenarios. Based on the multidisciplinary judgement of experts, the study assessed hazards in terms of frequency and severity and found that unacceptable risks were concentrated mainly in complex, time-critical situations and in vessels with higher levels of automation. The study demonstrates the suitability of HAZID for the early-stage assessment of emerging inland waterway technologies across technical, operational, environmental, and human-factor domains. Compared with the broader screening function of HAZID, HAZOP is primarily a deviation-based method and typically requires a clearly defined design intent, process parameters, and guide words. It is therefore more suitable for the detailed analysis of a specific operation or subsystem. STPA is particularly useful for identifying hazards arising from unsafe control actions and inadequate interactions among humans, software, and hardware. However, it requires the development of a detailed hierarchical control structure and does not directly provide indicators of transport-network connectivity, fragmentation, or critical removal thresholds.

Broader systemic-risk studies reinforce this point by extending the focus beyond the transport network itself. Wehrle et al. [15], for instance, conceptualized inland waterway transport as a System-of-Systems and assess systemic risks by connecting infrastructure vulnerability with downstream industrial and societal consequences. The framework developed in that study showed that the consequences of infrastructure disruption may extend beyond the failed asset itself and propagate into production, supply, and population exposure domains. This broader viewpoint is highly relevant for logistics systems, where infrastructure failure may trigger indirect operational and economic consequences well beyond the original event location, however the scope of the task is the supply chain delay.

Finally, multihazard and cascading impact approaches underline that risk should not always be treated as a set of isolated single-event scenarios. Dunant et al. [16] show that hazard

Funded by the European Union
Grant Agreement: 101136257

interactions evolving in time and space may amplify losses and that assessments which ignore these interactions may underestimate total risk. Complementing this perspective, Brunner et al. [17] emphasized that the consequences of disruption should also be examined through the dependency structures that connect infrastructures, services, and users. This perspective is particularly relevant to inland waterway transport systems, where disruptions affecting a single node, route, or supporting asset may extend beyond the point of origin and generate indirect operational impacts across the wider logistics network. Their contribution is therefore methodologically important for risk and resilience assessment in inland waterway transport. It highlights the need to assess not only direct hazard exposure, but also the propagation of service disruption through interdependent system elements and its implications for supply chain delay and overall network performance.

2.2 OVERVIEW OF HAZARDS IN IWW

Hazards affecting IWT should be understood not only as isolated accident events but rather as a broader constellation of environmental, infrastructural, operational, technical, and organizational conditions that can undermine both navigational safety and supply chain continuity. In their systematic review of inland waterways freight transport, Gbako et al. [18] argued that, despite the strategic significance of IWT as a sustainable transport mode, its effective operation remains limited due to insufficient infrastructure. This broader perspective is consistently supported in the literature, which identifies physical limitations of waterways as fundamental constraints on inland navigation performance and safety.

In particular, Totakura et al. [19] identified infrastructure-related factors as the most critical group influencing container shipping through inland waterways, ranking them above economic, geographical, and regulatory considerations. Among these, inadequate river depth act as one of the most significant subfactors, while terminal capacity, container availability, and supporting infrastructure are also important determinants of system performance. Similarly, Chen et al. [20] considered insufficient channel width and depth, and high vessel traffic density among the most important Risk-influencing factors (RIF) across different river sections, proposing mitigation measures such as dredging, shoal removal, traffic restrictions, and improved channel management. Taken together, these results suggest that shallow depth, narrow fairways, bottlenecks, and traffic concentration should not be regarded solely as efficiency-related limitations, but rather as core causes capable of triggering delays, disruptions, groundings, collisions, and broader network fragility.

A second major category of hazards concerns environmental conditions. According to Chen et al. [20], inland waterways are increasingly exposed to extreme weather events, while the trend toward larger vessels and increasing traffic volumes introduces extra safety challenges. Their study explicitly noted that inland waterway risks include ship collisions, grounding, fires, and explosions, while also showing that the relative importance of specific risk sources varies across river sections depending on local navigational and environmental conditions. In the same study, adverse weather, natural causes such as landslides, earthquakes, floods, and droughts, as well as swings in water levels, are identified as the principal RIFS affecting inland navigation. These observations underline that hydrometeorological variability and climate-related disruption constitute central dimensions of hazard exposure in IWT systems.

A third category concerns technical and navigational support hazards. Pham and Hoang [21] noted that failures in navigational support systems can significantly compromise safe vessel

Funded by the European Union
Grant Agreement: 101136257

operation. More specifically, their study detects risks associated with malfunctioning electronic navigation systems, such as Global Positioning System (GPS) and radar, outdated navigational charts, limited visibility of navigational aids, and the absence of redundancy and backup systems. Although their case study focuses on ferry operations, the essential mechanisms are directly relevant to inland waterways, particularly in narrow channels, low visibility environments, and high-density traffic areas, where limited manoeuvring margins may rapidly transform technical failure into collision, grounding, or operational stoppage.

A fourth category includes traffic management and emergency response hazards. In the Yangtze-based inland waterway study, Chen et al. [20] identified high ship traffic density, improper management of berthing ships, insufficient maritime supervision, and inadequate emergency-response capability as important risk sources. Similarly, Pham and Hoang [21] classified marine traffic congestion and inadequate evacuation and emergency-response features among the extreme-risk factors in ferry navigation. These hazards are particularly significant in inland waterway networks because they not only increase the probability of accidents, but also decrease the system's capacity to absorb, manage, and recover from disruptions once an incident has occurred. In this respect, weaknesses in emergency response represent not only safety hazards in their own right, but also clear indicators of reduced system resilience.

The above literature review referred to hazards associated with inland waterway transport systems. This was undertaken to ensure that the hazard identification process was sufficiently comprehensive and that all relevant hazards applicable to the examined case were captured in a greater detailed way in the Appendix. Overall, the literature suggests that hazard exposure in inland waterway transport is multidimensional and systemic. Several factors can affect the likelihood of accidents and disrupt normal operations, including inadequate infrastructure, environmental conditions, technical failures, and limitations in traffic management or emergency response. Human-related issues, such as strikes, labour protests, or shortages of personnel needed for essential operations, may also affect operational continuity and system performance. When these factors occur individually or in combination, they can reduce operational continuity and lead to delays that may affect the wider transport and supply chain network.. Even where physical infrastructure and technical systems remain operational, workforce-related disruptions may still interrupt cargo-handling activities, vessel servicing, and terminal functions, thereby undermining operational continuity and supply chain reliability. In this sense, the consequences of such hazards extend beyond immediate navigational safety, affecting the continuity, reliability, and temporal performance of freight flows. As a result, hazard assessment in IWT should move beyond an event-based perspective and adopt a more integrated understanding of the conditions that may impair operational continuity, navigational safety, network resilience and overall supply chain efficiency. In the AUTOFLEX inland waterway (IWW) transport system, all the above hazardous events are relevant, along with additional hazards arising from the system's innovations, which will be briefly examined in Section 4.

.

Funded by the European Union
Grant Agreement: 101136257

3 METHODOLOGY

Task 3.6 addresses the need for a structured and operationally relevant methodology for assessing the safety, security, and resilience of the AUTOFLEX transport system under conditions of increasing technological complexity and network interdependence. As highlighted by the preceding literature review, the assessment of risks in interconnected transport systems cannot rely exclusively on structural network analysis, nor can it be limited to the isolated examination of individual hazardous events. Inland waterway transport systems operate as interconnected logistics networks in which local disruptions may propagate across nodes, routes, supporting infrastructures, and subsequent supply chain stages. This challenge becomes even more pronounced in the case of the AUTOFLEX IWW Transport System, where the integration of autonomous solutions introduces new interactions with existing transport infrastructure, recreational and non-professional waterway users, physical and cyber threats, and the wider operational environment. For this reason, the task requires an approach that combines both network-based and hazard-informed logics, capable of identifying heterogeneous hazardous scenarios, using the quantitative risk-level results directly as weights in the network analysis, and supporting the formulation of targeted mitigation measures.

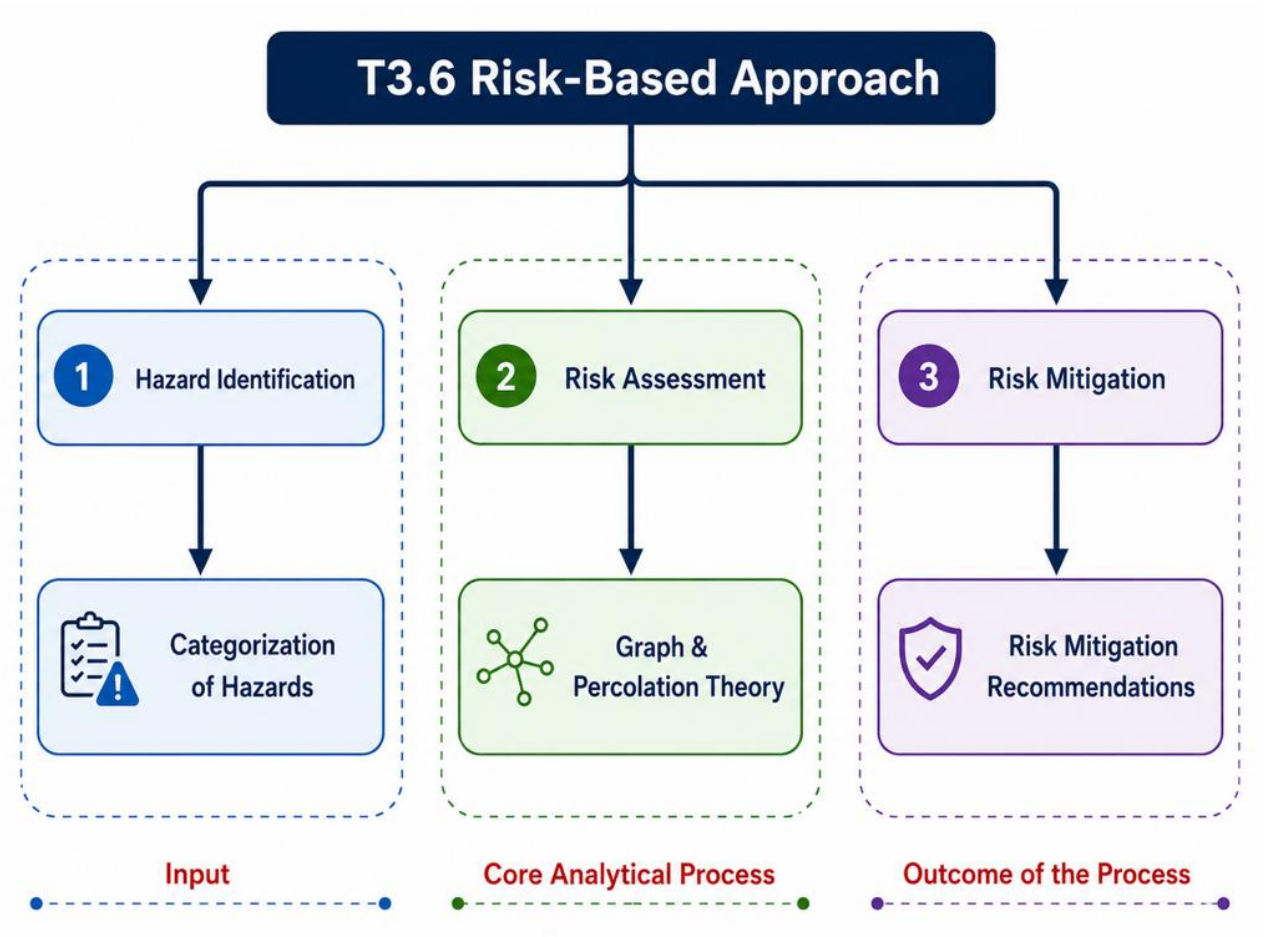

Figure 3-1: Three-Pillar Task Decomposition Plan.

Funded by the European Union
Grant Agreement: 101136257

To address these needs, the task is decomposed into three closely connected pillars: Hazard identification, Risk assessment, and Risk mitigation, as shown in Figure 3-1. This decomposition ensures that the overall methodology progresses from the systematic identification of hazardous scenarios to the evaluation of their implications for network vulnerability and resilience, and finally to the formulation of actionable risk control options.

The first pillar, Hazard Identification, focuses on the systematic identification, categorization, and ranking of hazards associated with the AUTOFLEX transport system. This includes hazards linked to the design and operation of AUTOFLEX innovations, their interaction with existing infrastructure, the presence of third-party and non-professional waterway users, and the emergence of safety, security, and resilience-related threats. In practical terms, this pillar establishes the hazard basis of the work performed in the context of this task by identifying relevant disturbance scenarios, defining their causes and consequences, and organizing them into a structured set of risk-relevant events.

The second pillar, risk assessment, translates the identified hazard environment into a network-oriented analytical framework. At this stage, the transport system is represented as a graph of nodes and edges, and the hazardous scenarios associated with individual elements are incorporated into the network as weighted conditions affecting connectivity, accessibility, and operational continuity. In line with the methodological logic presented in the task description, in the second pillar, percolation-theory principles and related network-vulnerability concepts are applied, in order to examine how disruption affects the cohesion and functionality of the studied transport system. The purpose is to determine which elements are exposed to risk, the nodes and routes are that are critical to the preservation of overall performance, how disruption may propagate through the network, and how the system behaves under conditions of partial degradation.

The third pillar, risk mitigation, constitutes the applied outcome of the task. Building on the results of the previous two pillars, this stage focuses on the development of risk-control options, mitigation measures, and recommendations capable of reducing the adverse effects of identified risks on the normal operation of the logistics system. These measures may address technical, operational, organizational, infrastructural, or cyber-related vulnerabilities, depending on the type and location of the critical risks identified. In this sense, the mitigation pillar seeks to support the resilient operation of the AUTOFLEX transport system by prioritizing interventions where they are expected to have the greatest effect on continuity, safety and system-wide performance.

The adopted three-pillar decomposition provides a coherent implementation plan ensuring that the task addresses its core methodological objectives – namely, to connect hazard identification with system-level network assessment and, ultimately, with actionable resilience-enhancing recommendations. By structuring the work in this way, the applied methodology is able to bridge the gap between heterogeneous hazard characterization and transport-network vulnerability analysis

Figure 3-2 provides an overview of the methodology developed and applied in the context of Task 3.6. It supports a structured workflow for risk identification, risk assessment and mitigation for the AUTOFLEX inland waterway transport system, addressing safety, cybersecurity, and resilience concerns in an integrated manner. The applied methodology combines conventional hazard-based risk analysis with network science (through graph and percolation theory application). It enables hazards and threats to be examined and evaluated

Funded by the European Union
Grant Agreement: 101136257

in terms of likelihood and consequences, at the level of individual transport system components, as well as on how they could propagate through or disrupt the underlying transport network and the supply chain.

The methodology is divided into three main stages:

- Hazard identification: Hazards are categorized as the key elements of the transport system and assessed through a Hazard Identification (HAZID)-based process in order to derive a relevant risk level. These results are translated into node and edge weights and used to construct a graph representation of the AUTOFLEX IWW network.
- Risk assessment: Graph theory is applied to model the AUTOFLEX IWW transport system as a network and to quantify its structural properties through key graph metrics, while percolation theory is applied through a set of deletion scenarios—random and targeted removals of nodes or edges to quantify resilience, robustness, and degradation patterns.
- Risk mitigation: The outcomes of the previous process are interpreted to formulate practical measures and recommendations for a more resilient AUTOFLEX transport network.

More detailed descriptions of each methodological step, together with the underlying assumptions, datasets, and analytical procedures, are presented in the following sections.

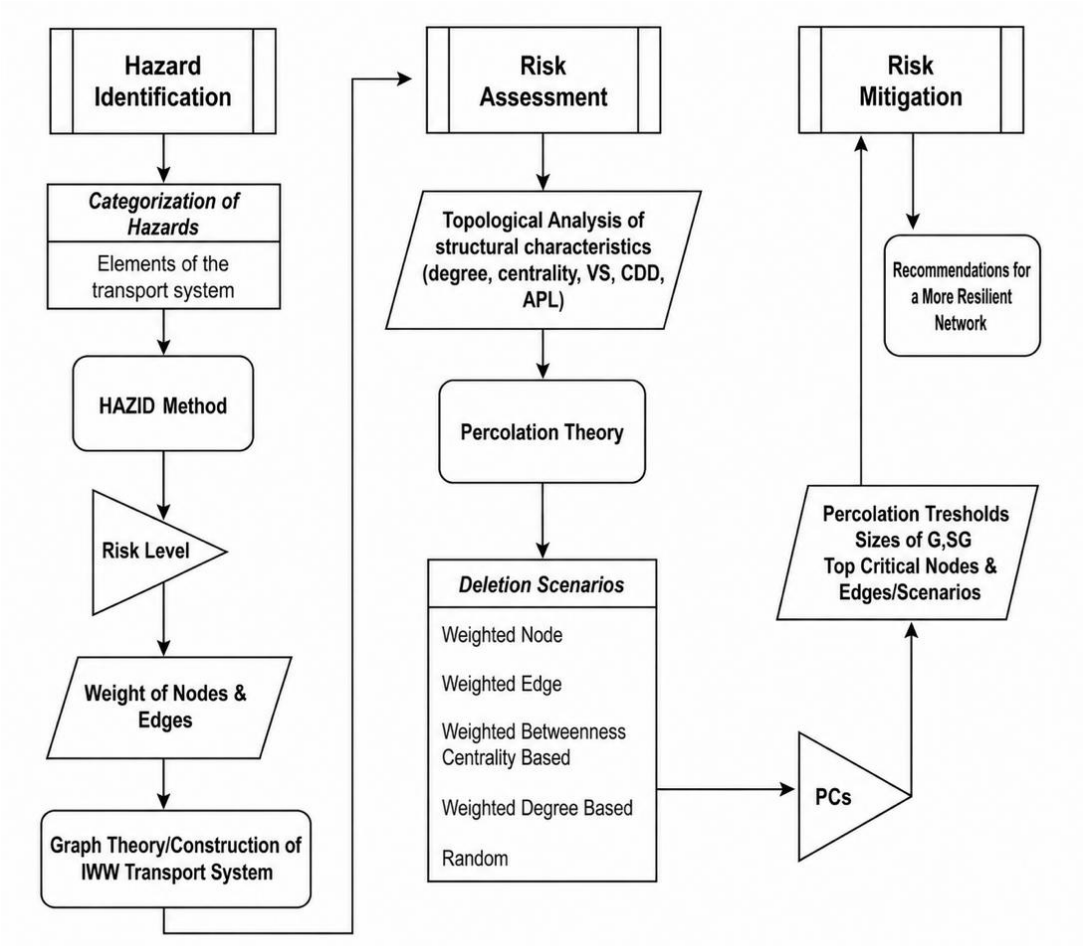

Funded by the European Union
Grant Agreement: 101136257

Figure 3-2: Risk and Resilience Assessment Method for AUTOFLEX IWTS.

3.1 STEP 1: HAZARD IDENTIFICATION - HAZID METHOD

The process begins with the identification of hazards linked to the key system elements that could affect cargo flow across the network by causing delivery delays or operational disruptions. The hazard identification and ranking processes were supported by a targeted literature review, described in Section 2, and a series of online workshops with consortium partners with relevant expertise on the field, i.e. DST[2], DFDS[3], and ISE[4], in order to identify hazards and hazardous events that may lead to cargo delays. The hazards and hazardous events were associated with the MDCs, TPTs, and S&C hubs respectively. In addition, hazards associated with ports and vessel routes were also considered, as these constitute critical segments of the end-to-end supply chain from the point of origin to the final terminal.

Subsequently, a HAZID approach is applied to systematically document the identified potential hazardous scenarios, along with their initiating causes and expected consequences. Each scenario is then ranked using a 5×5 risk matrix as shown in Table 3-1

Table 3-1: 5X5 Risk Matrix for AUTOFLEX IWW Transport System.

Probability/Severity	Insignificant 1	Minor 2	Significant 3	Major 4	Severe 5
5 Almost Certain	Medium 5	High 10	Very high 15	Extreme 20	Extreme 25
4 Likely	Medium 4	Medium 8	High 12	Very high 16	Extreme 20
3 Moderate	Low 3	Medium 6	Medium 9	High 12	Very high 15
2 Unlikely	Very low 2	Medium 4	Medium 6	Medium 8	High 10
1 Rare	Very low 1	Very low 2	Low 3	Medium 4	Medium 5

The adopted 5×5 Risk Matrix is the typical and widely used risk matrix scoreboard (similarly to NASA [22]), intended as an initial qualitative tool for prioritizing technical safety concerns. The matrix evaluates each hazardous event by combining its probability of occurrence with its severity on the AUTOFLEX Transport System, colour coded as very low, low, medium, high, very high and extreme risk. Probability refers to the general likelihood that a hazardous event may occur, classified from Rare to Almost Certain. Severity refers to the expected disruption caused to the AUTOFLEX transport system, expressed as delivery delay. Insignificant impacts cause delays of 0–3 hours, while severe impacts mean the delivery is not completed. The matrix provides a structured means of prioritising identified hazards. Each risk is assigned to a qualitative level, allowing higher-priority risks to be clearly identified and supporting the selection of appropriate risk control options. The risk levels, which have

[2] Entwicklungszentrum fur schiffstechnik und transportsysteme ev
[3] Det Forenede Dampskibs-Selskab
[4] Institut für Strukturleichtbau und Energieeffizienz gGmbH

Funded by the European Union
Grant Agreement: 101136257

resulted from the evaluation of the expert group, are assigned as weights to the corresponding network elements. Finally, the transport system is represented as a weighted graph, where nodes capture operational locations and system components, and edges represent vessel routes connecting them.

3.1.1. NODE EVALUATION

The TPT building blocks concept defines the main functional elements required for the development of a Temporary Port Terminal concept. They cover key aspects such as cargo handling, cargo storage, site utilities, waterborne and hinterland interfaces, public access, temporal availability, and the operating model. Since each building block includes different configuration options, the TPT concept can be adapted to the physical, operational, and social conditions of each location. In this case study, it is also noted that TPT building block characteristics are integrated into the ports.

Using information from Deliverable 3.1 [23], specific characteristics were identified through the relevant building blocks and linked to hazardous events that may affect supply chain continuity. As these characteristics differ among the examined configurations, they were used as an additional risk refinement layer for the node-level risk assessment. More specifically, selected hazardous events associated with the building blocks were correlated with the existing risk levels derived from the risk matrix and were further classified into categories. Based on this classification, the initial risk level was adjusted by applying a reduction factor (RF) calculated as $R_{baseline}$ divided by a risk category, where $R_{baseline}$ represents the baseline reduction factor assigned to the initial risk level. In this way, TPT or port characteristics indicating better operational performance or lower vulnerability result in a lower adjusted risk score, while characteristics associated with higher exposure to supply chain delay maintain a higher risk contribution. Table 3-2 presents the relevant building blocks, and the corresponding risk category assigned to each case.

The node-level reduction factor was calculated through a sequential adjustment process. Starting from $R_{baseline}$, the value was progressively divided by the risk category assigned to each relevant building block. Each building block was classified as High, Medium, or Low, corresponding to numerical values of 1, 2, and 3, respectively. Therefore, the final node-level reduction factor is expressed as:

$$RF_{nodes} = \frac{R_{baseline}}{RF_A \cdot RF_F \cdot RF_G \cdot RF_H} \quad (1)$$

where RF_A, RF_F, RF_G, and RF_H correspond to the risk categories assigned to the relevant Building Blocks.

Table 3-2: Building Block structure for AUTOFLEX IWW Transport System.

Building Block	Block Configuration	Short Description	Risk Category
A. Cargo Handling	A1. Fixed, ashore, cargo handling	Fixed Equipment on land	3 (Low)
	A2. Mobile ashore cargo handling	Mobile Equipment on land	2 (Medium)
	A3. Fixed afloat cargo handling	Afloat fixed equipment	2 (Medium)

Funded by the European Union
Grant Agreement: 101136257

	A4. Mobile afloat cargo handling	Afloat mobile equipment	1 (High)
F. Public Interface	F1. Open access	Without Fence	1 (High)
	F2. Limited access	Industrial site with gate	2 (Medium)
	F3. Restricted access	Industrial area with many companies	3 (Low)
G. Temporal Availability	G1. Continuous availability	24/7 operated	3 (Low)
	G2. Constrained availability	Specific time windows	2 (Medium)
	G3. Contingent availability	Occasionally, for specific need	1 (High)
H. Operating Model	H1. Independent TPT	Independent small terminal	3 (Low)
	H2. Integrated TPT	Integrated into an existing installation	2 (Medium)
	H3. Ecosystem TPT	Many companies, clusters	1 (High)

3.1.2. EDGE EVALUATION

Correspondingly, for the vessel routes, specific route-related characteristics were also considered in order to further refine the risk levels obtained from the risk matrix. These characteristics include traffic conditions, CEMT class and route length in kilometres, as they may influence the likelihood or severity of delays within the AUTOFLEX Transport System. Traffic was assessed using three parameters: The vessel routes that connect ports to specific locations, the level of route utilisation, and the presence of common routes within the AUTOFLEX Transport System. A traffic reduction factor was calculated as:

$$RF_{traffic} = R_{baseline} \cdot \frac{RF_{port} + RF_{corridor} + RF_{route}}{3} \quad (2)$$

where RF_{port}, $RF_{corridor}$ and RF_{route} are binary traffic multipliers, such that $RF_{traffic} = RF_{baseline}$ if all three apply.

In addition, each route was classified according to its European Conference of Ministers of Transport (CEMT) class, where routes of classes I≤CEMT<III, III≤CEMT<IV, IV≤CEMT≤VI were assigned RF values of 1, 2, and 3 from high to low (RF_{CEMT}), as the wider a corridor, the fewer hazards may occur. Finally, route length was considered through distance-based categories, with routes of 1–25 km, 25–50 km, and 50–80 km assigned RF values of 3, 2 and 1 from high to low (RF_{Km}), as the longer the route, the more hazardous events may occur. These RFs are summarised in Table 3-3 Table 3-4. They were used to adjust the initial risk score, allowing the assessment to better reflect the operational characteristics and delay potential of each vessel route. The final risk level for each route of the AUTOFLEX Transport System is derived as follows:

$$RF_{edges} = \frac{RF_{traffic}}{RF_{CEMT} \cdot RF_{Km}} \quad (3)$$

Table 3-3: CEMT Reduction Factors for AUTOFLEX IWW Transport System.

Funded by the European Union
Grant Agreement: 101136257

CEMT	Reduction Factor (R_{CEMT})	Risk Category
I≤CEMT<III	1	High
III≤CEMT<IV	2	Medium
IV≤CEMT≤VI	3	Low

Table 3-4: Km Reduction Factors AUTOFLEX IWW Transport System.

Km	Reduction Factor (R_{Km})	Risk Category
1≤km<25	3	Low
25≤km<50	2	Medium
50≤km≤80	1	High

3.2 STEP 2: RISK ASSESSMENT – GRAPH & PERCOLATION THEORY

The risk assessment analysis in this work is performed through a graph-theoretical framework in combination with percolation theory, using the reduction factors presented in the previous section to build a graph of the transport system. Graph theory offers a suitable analytical framework for the transport system with nodes and edges and for examining its structural and functional properties through network indicators. Nevertheless, a purely unweighted representation may be insufficient for capturing the real operational significance of the network. Not all nodes and edges contribute equally to system performance, and not all disruptions have the same consequences. From this point of view, it is useful to examine the transport network in both unweighted and weighted forms. The unweighted graph captures the pure structural topology of the system by considering only the existence of connections between nodes and is therefore appropriate for investigating the backbone of network connectivity and the general organization of flows [24]. By contrast, the weighted graph incorporates functional information into the network representation and is better suited to reflect the heterogeneous operational significance of network elements. This distinction is particularly important in resilience and vulnerability analysis, since disruptions do not affect all nodes and edges equally. Furthermore, the consequences for network performance depend not only on whether a connection exists, but also on its relative importance within the system. Accordingly, the combined use of unweighted and weighted graph representations enables a more comprehensive understanding of the network, linking its structural properties with its functional behaviour under disruption. Based on this dual structural and functional perspective, a set of graph-theoretic metrics is employed below to quantify the main topological and weighted properties of the network. The definitions (1-7) presented below are applied to the unweighted graph to characterise the system's structural topology based solely on the presence or absence of connections. The percolation theory methodology is applied to a weighted graph in order to determine the removal order per removal scenario. Is also useful for assessing network robustness and resilience under progressive disruption By monitoring the size of the connected components during this process, the analysis identifies

Funded by the European Union
Grant Agreement: 101136257

the percolation threshold, namely the point at which the network undergoes a major transition from a predominantly connected structure to a fragmented one.

(1) Cumulative degree distribution (CDD): One common way to quantify a node's connectivity within a network is by using the concept of degree, i.e., how many edges a node connects to. The degree of node *i* can be determined using the following formula:

$$k_i = \sum_{j=0}^{N} a_{ij} \qquad (4)$$

The a_{ij} represents the connection between 2 nodes in the AUTOFLEX IWTS. It takes the value 1 when nodes i and j form an origin–destination pair, indicating that a connection exists between them, and 0 otherwise. In the network analysis, higher-degree nodes provide easier access to more nodes. In the IWT Systems, the CDD represents the minimum degree (P(k)) used to calculate the probability of randomly (p(k')) selecting a node with a degree of at least *k*, and it is calculated as follows:

$$P(k) = \sum_{k\prime=k}^{\infty} p(k') \qquad (5)$$

The CDD plays a key role in identifying various network behaviours in actual transportation systems, such as the spread of traffic flow and the resilience of the network [22].

(2) In-degree and Out-degree: Represent the number of incoming and outgoing connections per node, respectively, and are calculated as follows [25]:

$$k_i^{in} = \sum_j a_{ji} \qquad (6)$$

$$k_i^{out} = \sum_j a_{ij} \qquad (7)$$

where: a_{ji} *or* a_{ij} $\begin{cases} 1, if\ there\ is\ an\ edge \\ 0, if\ there\ is\ not\ an\ edge \end{cases}$

In-degree and Out-degree are useful for identifying important destinations and distribution points whose disruption could significantly affect the network.

(3) Average path length (APL): The formula below is applied to calculate the APL, representing the mean of the shortest number of edges between any randomly selected pair of nodes in the IWTS.

$$L = \frac{1}{N(N-1)} \sum_{i \neq j} d_{ij} \qquad (8)$$

Where d_{ij} is the fewest number of edges that connect nodes *i* to *j* [25]. APL measures network efficiency by indicating how many intermediate connections are typically required to travel between nodes.

(4) Clustering coefficient (CC): Quantifies how many nodes in a graph are inclined to form clusters. In real world networks, nodes often form closely connected groups with a higher density of edges. The CC is defined by the following equation:

$$C_i = \frac{E_i}{C_{ki}^2} \qquad (9)$$

Funded by the European Union
Grant Agreement: 101136257

where C_i denotes the local CC of node *i*, E_i indicates the number of realized connections among the neighbours of node *i*, while C^2_{ki} refers to the total number of potential connections among those neighbours [25]. The CC reveals closely interconnected groups of nodes and indicates whether alternative routes are locally available.

(5) Betweenness centrality (BC): Quantifies how much a node influences the shortest paths between all node pairs. A higher value indicates a more important role for transfer of a node *i*. The betweenness of node *i* is determined by the fraction of shortest paths that pass through it:

$$BC_i = \sum_{s \neq i \neq t} \frac{n^i_{st}}{g_{st}} \quad (10)$$

where g_{st} indicates the total number of shortest paths from *s* to node *t and* n_{st} refers to the count of those shortest paths in g_{st} that pass through node *i* [25]. It is useful for detecting critical transfer or bridge nodes whose failure could interrupt flows between different parts of the network.

(6) Network density (d): The ratio of the number of its edges to the largest possible number of edges that may be stretched on the vertices of the graph [22], calculated as:

$$d = \frac{m}{n(n-1)} \quad (11)$$

where n is the number of nodes and m is the number of edges. Network density indicates the overall degree of connectivity and the availability of alternative routes within the network.

(7) Diameter D(G):

The maximum distance (steps) over all pairs of nodes in a graph where d(i,j) is the minimum number of edges required to connect nodes i and j[24].

$$D(G) = max_{\,i,j \in V}\, d(i,j) \quad (12)$$

Diameter helps evaluate overall network efficiency by showing the maximum number of connections needed to travel between any two nodes.

Subsequently, percolation theory is used to examine the response of the network to disruptions by evaluating the evolution of its cohesion and connectivity as nodes or edges are progressively removed.

The analysis focuses on the critical percolation threshold p_c, which denotes the phase transition point of the network and is determined from the behavior of the largest connected giant component, (G), and the second-largest giant connected component(*SG)*, with respect to the node or edge removal rate q [26]. A connected component is a maximal group of nodes in which every pair of nodes can be connected through a path. More specifically, G and SG represent the numbers of nodes contained in the largest and second-largest such groups, respectively. The percolation threshold p_c is defined as the first removal fraction *q* at which the SG reaches its global maximum, meaning its highest value over the complete removal process, signalling the onset of large-scale fragmentation or, conversely, the loss of global connectivity. Here, *q* represents the proportion of nodes or edges removed from the network. For low values of *q*, the G remains dominant, indicating that most nodes are still

Funded by the European Union
Grant Agreement: 101136257

interconnected. As q increases, the network becomes progressively fragmented.SG initially increases when a substantial group of nodes becomes detached from G and subsequently decreases as that group is further divided into smaller components as illustrated in .

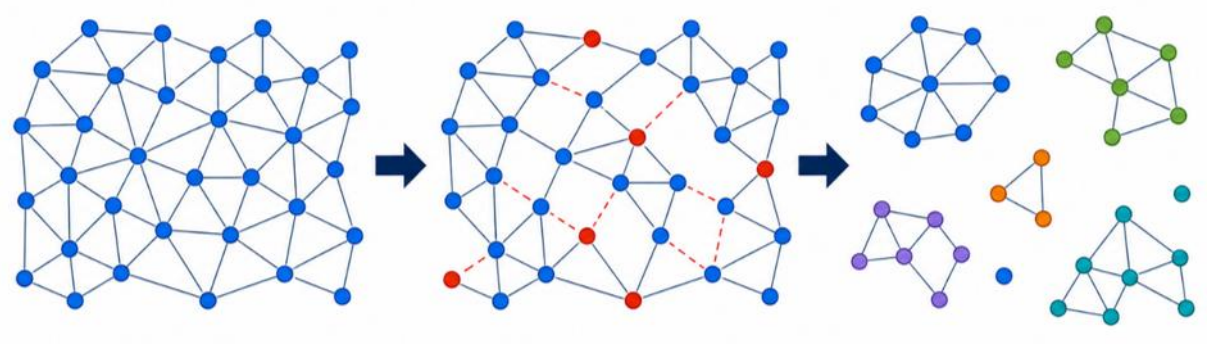

Figure 3-3: Three phases of percolation theory in graph networks.

3.2.1. CYBERSECURITY-INFORMED PERCOLATION ASSESSMENT

. Once q exceeds p_c, global connectivity is lost and the network becomes divided into smaller, disconnected components. In transportation networks, for q < p_c, cargo can be routed to most destinations through connected paths.

The percolation theory analysis is performed under five different disruption scenarios, including the targeted removal of nodes or edges, according to:

1) Weighted betweenness centrality, where nodes serving as critical bridges are removed first;
2) Weighted degree, where the most highly connected nodes are prioritized for removal;
3) Weighted node;
4) Weighted edge removal in descending order, and;
5) Random removal [27].

When multiple nodes or edges have the same score, the algorithm randomly selects one of them for removal (scenario 3). For scenario 2, each node's weighted degree score is calculated by summing its in-degree and out-degree, as defined in Equations (6) and (7), and multiplying the result by its corresponding node weight. Nodes are then removed in descending order of the resulting score. For scenario 1, the procedure is more complex, as the removal score combines each node's edge-weighted betweenness centrality with its corresponding node weight. It is calculated as follows:

$$Weigthed\ BC_i = \frac{1}{(N-1)\times(N-2)} \sum_{s\neq i\neq t} \frac{n_{st}^{i,(w)}}{g_{st}^{(w)}} \times Node\ Weight \qquad (13)$$

where $n_{st}^{i,(w)}$ is the number of these weighted shortest paths passing through node i, and $g_{st}^{(w)}$ is the number of paths whose cumulative edge weight achieves the minimum value of $d_w(s,t)$. The weighted shortest path distance is defined as:

$$d_w(s,t) = min_{\ P\in P_{st}} \sum_{e\in P} weight_{edge} \qquad (14)$$

Funded by the European Union
Grant Agreement: 101136257

where P_{st} is the set of all paths from s to t. The factor $\frac{1}{(N-1)\times(N-2)}$ is used as a normalization factor for directed networks.

For each scenario, the variation of *G* and *SG* is monitored as the removal rate changes, and the results are illustrated through diagrams showing the progressive deterioration of network connectivity. This approach makes it possible to determine the percolation threshold for each failure mechanism, identify the nodes and edges that are most critical to overall network integrity, and assess which disruption patterns produce the fastest or most severe fragmentation, thereby highlighting the elements that require priority risk mitigation. The three phases of this type of network, according to percolation theory, are illustrated in Figure 3-3.

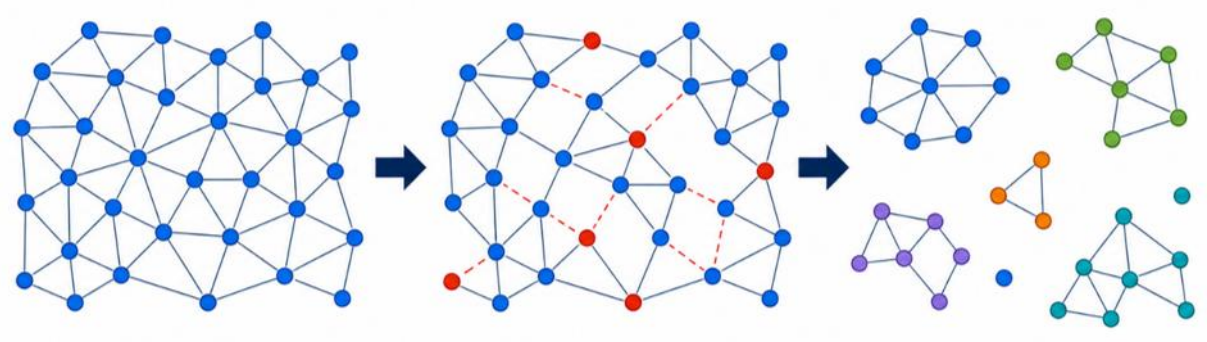

Figure 3-3: Three phases of percolation theory in graph networks.

3.2.2. CYBERSECURITY-INFORMED PERCOLATION ASSESSMENT

Penetration testing is a controlled cybersecurity assessment method used to identify, validate, and evaluate vulnerabilities in digital systems, networks, or applications. In contrast to a purely theoretical vulnerability assessment, penetration testing attempts to determine whether identified weaknesses can actually be exploited in practice [28]. It is performed in a legal and controlled manner, usually by cybersecurity specialists, with the objective of understanding how an attacker could gain unauthorised access, disrupt system operation, manipulate data, or compromise critical services. In the context of autonomous or remotely operated inland waterway transport systems, penetration testing is particularly relevant because vessel operations increasingly depend on digital communication, vessel management systems, remote-control interfaces, data exchange platforms, and monitoring infrastructure.

This analysis does not involve penetration testing of vessel Information Technology (IT) systems in the conventional technical sense. Instead, it enables additional cybersecurity-related events that were not previously considered to be identified and incorporated into the graph, allowing their potential effects on the connectivity and resilience of the transport network to be assessed. Within the AUTOFLEX network, this issue can be represented as a cybersecurity-related hazardous event affecting the vessel route edges of the graph. The hazardous event identified in the AUTOFLEX IWTS refers to the potential compromise of vessel IT management systems that support vessel operations along specific route segments. [29]. These systems may be affected by cyberattacks, including attacks against the IT management system itself, data breaches, unauthorised access, or denial-of-service incidents. The main causes of this hazardous event are vulnerable systems and inadequate security controls, such as weak authentication mechanisms, insufficient network segmentation,

Funded by the European Union
Grant Agreement: 101136257

outdated software, poor monitoring, or limited protection against external attacks [30]. If such weaknesses are exploited, the consequences may include incorrect or corrupted operational data, temporary loss of system availability, out-of-order vessel management functions, damage to the vessel, and, in severe cases, damage to surrounding infrastructure. Therefore, the hazardous event does not only represent a local cybersecurity problem, but also a potential source of operational disruption along the affected vessel route.

3.3 STEP 3: RISK MITIGATION

Finally, the findings of the previous stages are translated, in the third step of the process, into targeted risk control options and recommendations aimed at strengthening overall network resilience. Following the identification of critical nodes and edges, as well as the most disruptive failure scenarios, appropriate measures are defined to reduce the vulnerability of the system and preserve its functionality even under severe disruption conditions. Here, critical nodes and edges refer to structural weak points of the system, i.e., network elements whose failure or removal would significantly affect network connectivity, increase fragmentation, disrupt major flow paths, or reduce the overall resilience of the IWW network [31]. Appropriate measures may include reducing the risk level of specific scenarios associated with critical network elements, strengthening or protecting key infrastructures, increasing redundancy through the development of alternative routes, redesigning connections at central points of the network, and implementing organizational and operational continuity measures. In this respect, mitigation is not limited to the protection of individual assets, but also aims at promoting a more cohesive graph structure, characterized by improved connectivity, greater route diversity, and reduced dependence on single critical hubs or bottleneck edges [32].

Based on these findings, an alternative and more cohesive graph configuration will also be presented, with the aim of examining whether and to what extent the vulnerabilities identified in the previous stages can be reduced through a structurally improved network design. In this way, the analytical results are transformed into practical interventions that support a more resilient IWW network, capable of maintaining its cohesion and functional performance even when exposed to significant disruptions.

Funded by the European Union
Grant Agreement: 101136257

4 RESULTS

4.1 HAZARD IDENTIFICATION - HAZID METHOD RESULTS

This section presents the results of the hazard identification and risk evaluation process conducted for the AUTOFLEX IWW Transport System, with particular emphasis on the hazards and hazardous events that may adversely affect operational and cargo flow continuity, navigational reliability, and the overall performance of the logistics chain. . Equally important is a clear understanding of each part of the AUTOFLEX transport system, since alongside conventional route components such as ports and vessel routes, the system also incorporates a number of innovations that were fully described in Deliverable D3.1 entitled "Transport Concepts".

In the context of this deliverable, these elements are examined from the perspective of supply chain delay. The analysis is based on the HAZID method and approaches the AUTOFLEX system as an integrated operational framework composed of interconnected infrastructure, transport, energy, and cargo-handling elements. Within this context, the following subsections first provide a description of the main parts of the AUTOFLEX transport system and its key innovations from a supply chain delay perspective and subsequently present the hazard identification process and the resulting classification of the main hazards and hazardous events.

4.1.1. DESCRIPTION OF THE PARTS AUTOFLEX TRANSPORT SYSTEM AND ITS INNOVATIONS

a) AUTOFLEX Vessel

Figure 4-1: AUTOFLEX IWW Vessel [30].

The AUTOFLEX vessel is a small, fully electric and uncrewed inland container vessel concept designed for operation on CEMT Class II inland waterways [33]. It aims to provide a zero-emission, flexible, and logistically efficient alternative for inland freight transport, particularly in shallow, narrow, and infrastructure-constrained waterways where larger conventional vessels may face operational limitations. The vessel concept integrates autonomous navigation, remote monitoring and control, modular Zero Emission Services

Funded by the European Union
Grant Agreement: 101136257

(ZES) battery units, and a containerized cargo arrangement compatible with standard 20-foot ISO and pallet-wide containers. Its design is shaped by key operational and regulatory constraints, such as lock dimensions, bridge clearance, shallow-draft requirements, stability needs, and compliance with relevant inland navigation rules. Overall, the AUTOFLEX vessel represents a scalable concept for automated and sustainable inland shipping, supporting the wider transition toward greener and more digitally integrated freight transport systems. An illustration of the AUTOFLEX vessel is shown in Figure 4-1.

b) WACS-Vessel Route

Waterborne Alternative Corridors (WACs) are inland waterway routes identified as alternatives to highly congested road corridors. In the AUTOFLEX context, WACs are defined by matching Traffic-Intense Corridors (TICs) with nearby or parallel canals and inland waterways that can provide similar transport connections. Their purpose is to support modal shift from TICs, especially in areas where external costs, and underutilized waterways create opportunities for more sustainable logistics. Therefore, WACs form the basis for identifying where TPTs, and S&C hubs could be developed within the AUTOFLEX transport network, while vessel routes between WACs, represent the connecting edges between the various operational nodes of the AUTOFLEX transport system. Any disruption affecting route availability, navigability, or travel time may therefore have a direct impact on service reliability and the overall synchronisation of logistics activities. Potential delays may arise due to insufficient water depth, traffic congestion, lock or bridge restrictions, adverse weather conditions, navigational obstacles, reduced manoeuvrability in complex passages, or deviations caused by operational and energy- related constraints. Since vessel routes are closely tied to planned schedules, battery range limitations, and port or terminal time windows, even relatively small disruptions may lead to cascading effects across the network, including missed berthing slots, delayed cargo handovers, and rescheduling of downstream transport operations. For this reason, vessel routes should be considered not merely as transport corridors, but as time-critical operational elements whose reliability, accessibility, and adaptability strongly influence supply chain performance.

c) Ports

Ports constitute critical interface nodes within the AUTOFLEX transport system, as they support the transfer of cargo between waterborne and landside operations and enable the coordination of vessel arrivals, loading and unloading activities and onward distribution. From a supply chain delay aspect, ports play a central role in maintaining cargo flow continuity, since any inefficiency or disruption in berth allocation, cargo handling, terminal coordination, or hinterland connectivity may directly affect vessel turnaround times and delay subsequent logistics operations. In this context, congestion, limited handling capacity, equipment unavailability, restricted access, labour constraints, or poor synchronisation between terminal and vessel operations may result in waiting times, cargo accumulation, and reduced operational reliability. Because port operations are closely linked with logistics processes, delays occurring at port level may propagate across the wider transport chain, affecting delivery schedules, transshipment planning, and resource allocation. Therefore, ports should be assessed not only as physical transfer points, but also as operational coordination hubs whose efficiency and resilience are essential for avoiding supply chain disruptions and maintaining the timely movement of goods.

Funded by the European Union
Grant Agreement: 101136257

d) Temporary Port Terminals (TPTs)

Figure 4-2: Example of TPT for the AUTOFLEX Inland Waterway Transport Network in Haarlem, the Netherlands [23].

TPTs represent critical intermediate nodes in the logistics chain, particularly in areas where permanent port infrastructure is unavailable, constrained, or not economically justified. An example of a TPT is shown in Figure 4-2. From a supply chain delay perspective, their importance lies in their role in enabling timely cargo handling, temporary storage, and modal transfer under flexible and often spatially restricted conditions. Because they are deployed in non-permanent or underutilised locations, their operational performance may be more sensitive to infrastructure limitations, restricted accessibility, limited handling capacity, or security and coordination challenges, all of which can affect cargo flow continuity. In this context, any disruption in loading, unloading, transhipment, temporary storage, or terminal access control may result in delays that extend beyond the terminal itself and affect subsequent transport operations. Such delays may lead to increased vessel waiting times, road transport rescheduling, cargo accumulation, and reduced synchronisation between different transport modes. At the same time, while TPTs are intended to relieve congestion at major ports and improve system flexibility, inadequate configuration of their modular functions or insufficient adaptation to local logistical needs may create bottlenecks rather than reduce them. Therefore, TPTs should be assessed not only as flexible logistics solutions, but also as operational nodes whose efficiency, accessibility, and functional adequacy are essential for preventing supply chain disruptions and maintaining the smooth flow of goods across the wider transport network.

e) Stow & Charge hubs (S&C)

Funded by the European Union
Grant Agreement: 101136257

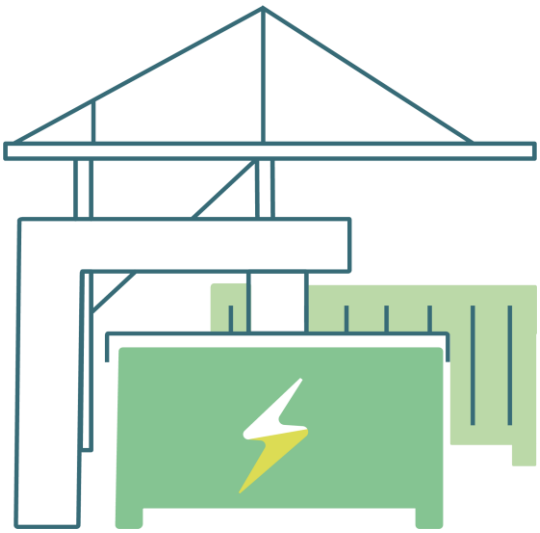

Figure 4-3: Illustration of an S&C Hub for AUTOFLEX Inland Waterway Transport Network [23].

S&C hubs constitute critical operational nodes within the AUTOFLEX logistics chain, as they combine freight transfer functions with the energy replenishment required for the continuous operation of battery-powered vessels [34]. An example of an S&C hub is shown in Figure 4-3 where the S&C hubs concept is illustrated. Their performance is also highly time-sensitive, since any disruption in battery swapping, charging availability, berth access, or cargo handling operations may directly affect vessel turnaround times and, consequently, the reliability of downstream transport and delivery processes. The effectiveness of these hubs depends on the availability of sufficient space for vessel berthing and battery storage, adequate handling equipment for the fast exchange of ZES-packs, and reliable access to high-voltage grid connections and nearby renewable energy sources. If any of these enabling conditions are not met, delays may arise in the swapping process, vessel queuing may increase, and planned sailing schedules may be disrupted. Such delays may propagate further across the network, particularly where vessel operations are tightly coordinated with cargo collection, transshipment, or onward distribution activities. Moreover, because hub placement is determined according to vessel sailing range and energy consumption calculations, any mismatch between hub location and actual operational conditions may create additional delay. Deviations in energy demand, reduced propulsion efficiency, adverse environmental conditions, or limited hub accessibility may reduce the vessel's effective range and increase dependency on intermediate charging or swapping operations. As a result, Stow & Charge hubs should be assessed not only as energy supply points, but also as strategic infrastructure elements whose operational reliability, spatial adequacy, and network positioning are essential for avoiding service interruptions and maintaining supply chain continuity.

f) Mobile Distribution Centres (MDCs)

Funded by the European Union
Grant Agreement: 101136257

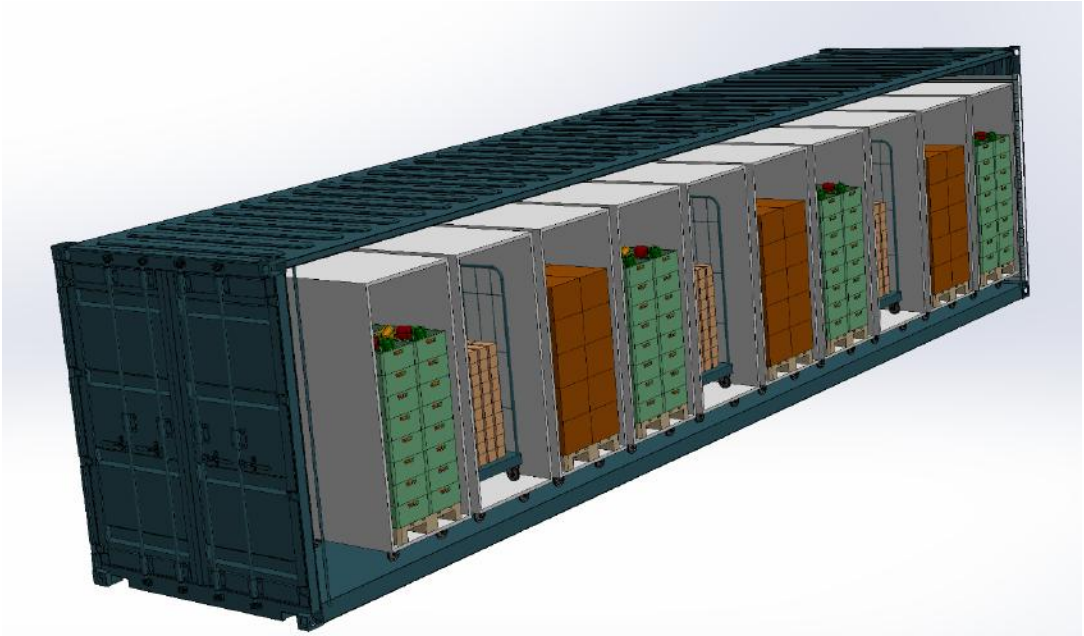

Figure 4-4: Example of an MDC for the AUTOFLEX Inland Waterway Transport Network [20].

MDCs constitute a critical interface between inland waterway transport, temporary storage, and last-mile distribution [23]. An example of an MDC is shown in Figure 4-4. Their operation is particularly time-sensitive, as they are deployed at predefined locations for limited dwell times and are expected to support both cargo pick-up and cargo consolidation activities within strict operational windows. As a result, any disruption affecting the arrival of the vessel, the transshipment of the MDC to shore, the accessibility of the unit, or the timely retrieval of goods by end users may directly translate into delays across subsequent logistics operations. In particular, the reliance of MDCs on fixed collection points and predefined collection deadlines means that delays in vessel schedules, berth availability, loading and unloading operations, or customer pick-up can reduce system efficiency and create knock-on effects for depot return, emptying, re-filling, and redeployment. Similar impacts may arise from handling constraints at the transshipment point, especially in urban, temporary, or spatially restricted environments where forklifts, pallet trucks, or other industrial vehicles may face operational limitations. In addition, MDC performance depends on the reliable functioning of several enabling systems, including energy supply, battery backup, digital access management, automated locks, surveillance systems, and user authentication interfaces. Failures in these systems may not only affect security and cargo integrity but may also temporarily prevent users from accessing their shipments, thereby interrupting the planned flow of goods. For temperature-sensitive cargo, disruptions in power supply or cooling capability may further compromise cargo availability and lead to additional handling, replacement, or rescheduling requirements.

4.1.2. HAZID PROCESS

In addition to the literature review on hazards in inland waterways, particular emphasis was placed on the identification of hazardous events that could disrupt operations and delay the logistics chain in relation to the AUTOFLEX innovations referred to risk evaluation which is

Funded by the European Union
Grant Agreement: 101136257

presented in the next section. Given that these innovations concern novel systems intended for market introduction, it was considered essential to develop a thorough understanding of them from both a structural and an operational perspective. Such an understanding was necessary in order to identify potential hazardous events that may arise during their deployment and operation, as well as to assess their possible implications for operational continuity, navigational safety, and supply chain performance.

To this end, three dedicated online workshops were organized with relevant project partners, building upon a preliminary set of hazardous events that had been identified internally by the NTUA team. The workshops were organised separately in order to allow more focused discussions, obtain more targeted feedback, and improve the overall quality and reliability of the results. During each workshop, the hazardous events and risk-related items already identified were discussed and analysed in real time with the participants. This enabled the NTUA project team to validate the relevance of the identified items, receive feedback on possible additional hazardous events, and identify items that could be considered irrelevant or less applicable to the specific AUTOFLEX context and assist the risk evaluation process.

Figure 4-5: Participants of the online workshop #1 (11/03/2026).

The workshop process also supported the collection of partner feedback regarding the severity and probability values associated with the identified hazardous events. Following the workshops, this feedback was further reviewed and ranked by the project team in order to ensure consistency across the overall risk assessment framework. The three workshops were organised as follows:

- Workshop #1 with ISE on 11/03/2026 as shown in Figure 4-5.
- Workshop #2 with DFDS on 11/03/2026.
- Workshop #3 with DST on 16/03/2026 as illustrated in Figure 4-6.

Funded by the European Union
Grant Agreement: 101136257

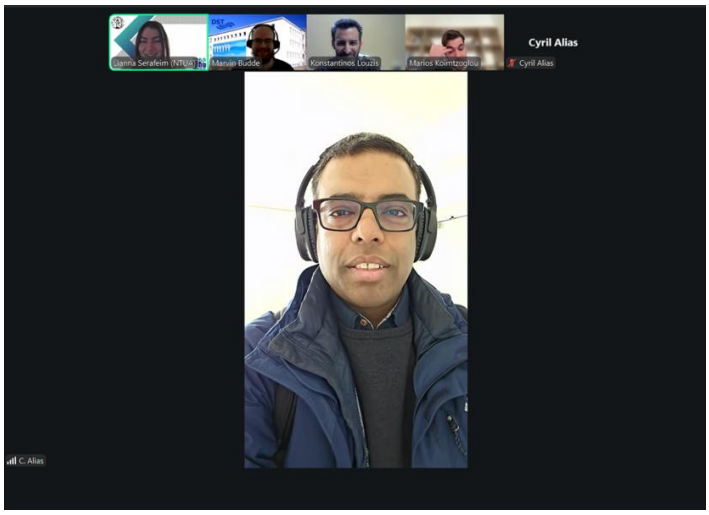

Figure 4-6: Participants of the online workshop #3 (16/03/2026)

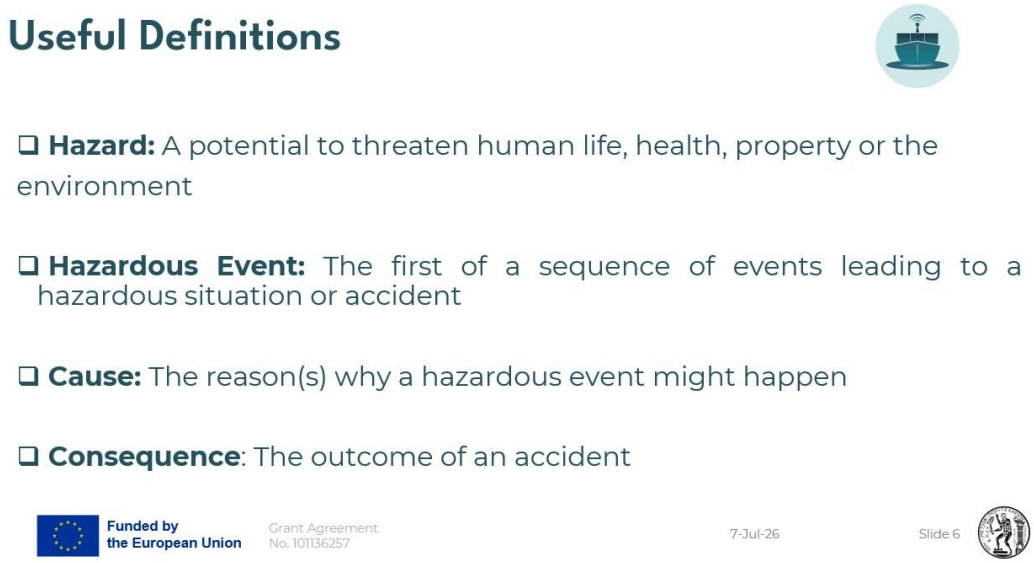

Figure 4-7: Excerpt from the workshop's presentation.

Overall, this iterative process supported a more robust understanding of the AUTOFLEX innovations, not only as standalone technical solutions, but also as integrated operational systems within a broader transport and logistics environment. In this respect, the analysis helped ensure that potential sources of disruption, inefficiency, or operational failure affecting the logistics chain could be identified at an early stage and considered within the overall risk assessment framework. An excerpt from the workshop's presentation is illustrated in Figure 4-7.

The tables in the Appendix present the overall list of the main hazards and hazardous events, classified by each part of AUTOFLEX IWW Transport System and further analysed in terms of their causes and consequences relevant to supply chain delays, as well as the probability and severity of each hazardous event, as derived in the methodology of the previous sections

[35]. The final column is defined as the risk level, calculated as the product of probability and severity.

4.1.3. RISK EVALUATION

Based on the above analysis, Table 4-1 presents the final risk levels, which are used as the weights assigned to the nodes and edges of the graph. The weights per node were calculated by summing all Final Risk Level values associated with the corresponding Hazards (system element) as presented in the Appendix. For example, the Port weight is calculated as the sum of all port-related Final Risk Level values and is equal to 80 (Port weight = 6.5 + 3.5 + 6 + 4 + 9 + 6.5 + 6.5 + 10 + 9 + 7.5 + 7.5 + 4 = 80). The weight of each edge is calculated in the same manner. The risk level of each hazardous event is calculated by averaging the probability and severity assessments provided by all experts. The fact that a node can have a dual role, for example, functioning as both a port or a TPT and a S&C hub at the same time, differentiates the weight of each node because it adds the additional weight of the S&C hub, while all nodes additionally incorporate the weight associated with the MDCs. Table 4-2 and Table 4-4 provides a detailed overview of the role, characteristics (as described detailed in Table 3-2) and corresponding weight of each node, as well as the manner in which these nodes are represented in the graph.

Based on the above, and in line with D3.1 and input provided from T3.4[5] and T3.5[6] , the following Table 4-3 and Table 4-5 present a case study/illustrative scenario of the routes of the AUTOFLEX Transport System and the corresponding five routes. Table 4-2 should be interpreted together with Table 3-2.

Table 4-1: Corresponding Weights for AUTOFLEX IWTS.

Node	Weight
Vessel Route	188
TPT	111
MDC	87
Port	80
S&C	68

Table 4-2: AUTOFLEX Building Blocks Configurations.

Nodes	A. Cargo Handling	F. Public Interface	G. Temporal Availability	H. Operating Model
Leiden	A4	F2	G2	H2
Katwijk	A2	F2	G2	H3
Haarlem	A2	F2	G2	H1
Den Haag	A2	F2	G2	H2
Delft	A2	F2	G2	H1

[5] Transport system architecture re-design
[6] Transport system performance validation

Funded by the European Union
Grant Agreement: 101136257

Eindhoven 1	A2	F1	G1	H2
Eindhoven 2	A1	F2	G1	H1
Breda 1	A2	F3	G1	H2
Breda 2	A2	F3	G1	H1
Roosendaal	A4	F3	G1	H2
's-Hertogenbosch	A1	F1	G2	H2
Amsterdam	A3	F1	G1	H2
Alphen a/d Rijn	A1	F1	G2	H1
Rotterdam	A2	F2	G2	H3
Moerdijk	A2	F1	G2	H2
Utrecht	A2	F1	G2	H3

Table 4-3: AUTOFLEX IWW Routes.

WAC	Route	Places
WAC1	Route 1	Alphen a/d Rijn → Leiden
WAC1	Route 2	Leiden → Katwijk
WAC1	Route 3	Amsterdam → Haarlem → Leiden → Den Haag → Delft → Rotterdam
WAC2	Route 1	Amsterdam → Utrecht → 's-Hertogenbosch → Eindhoven 1 → Eindhoven 2
WAC3	Route 1	Rotterdam → Utrecht
WAC4	Route 1	Rotterdam → Moerdijk
WAC5	Route 1	Eindhoven1 → Eindhoven2 → Moerdijk
WAC5	Route 2	Eindhoven 1 → Eindhoven 2 → Breda 1 → Breda 2 → Roosendaal

Funded by the European Union
Grant Agreement: 101136257

4.2 RISK ASSESSMENT RESULTS - GRAPH THEORY

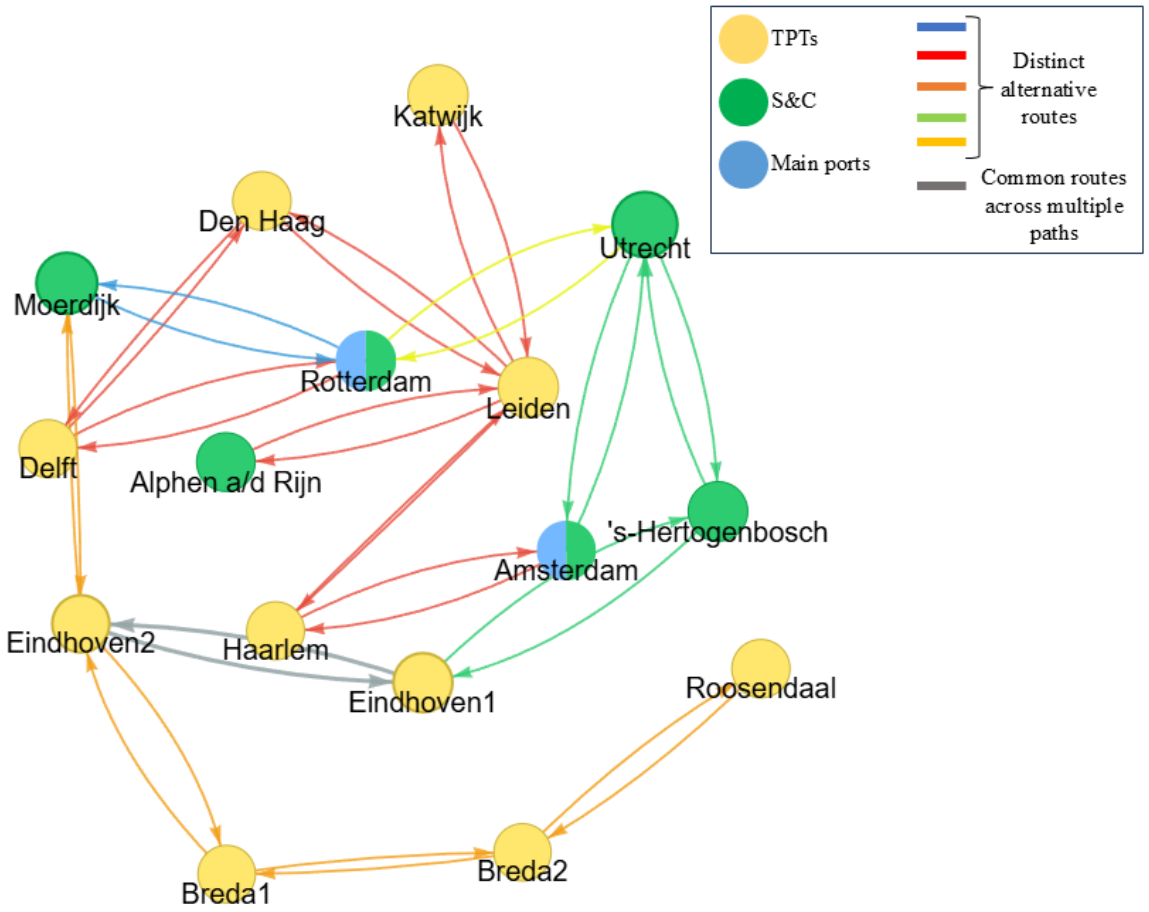

Figure 4-8: Graph Presentation of the latest AUTOFLEX IWW Transport System

Figure 4-8 presents the AUTOFLEX transport system used in this study. The main ports are represented in blue, whereas all other nodes are classified as TPTs and shown in yellow. Locations equipped with S&C hubs are marked in green. All routes are represented as bidirectional. The basic topological representation treats all connections as unweighted reciprocal edges, while the subsequent risk-informed analyses assign route-specific weights to these edges. The five alternative IWW routes are distinguished by different colours, while grey indicates segments common to multiple routes. In total, the network comprises 16 nodes and 34 edges. The roles of the locations within the network, including ports, TPTs, and the presence of S&C hubs, are provided below in Table 4-4, in combination with their normalized weight derived from the equations in Section 3.1.1. Accordingly, Table 4-5 illustrates each edge of the system as a route segment, including its characteristics and the corresponding weight derived from the associated risk level and from the equations in the Section 3.1.2. Regarding the traffic factor, nodes connected to a port are assigned to value “1”, whereas all other nodes are assigned to value “0”. Similarly, routes passing through utilised corridors receive “0”, while those traversing unutilised corridors receive “1”. For the grey-route factor, routes that overlap with common routes are assigned “1”, as illustrated in Figure 4-8. For example, the route Amsterdam → Utrecht is assigned a value of:

Funded by the European Union
Grant Agreement: 101136257

$$RF_{traffic} = 188 \cdot \frac{1+1+0}{3} = 125.3$$

$$RF_{\text{Amsterdam} \rightarrow \text{Utrecht}} = \frac{125.3}{1 \cdot 2} \approx 63$$

Based on these criteria, together with the CEMT classification and route length (km), partly obtained from Deliverables D3.1 and D3.2 [36], the final column of Table 4-5 presents the normalised edge weights.

Table 4-4: Final Weights for the nodes of the AUTOFLEX IWW Transport System

Nodes	Innovation	Weight
Utrecht	TPT, S&C Hub	66
Moerdijk	TPT, S&C Hub	33
Rotterdam	Port, S&C Hub	30
Leiden	TPT	25
Katwijk	TPT	25
's-Hertogenbosch	TPT, S&C Hub	22
Amsterdam	Port, S&C Hub	20
Eindhoven 1	TPT	17
Alphen a/d Rijn	TPT, S&C Hub	15
Den Haag	TPT	12
Roosendaal	TPT	11
Haarlem	TPT	8
Delft	TPT	8
Breda 1	TPT	6
Eindhoven 2	TPT	4
Breda 2	TPT	4

Table 4-5: Final Weights for the edges of the AUTOFLEX IWW Transport System

Routes	Traffic			CEMT	Km	Weight
	Port	Utilised	Grey Route			
Amsterdam → Utrecht	1	1	0	VI	40	63
Rotterdam → Utrecht	1	1	0	VI	63	63
Amsterdam → Haarlem	1	0	0	II	22	42
Delft → Rotterdam	1	0	0	II	16	42
Utrecht → 's-Hertogenbosch	0	1	0	II–VI	71	42
Eindhoven 2 → Moerdijk	0	1	0	V	78	42
Haarlem → Leiden	0	0	0	II	33	31
Rotterdam → Moerdijk	1	1	0	VI	38	31
Alphen a/d Rijn → Leiden	0	0	0	II–III	18	21
Leiden → Katwijk	0	0	0	II	13	21
Leiden → Den Haag	0	0	0	II	18	21

Funded by the European Union
Grant Agreement: 101136257

Den Haag → Delft	0	0	0	II	11	21
's-Hertogenbosch → Eindhoven 1	0	1	0	II–VI	71	21
Eindhoven 2 → Breda 1	0	0	0	IV–VI	61	21
Eindhoven 1 → Eindhoven 2	0	0	1	II–VI	2	14
Breda 2 → Roosendaal	0	0	0	IV–VI	42	10
Breda 1 → Breda 2	0	0	0	IV–VI	3	7

Figure 4-8 reveals a centralized hub-and-spoke configuration that is inherently vulnerable, with Rotterdam's total betweenness centrality of 0.39, underlining its dominant role in cargo flows. It should be noted that the above metrics were derived from the unweighted version of the network, as the purpose of this analysis is to assess the graph from a purely structural perspective, independently of the risk-based weights assigned to nodes and edges. The network also contains weakly connected nodes, as reflected by its low density (0.142), which indicates a sparse topology with limited interconnectivity. A diameter of 9 in a 16-node network further suggests a relatively stretched structure, lacking shortcuts between distant areas. Together with the complete absence of clustering (CC = 0) and an average path length of 3.62, these characteristics describe a network that connects the examined locations through relatively short topological paths, while exhibiting limited local connectivity and redundancy. Overall, the system displays a tree-like architecture in which the majority of paths rely heavily on a small number of central nodes. The Table 4-6 below provides a detailed presentation of the unweighted basic metrics for each node, as analysed in Section 3.2. These metrics offer an overview of the transitivity and connectivity properties of the network nodes. It should be noted that the values of $k^{in}$and k^{out} are equal, as all node connections are bidirectional.

The following tables Table 4-7 to Table 4-12 present the main network analysis results used to identify the most critical nodes and edges within the AUTOFLEX transport network as represented in Section 3.2. First, the unweighted indicators, namely total degree and betweenness centrality, describe the structural importance of each node based only on the network topology. These results show which nodes are more connected and which nodes act as important intermediaries along the shortest paths of the network.

In addition, the weighted indicators incorporate the assigned node weights, allowing the analysis to account not only for the position of each node in the network but also for its risk-related importance. The weighted degree highlights nodes with both high connectivity and high assigned risk weight, while the weighted betweenness centrality identifies nodes that combine a strong intermediary role with increased risk relevance. Finally, the node weight and edge weight rankings provide supporting information on the individual risk contribution of each location and route segment. Overall, these tables help distinguish between nodes that are topologically important and nodes that become critical when risk-related characteristics are also considered.

Table 4-6: AUTOFLEX IWW Transport System Basic Metrics

Node	k^{in}, k^{out}	Degree (k_{total})	CDD	BC
s-Hertogenbosch	2	4	0.8125	0.128571
Alphen a/d Rijn	1	2	1.000	0
Amsterdam	2	4	0.8125	0.171429

Funded by the European Union
Grant Agreement: 101136257

Breda1	2	4	0.8125	0.247619
Breda2	2	4	0.8125	0.133333
Delft	2	4	0.8125	0.257143
Den Haag	2	4	0.8125	0.209524
Eindhoven 1	2	4	0.8125	0.100000
Eindhoven 2	3	6	0.2500	0.371429
Haarlem	2	4	0.8125	0.123810
Katwijk	1	2	1.000	0
Leiden	4	8	0.0625	0.285714
Moerdijk	2	4	0.8125	0.300000
Roosendaal	1	2	1.000	0
Rotterdam	3	6	0.2500	0.395238
Utrecht	3	6	0.2500	0.266667

Table 4-7: Top 10 critical nodes related to degree.

Rank	Node	Degree
1	Leiden	8
2	Utrecht	6
3	Eindhoven 2	6
4	Rotterdam	6
5	Delft	4
6	Eindhoven 1	4
7	Amsterdam	4
8	Breda 1	4
9	Breda 2	4
10	Den Haag	4

Table 4-8: Top 10 critical nodes related to betweenness centrality.

Rank	Node	BC
1	Rotterdam	0.395238
2	Eindhoven 2	0.371429
3	Moerdijk	0.300000
4	Leiden	0.285714
5	Utrecht	0.266667
6	Delft	0.257143

Funded by the European Union
Grant Agreement: 101136257

7	Breda 1	0.247619
8	Den Haag	0.209524
9	Amsterdam	0.171429
10	Breda 2	0.133333

Table 4-9: Top 10 critical nodes related to weighted degree.

Rank	Node	Weighted Degree
1	Utrecht	396.00
2	Leiden	200.00
3	Rotterdam	180.00
4	Moerdijk	132.00
5	's-Hertogenbosch	88.00
6	Amsterdam	80.00
7	Eindhoven 1	68.00
8	Katwijk	50.00
9	Den Haag	48.00
10	Delft	32.00

Table 4-10: Top 10 critical nodes related to weighted betweenness centrality.

Rank	Node	Weighted BC
1	Utrecht	23.885714
2	Leiden	7.619048
3	Amsterdam	6.095238
4	Rotterdam	6.000000
5	's-Hertogenbosch	5.714286
6	Moerdijk	4.714286
7	Eindhoven 1	4.695238
8	Haarlem	2.057143
9	Eindhoven 2	1.561905
10	Breda1	1.485714

Table 4-11: Top 10 critical nodes related to their weight.

Rank	Node	Weight
1	Utrecht	66.00
2	Moerdijk	33.00
3	Rotterdam	30.00
4	Leiden	25.00
5	Katwijk	25.00

Funded by the European Union
Grant Agreement: 101136257

6	's-Hertogenbosch	22.00
7	Amsterdam	20.00
8	Eindhoven 1	17.00
9	Alphen a/d Rijn	15.00
10	Den Haag	12.00

Table 4-12: Top 10 critical edges related to their weight.

Rank	Node	Weight
1	Utrecht → Rotterdam	63.00
2	Rotterdam → Utrecht	63.00
3	Amsterdam → Haarlem	42.00
4	Haarlem → Amsterdam	42.00
5	Delft → Rotterdam	42.00
6	Rotterdam → Delft	42.00
7	's-Hertogenbosch → Utrecht	42.00
8	Utrecht → 's-Hertogenbosch	42.00
9	Eindhoven2 →Moerdijk	42.00
10	Moerdijk → Eindhoven 2	42.00

4.3 RISK ASSESSMENT RESULTS - PERCOLATION THEORY

This study examined five scenarios of network-element removal.

1. In the first scenario, 30 repetitions of random node removal were performed, with each node having the same probability of being removed, to examine the range of p_c values under untargeted failures. The mean p_c value obtained across these repetitions is presented as random removal result [37].

The remaining scenarios considered targeted removals in descending order one by one from the most critical to the least critical, based on:

2. Node importance measured through weight.
3. Edge importance measured through weight.
4. Weighted degree.
5. Weighted betweenness centrality.

This approach makes it possible to assess network fragmentation not only from a topological perspective but also in relation to weighted attributes, where the assigned weights correspond to risk levels and reflect the structural and functional vulnerability of the network. The corresponding results are discussed in the next subsections.

Funded by the European Union
Grant Agreement: 101136257

4.3.1. SCENARIO 1: RANDOM REMOVAL SCENARIO

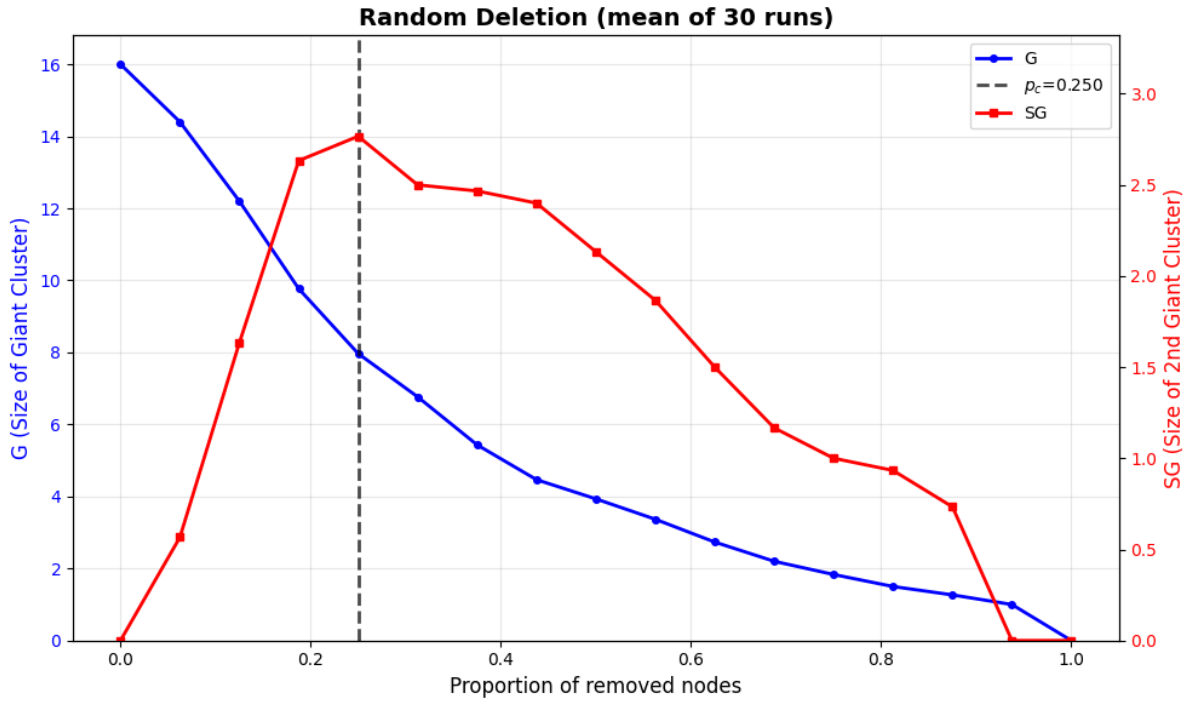

Figure 4-9: The percolation process under Random scenario.

As illustrated in Figure 4-9, the random removal scenario results in a percolation threshold of $p_c = 0.250$, showing that the network remains relatively largely connected even after the random removal of nearly 25% of its nodes. The progressive decrease of the G, along with the gradual rise of the SG, indicates a relatively resilient response to non-targeted and unforeseen failures. The blue curve represents the size of the largest connected component, G, with its values shown on the left vertical axis. It progressively decreases from 16 to zero as an increasing percentage of nodes is removed, indicating the gradual deterioration of the giant connected system of the network. The red curve represents the size of the second-largest connected component, SG, with its values shown on the right vertical axis. It initially increases as groups of nodes are detached from the largest component and reaches a maximum at a removal fraction of 0. 250.The grey dashed line identifies this point as the filtration threshold, which corresponds to the random removal of 4 from the original 16 nodes specifically Amsterdam, Roosendaal, Katwijk and Den Haag. The following diagrams (

Funded by the European Union
Grant Agreement: 101136257

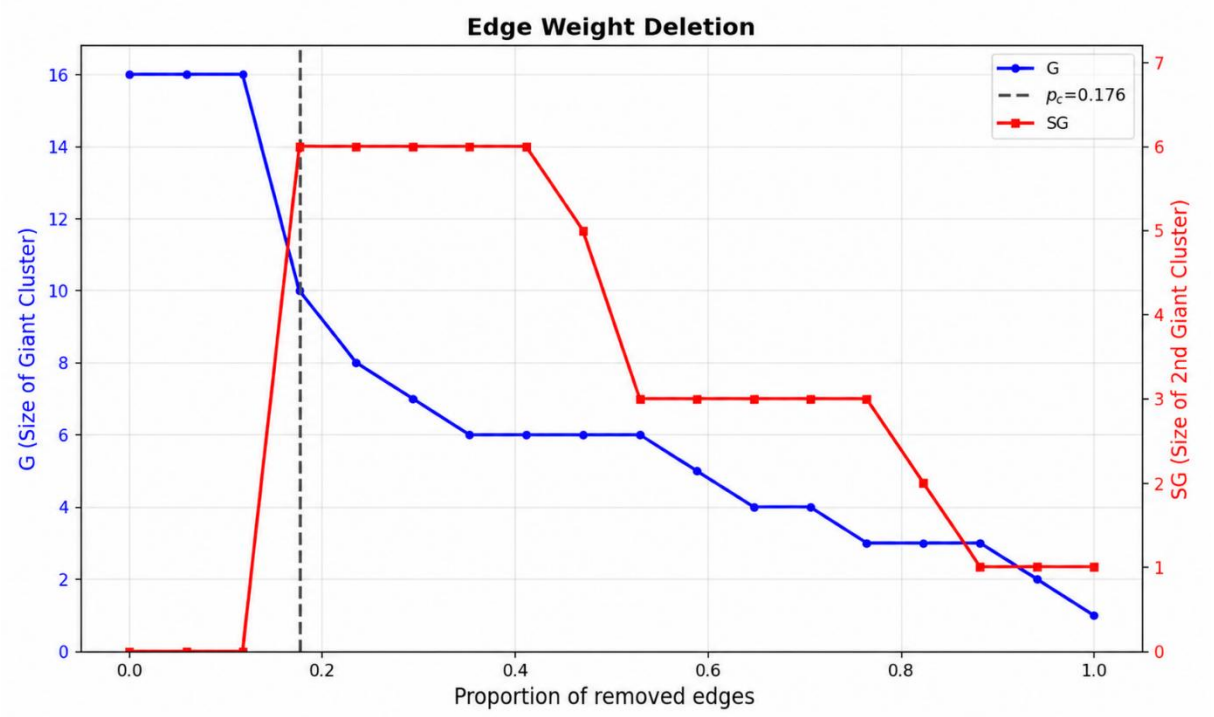

Figure 4-10 to Figure 4-13) in the remaining scenarios are interpreted with the same logic. These findings suggest that random failures are not immediately catastrophic, since the network can tolerate a moderate level of damage before losing its overall cohesion [38]. As the mean curves cannot be associated with a unique set or sequence of removed nodes, the removal of Amsterdam, Roosendaal, Katwijk, and Den Haag refers only to an illustrative representative run near to the mean of p_c.

Funded by the European Union
Grant Agreement: 101136257

4.3.2. SCENARIO 2: EDGE WEIGHT REMOVAL SCENARIO

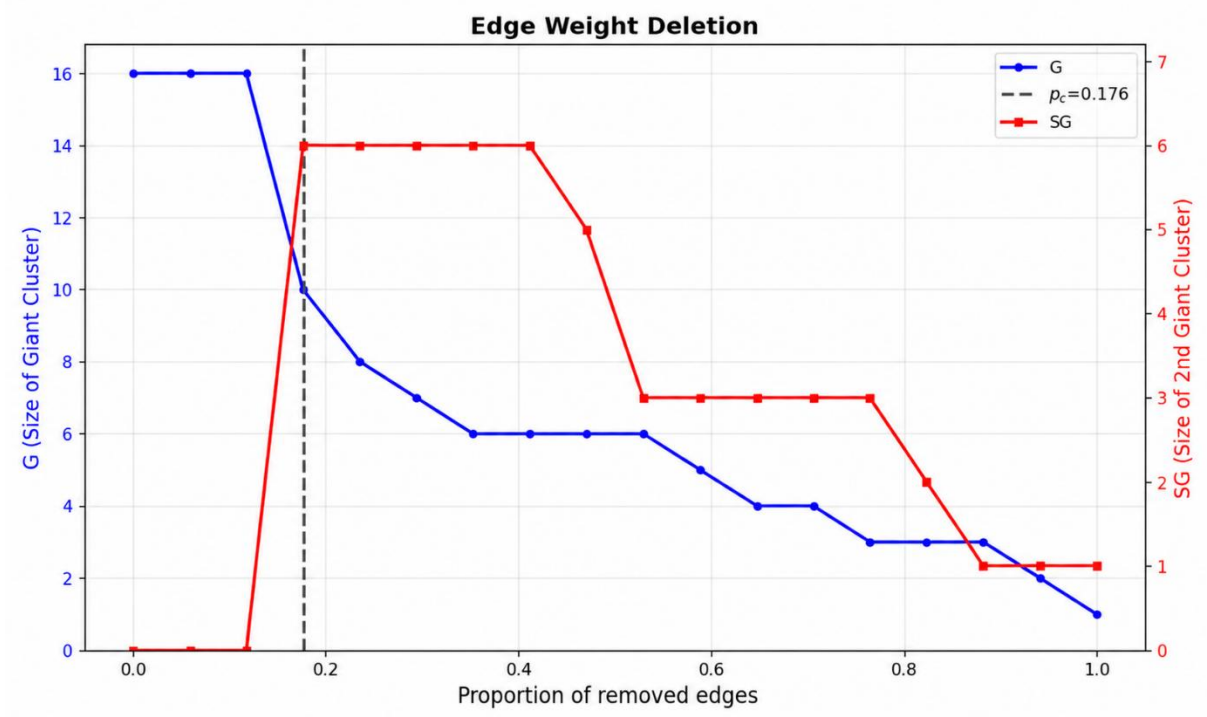

Figure 4-10: The percolation process under Edge Weight scenario.

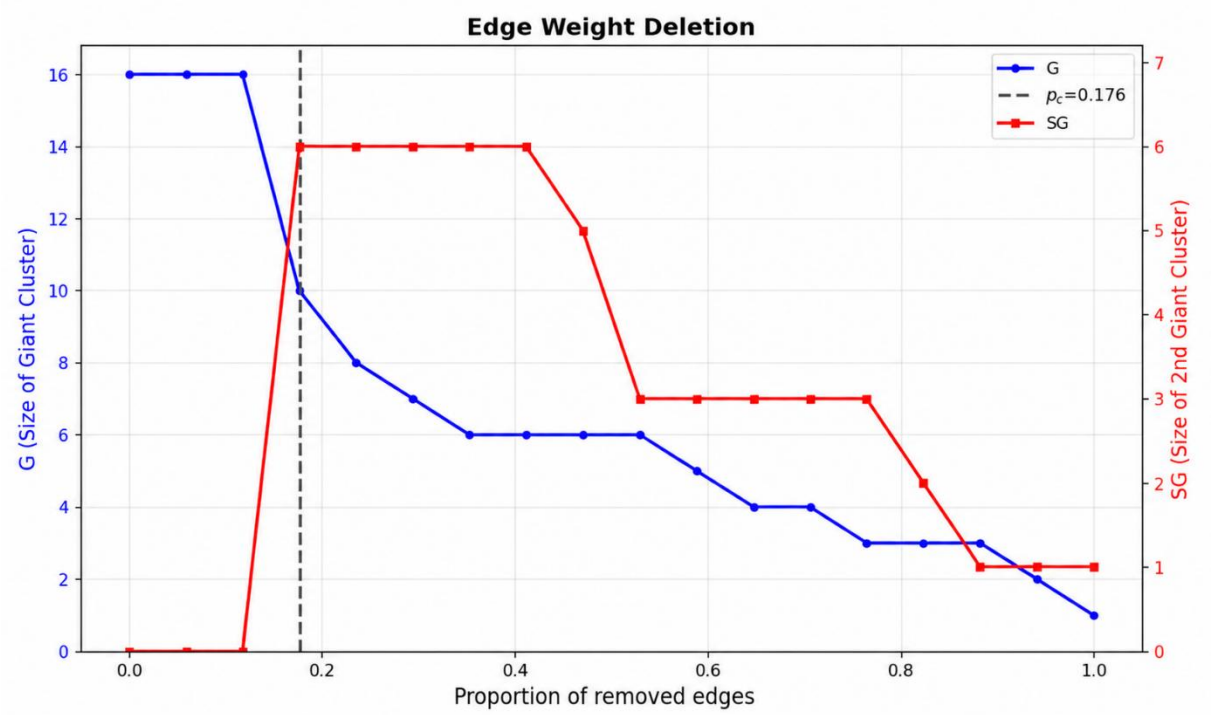

Figure 4-10 illustrates the results of the edge weight-based removal strategy, with a percolation threshold of $p_c = 0.176$. The percolation threshold corresponds to the first removal fraction, q, at which the second-largest connected component, SG, reaches its maximum value, indicating the progressive fragmentation of the network into smaller connected components. Accordingly, the percolation threshold is taken as $p_c = 0.176$ rather

Funded by the European Union
Grant Agreement: 101136257

than 0.41. This indicates that the AUTOFLEX IWTS network remains functional until approximately 17.6% of its edges, corresponding to 6 out of 34 directed edges, are removed, after which fragmentation occurs abruptly. Since the removed edges are those with the highest weights, the results suggest that the network can initially absorb the disruption of a limited number of vulnerable or risk-critical route segments through alternative connections. This reflects a certain degree of structural redundancy, as highly important edges can, to some extent, be substituted by alternative paths. However, once the threshold is exceeded, the compromise of a relatively small subset of high-risk vessel routes may generate wider system-level consequences. Therefore, although rerouting can temporarily preserve connectivity, it is likely to increase cargo-flow delays and place additional pressure on the remaining parts of the inland waterway transport network.

4.3.3. SCENARIO 3: WEIGHTED DEGREE REMOVAL SCENARIO

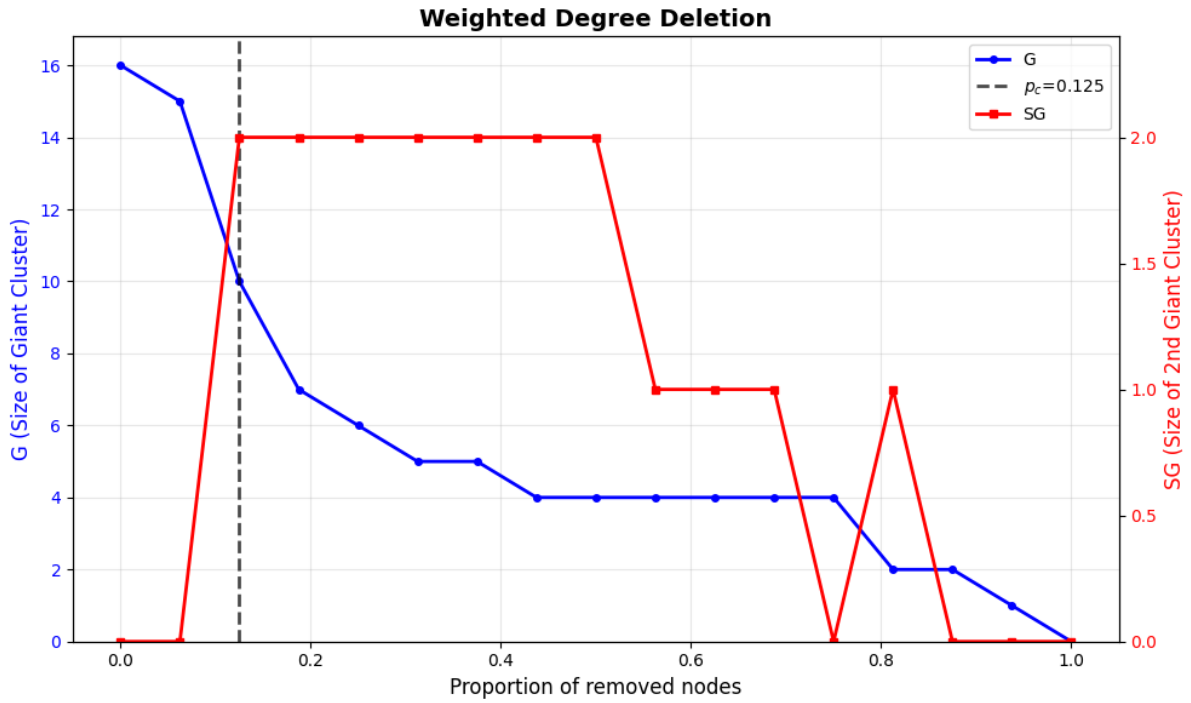

Figure 4-11: The percolation process under Weighted Degree Scenario.

As presented in Figure 4-11, the weighted degree strategy results in a low percolation threshold of $p_c = 0.125$. The percolation threshold is identified as the first removal fraction, q, at which the second-largest connected component, SG, reaches its peak, marking the point where the network begins to fragment into smaller connected components. Accordingly, the percolation threshold is taken as $p_c = 0.125$ rather than 0.5. This indicates that the removal of only 2 nodes, specifically first Utrecht and then Leiden, is sufficient to push the system beyond its critical fragmentation point. The abrupt decline of the G, together with the sharp rise of the SG around the threshold, reveals a rapid loss of network cohesion and highlights the system's strong dependence on nodes that combine high connectivity with high-risk weights. This fact contrasts with the intuitive expectation that Leiden would appear first, as shown in the pure topological analysis (Table 4-7). This result highlights that node importance

Funded by the European Union
Grant Agreement: 101136257

cannot be inferred solely from conventional topological prominence but must also incorporate the node-specific risk profile.

4.3.4. SCENARIO 4: WEIGHTED BETWEENNESS CENTRALITY REMOVAL SCENARIO

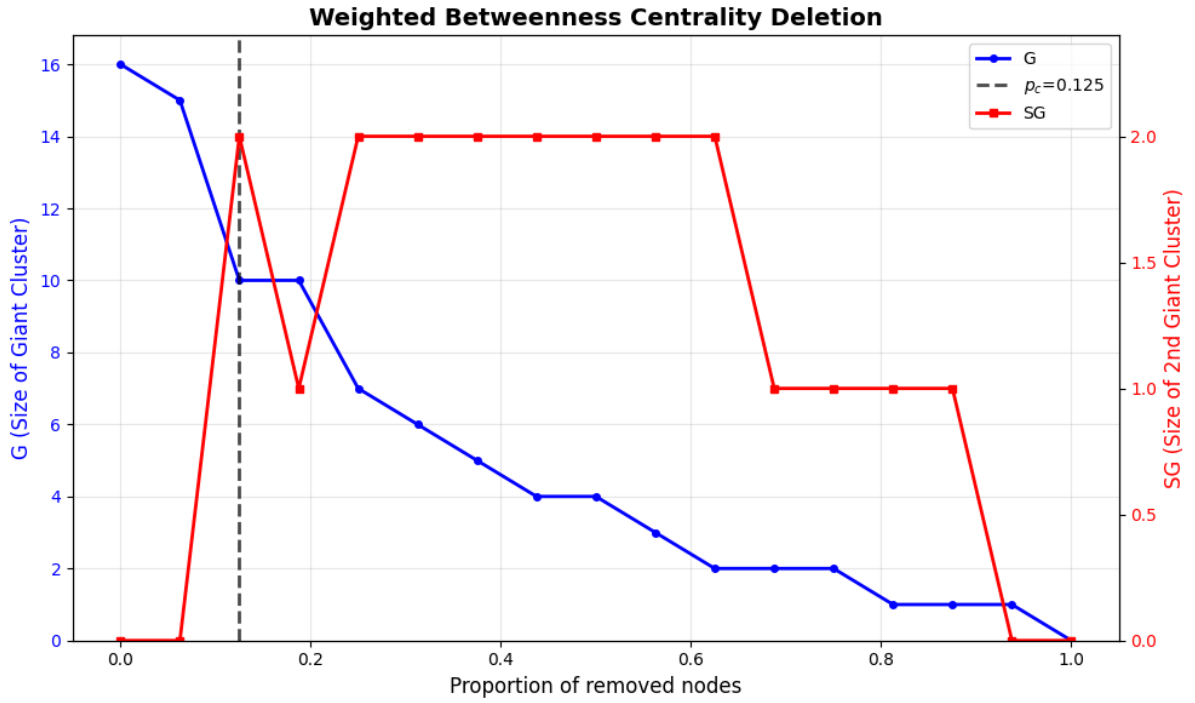

Figure 4-12: The percolation process under Betweenness Centrality Scenario.

A similarly low threshold is observed in the weighted-betweenness-centrality scenario, shown in Figure 4-12. Here, the percolation threshold is $p_c = 0.125$, indicating that the removal of only 2 nodes is enough to disconnect the network. The corresponding node removal order is Utrecht first, followed by Leiden. This means that, under the weighted betweenness centrality criterion, the network collapses after removing these two nodes in sequence. Therefore, the removal sequence confirms that the network's vulnerability is concentrated around a limited number of strategically important and risk-relevant nodes. This confirms the network's strong reliance on a small set of nodes that act both as major flow mediators and as high-risk elements.

Funded by the European Union
Grant Agreement: 101136257

4.3.5. SCENARIO 5: NODE WEIGHT REMOVAL SCENARIO

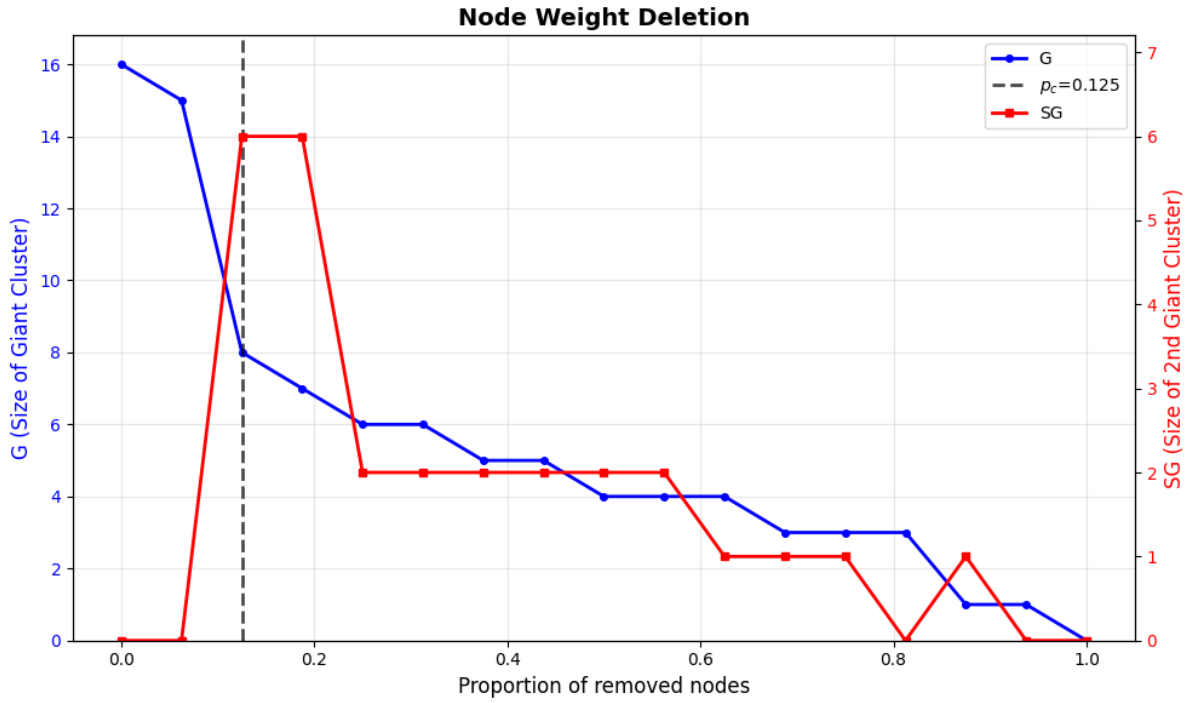

Figure 4-13: The percolation process under Node Weight Scenario.

The last outcome, which is the same as the weighted degree deletion scenario, is observed in the node weight removal scenario, depicted in Figure 4-13, where network collapse occurs at $p_c = 0.125$. This result implies that removing only 12.5% of the highest weight nodes, corresponding to 2 nodes (first Utrecht and then Moerdijk), is enough to trigger immediate network disconnection. The finding demonstrates that when node importance is assessed exclusively based on risk level, the most highly weighted nodes emerge as the most critical elements in the system. Consequently, these nodes should be treated as top-priority targets for protection, monitoring, and mitigation planning. The fact that the weighted degree and node weight strategies produce the same threshold suggests that nodes with many connections also tend to operate as critical bottlenecks for cargo flows. However, the fragmentation patterns differ between the two strategies. In this case, the node removal order is Utrecht → Moerdijk, underlining once more that a purely topological interpretation is insufficient, unless combined with node risk levels.

4.4 IMPACT ANALYSIS

Table 4-13 below illustrates the structural consequences of removing Utrecht, which was identified as the most critical node in the AUTOFLEX network based on the node weighted betweenness centrality deletion scenario. This indicator, calculated as the product of betweenness centrality and node weight (NW), captures both the topological brokerage role of a node and its risk-related or functional importance within the network. In this context, Utrecht represents a key intermediary through which a substantial share of shortest-path connections and weighted network responsibility is concentrated. To evaluate its structural

Funded by the European Union
Grant Agreement: 101136257

and functional significance, Utrecht was removed from the network, and the resulting changes in betweenness centrality were recalculated for all remaining nodes.

Table 4-13: Impact Analysis of Utrecht Removal on Betweenness Centrality

Node	NW	NW × BC Before	NW × BC After	Δ (NW × BC)	Rate % NW × BC
Moerdijk	33	4.714	17.407	12.692	269.2
Rotterdam	30	6.000	16.154	10.154	169.2
Den Haag	12	1.143	5.934	4.791	419.2
Leiden	25	7.619	12.363	4.744	62.3
Delft	8	0.990	4.220	3.229	326.0
Eindhoven 2	4	1.562	2.242	0.680	43.5
Breda 1	6	1.486	1.582	0.097	6.5
Breda 2	4	0.533	0.571	0.038	7.1
Roosendaal	11	0.000	0.000	0.000	0.0
Katwijk	25	0.000	0.000	0.000	0.0
Alphen a/d Rijn	15	0.000	0.000	0.000	0.0
Haarlem	8	2.057	1.143	-0.914	-44.4
Eindhoven 1	17	4.695	2.429	-2.267	-48.3
's-Hertogenbosch	20	5.714	0.000	-5.714	-100.0
Amsterdam	20	6.095	0.000	-6.095	-100.0

The results indicate and confirm that Utrecht acts as a primary critical hub within the AUTOFLEX network. Its removal leads to a substantial redistribution of betweenness centrality across the remaining system, indicating that alternative nodes are forced to absorb part of the connectivity function previously associated with Utrecht [39]. However, this redistribution is not even across the network. The additional structural burden is concentrated on a limited number of nodes, mainly Moerdijk, Rotterdam, Den Haag, Leiden, Delft, and Eindhoven 2.

Moerdijk records the highest absolute increase in node-weighted betweenness centrality after the removal of Utrecht. Its betweenness centrality increases from 0.14285 to 0.52748, corresponding to an increase of 0.38463, or approximately 269.2%. Den Haag also experiences a very significant increase. Its betweenness centrality rises from 0.09525 before the removal of Utrecht to 0.49450 after the removal, corresponding to an increase of 0.39925, or approximately 419.2%. This indicates that Den Haag becomes one of the main alternative intermediary nodes in the disrupted network and absorbs a significant share of the rerouted connectivity.

A similarly important increase is observed for Rotterdam. This shows that Rotterdam becomes a critical inland intermediary after the loss of Utrecht, supporting the redistribution of network flows towards alternative inland routes.

Funded by the European Union
Grant Agreement: 101136257

Delft also becomes considerably more important in the disrupted configuration. Its betweenness centrality increases from 0.12375 to 0.52750, while its node-weighted betweenness rises from 0.990 to 4.220. The result suggests that Delft becomes part of the alternative routing structure that helps maintain connectivity after Utrecht is removed.

Leiden already had a relatively high centrality value before the disruption and continues to play an important role afterwards. Although its relative increase is lower compared with nodes such as Den Haag, Delft, or Moerdijk, Leiden still records one of the highest post-removal node-weighted betweenness values among the remaining nodes. This indicates that Leiden remains a highly critical node in the disrupted network due to the combination of its structural role and relatively high node weight.

Eindhoven 2 also shows a notable increase. Although Eindhoven 2's absolute node-weighted impact remains lower than that of Moerdijk, Rotterdam, Den Haag, Leiden, and Delft, the relative increase suggests that it becomes more important as an intermediary node in the disrupted network.

The results also show that some nodes experience only minor changes after Utrecht's removal. Eindhoven 2, Breda 1, and Breda 2 show limited increases in both betweenness centrality and node-weighted betweenness. These small changes suggest that, although these nodes remain connected to the network, they do not absorb a major share of the redistributed shortest-path flows under this disruption scenario.

Katwijk, Roosendaal, and Alphen a/d Rijn remain at zero node-weighted betweenness both before and after the removal of Utrecht. This indicates that these nodes do not function as intermediary nodes in the shortest-path structure of the network under either configuration. Their role may still be locally relevant, but they do not contribute significantly to network-wide shortest-path connectivity in this specific analysis.

In contrast, Haarlem, Eindhoven 1, 's-Hertogenbosch, and Amsterdam experience a decrease in betweenness centrality after the removal of Utrecht. Haarlem's node-weighted betweenness decreases from 2.057 to 1.143 while Eindhoven 1 decreases from 4.695 to 2.429, 's-Hertogenbosch and Amsterdam both fall to zero node-weighted betweenness, with 's-Hertogenbosch decreasing from 5.714 to 0.000 and Amsterdam decreasing from 6.095 to 0.000. This suggests that Utrecht's removal does not increase the importance of all surrounding or connected nodes. Instead, it redirects the main intermediary function towards specific alternative corridors while reducing the role of others.

Overall, the analysis demonstrates that the removal of Utrecht produces a concentrated redistribution of network criticality rather than a balanced redistribution across the whole system. The strongest absolute increase in node-weighted betweenness is observed for Moerdijk, followed by Rotterdam, Den Haag, Leiden, Delft, and Eindhoven 2. These nodes become the main secondary intermediaries in the disrupted configuration and should therefore be considered priority locations for resilience planning, redundancy enhancement, and contingency routing.

From a mitigation perspective, the results suggest that resilience measures should not focus only on protecting Utrecht itself. They should also strengthen the nodes that become critical after Utrecht's removal. In particular, Moerdijk, Rotterdam, Den Haag, Leiden, Delft, and Eindhoven 2 should be examined as priority locations for additional operational capacity, backup routing options, and infrastructure reinforcement. This would reduce the risk of

Funded by the European Union
Grant Agreement: 101136257

transferring excessive pressure from Utrecht to a small number of secondary bottlenecks and support a more balanced and resilient inland waterway transport network. The effects of removing the second- or third-ranked node, or of removing three nodes simultaneously, are not expected to follow the same pattern observed for the removal of Utrecht. This is because betweenness centrality is topology-dependent and is recalculated after each structural change in the network. Consequently, the impact of node removal depends on the specific position and connectivity of the removed node or nodes. For example, removing Leiden disrupts a different set of connections and may isolate specific parts of the network. By contrast, the removal of Amsterdam alone does not cause fragmentation, since all 15 remaining nodes can still be connected through alternative paths.

4.5 RISK MITIGATION RESULTS

This section presents the risk mitigation results for the inland waterway transport system, focusing on improving network resilience and reducing risk exposure across the examined IWW transport network. Based on the outcomes of the risk assessment and network analysis, different mitigation measure strategies were developed and evaluated in order to identify how the system's resilience robustness can be enhanced under different disruptive scenarios.

The mitigation analysis is structured around three main scenarios:

1. The first scenario focuses on improving the overall cohesion of the graph, aiming to strengthen connectivity and reduce the vulnerability of weakly connected nodes of the network.
2. The second scenario aims to minimize the risk level by prioritising interventions at nodes and edges with higher risk contribution.
3. Finally, the third scenario combines both perspectives, considering network connectivity and risk reduction at the same time. In this way, the proposed mitigation results support the identification of more effective strategies for improving the safety, reliability, and resilience of inland waterway transport operations.

4.5.1. REVISED GRAPH

Figure 4-14 illustrates an alternative configuration of the AUTOFLEX inland waterway transport system, with 30 nodes and 68 directed edges, corresponding to 34 bidirectional route segments. This enhanced version of the network includes additional routes and a larger number of nodes, with the aim of strengthening the existing system and improving its overall connectivity. The purpose of this extended network representation is to examine whether the system becomes less vulnerable to fragmentation under specific node or edge removal scenarios, following the same methodological approach applied in Sections 4.2 and 4.3. By introducing additional connections and alternative pathways, this configuration allows the assessment of how increased redundancy may affect the resilience of the AUTOFLEX network. In particular, the analysis investigates whether the expanded network is able to maintain a higher level of connectivity when critical nodes or route segments are disrupted.

Funded by the European Union
Grant Agreement: 101136257

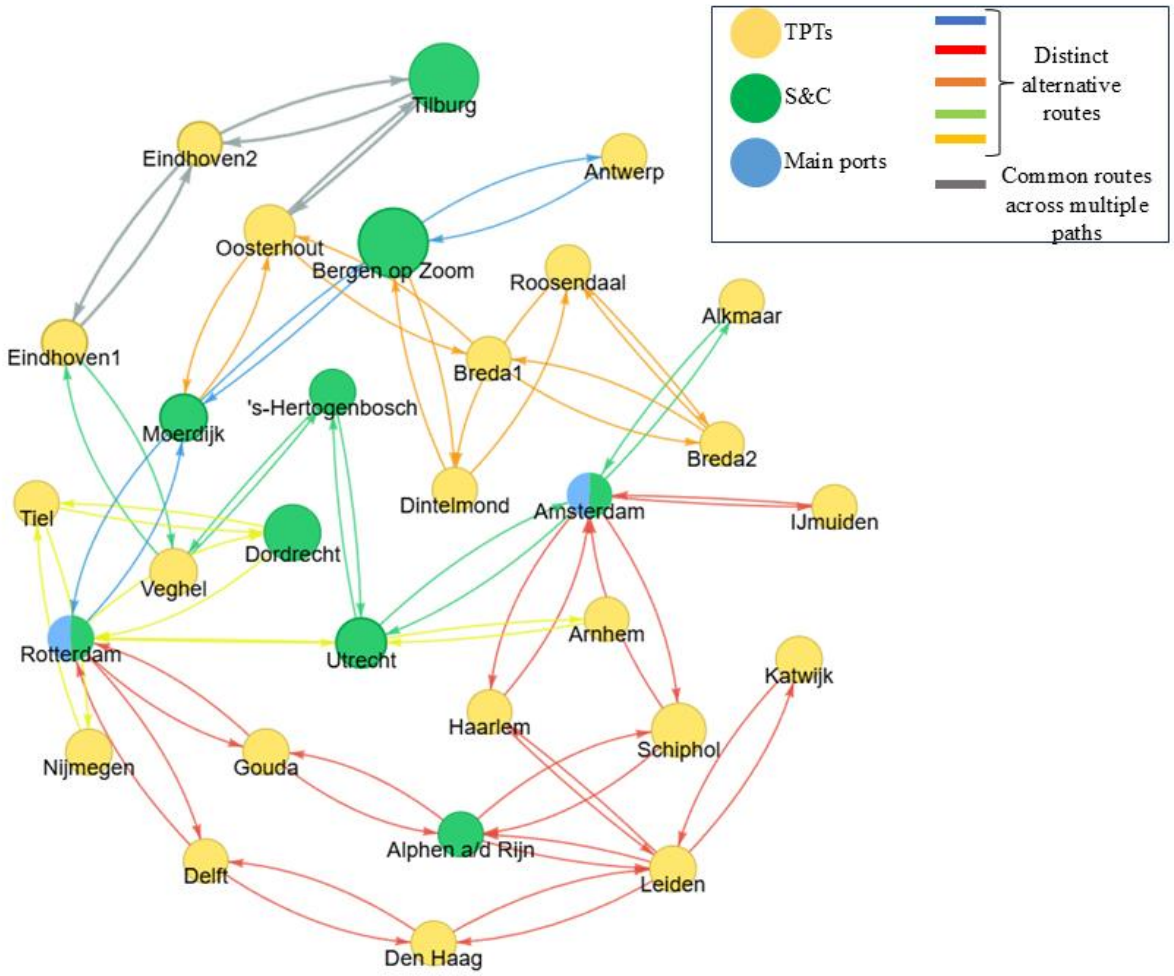

Figure 4-14: Graph Presentation of a revised AUTOFLEX IWW Transport System

The revised, more cohesive network configuration is presented as an illustrative topology-augmentation scenario. It preserves the nodes, edges, weights, and routes of the network analysed in Section 4.2, while adding additional nodes, connections, attributes, and assigned weights. This augmented configuration is not derived entirely from the outputs of Tasks 3.4 and 3.5. Where the relevant network characteristics had not yet been fully defined within those tasks, additional elements were introduced on the basis of the project-specific information available at this stage of AUTOFLEX and representative configurations consistent with the planned transport concepts, in order to explore how increased network cohesion and route redundancy could affect system resilience. Therefore, it should be interpreted as an exploratory scenario rather than a fully validated network configuration. The newly introduced elements are documented in Table 4-14 - Table 4-17. Table 4-14 should be interpreted together with Table 3-2.

Table 4-14: AUTOFLEX Building Blocks Configurations in revised graph.

TPTs	A. Cargo Handling	F. Public Interface	G. Temporal Availability	H. Operating Model
Leiden	A4	F2	G2	H2

Funded by the European Union
Grant Agreement: 101136257

Katwijk	A2	F2	G2	H3
Haarlem	A2	F2	G2	H1
Den Haag	A2	F2	G2	H2
Delft	A2	F2	G2	H1
Eindhoven 1	A2	F1	G1	H2
Eindhoven 2	A1	F2	G1	H1
Breda 1	A2	F3	G1	H2
Breda 2	A2	F3	G1	H1
Roosendaal	A4	F3	G1	H2
's-Hertogenbosch	A1	F1	G2	H2
Amsterdam	A3	F1	G1	H2
Alphen a/d Rijn	A1	F1	G2	H1
Rotterdam	A2	F2	G2	H3
Moerdijk	A2	F1	G2	H2
Utrecht	A2	F1	G2	H3
Bergen op Zoom	A4	F1	G3	H3
Tilburg	A4	F1	G3	H3
Dordrecht	A4	F2	G3	H3
Alkmaar	A1	F1	G1	H1
IJmuiden	A2	F2	G2	H2
Veghel	A3	F3	G3	H3
Gouda	A4	F1	G3	H3
Arnhem	A1	F2	G2	H2
Tiel	A3	F1	G1	H1
Nijmegen	A4	F2	G2	H2
Schiphol	A2	F1	G3	H3
Antwerp	A3	F2	G2	H2
Oosterhout	A4	F1	G1	H3
Dintelmond	A2	F2	G2	H2

Table 4-15: Final Weights for the nodes of the AUTOFLEX IWTS in revised graph

Node	Innovation	Weight
Leiden	TPT	25
Katwijk	TPT	25
Haarlem	TPT	8
Den Haag	TPT	12
Delft	TPT	8
Eindhoven 1	TPT	17
Eindhoven 2	TPT	4
Breda 1	TPT	6
Breda 2	TPT	4
Roosendaal	TPT	11
's-Hertogenbosch	TPT, S&C Hub	22
Amsterdam	Port, S&C Hub	20
Alphen a/d Rijn	TPT, S&C Hub	15

Funded by the European Union
Grant Agreement: 101136257

Rotterdam	Port, S&C Hub	30
Moerdijk	TPT, S&C Hub	33
Utrecht	TPT, S&C Hub	66
Bergen op Zoom	TPT, S&C Hub	266
Tilburg	TPT, S&C Hub	266
Dordrecht	TPT, S&C Hub	133
Alkmaar	TPT	7
IJmuiden	TPT	12
Veghel	TPT	33
Gouda	TPT	198
Arnhem	TPT	8
Tiel	TPT	11
Nijmegen	TPT	25
Schiphol	TPT	99
Antwerp	TPT	12
Oosterhout	TPT	66
Dintelmond	TPT	12

Table 4-16: AUTOFLEX IWW Routes in revised graph.

WAC	Route	Places
WAC1	Route 1	IJmuiden → Amsterdam → Schiphol → Alphen a/d Rijn → Gouda → Rotterdam
WAC1	Route 2	Alphen a/d Rijn → Leiden
WAC1	Route 3	Leiden → Katwijk
WAC1	Route 4	Amsterdam → Haarlem → Leiden → Den Haag → Delft → Rotterdam
WAC2	Route 1	Alkmaar → Amsterdam → Utrecht → 's-Hertogenbosch → Veghel → Eindhoven 1→ Eindhoven 2
WAC3	Route 1	Rotterdam → Utrecht → Arnhem
WAC3	Route 2	Rotterdam → Dordrecht → Tiel → Nijmegen
WAC4	Route 1	Rotterdam → Moerdijk → Bergen op Zoom → Antwerp
WAC5	Route 1	Eindhoven1→ Eindhoven2→ Tilburg → Oosterhout → Moerdijk
WAC5	Route 2	Eindhoven 1→ Eindhoven 2→ Tilburg → Oosterhout → Breda 1 → Breda 2 → Roosendaal → Dintelmond → Bergen op Zoom

Table 4-17: Final Weights for the edges of the AUTOFLEX IWTS in revised graph.

Routes	Traffic			CEMT	Km	Weight
	Port	Utilised	Grey Route			
IJmuiden -> Amsterdam	1	1	0	VI	23	21

Funded by the European Union
Grant Agreement: 101136257

Amsterdam -> Schiphol	1	0	0	III-V	14	21
Schiphol -> Alphen a/d Rijn	0	0	0	III-V	30	16
Alphen a/d Rijn -> Gouda	0	1	0	III-V	19	21
Gouda -> Rotterdam	1	1	0	III-V	26	47
Alphen a/d Rijn -> Leiden	0	0	0	II–III	18	21
Leiden -> Katwijk	0	0	0	II	13	21
Amsterdam -> Haarlem	1	0	0	II	22	42
Haarlem -> Leiden	0	0	0	II	33	31
Leiden -> Den Haag	0	0	0	II	18	21
Den Haag -> Delft	0	0	0	II	11	21
Delft -> Rotterdam	1	0	0	II	16	42
Alkmaar -> Amsterdam	1	0	0	IV–V	39	21
Amsterdam -> Utrecht	1	1	0	VI	40	63
Utrecht -> 's-Hertogenbosch	0	1	0	II–VI	71	42
s-Hertogenbosch -> Veghel	0	1	0	II–VI	20	14
Veghel -> Eindhoven1	0	0	0	II	39	31
Eindhoven 1 -> Eindhoven 2	0	0	1	II-VI	2	14
Rotterdam -> Utrecht	1	1	0	VI	63	63
Utrecht -> Arnhem	0	1	0	VI	71	42
Rotterdam -> Dordrecht	1	1	0	VI	21	21
Dordrecht -> Tiel	0	1	0	VI	61	42
Tiel -> Nijmegen	0	1	0	VI	31	21
Rotterdam -> Moerdijk	1	1	0	VI	38	31
Moerdijk -> Bergen op Zoom	0	1	0	VI	55	42
Bergen op Zoom -> Antwerp	0	1	0	VI	33	21
Eindhoven2-> Tilburg	0	0	1	II	33	63
Tilburg -> Oosterhout	0	1	1	IV	24	21
Oosterhout -> Moerdijk	0	1	0	V	26	14
Oosterhout -> Breda1	0	1	0	IV–VI	11	14
Breda1 -> Breda2	0	0	0	IV-VI	3	7
Breda2 -> Roosendaal	0	0	0	IV–VI	42	10
Roosendaal -> Dintelmond	0	1	0	IV–VI	14	14
Dintelmond -> Bergen op Zoom	0	1	0	IV–VI	34	21

Figure 4-14 reveals a sparse and highly centralised network configuration, in which a limited number of nodes perform a dominant intermediary role. Rotterdam records the highest unweighted betweenness centrality value, equal to 0.584975, confirming once again its dominant role in maintaining network connectivity and supporting freight flows throughout the AUTOFLEX transport system. Other nodes with high betweenness centrality include Moerdijk, Utrecht, Amsterdam, Oosterhout, Bergen op Zoom, Dordrecht, 's-Hertogenbosch, Leiden, and Gouda. This indicates that, although Rotterdam remains the most critical node, the updated network also includes a set of secondary intermediary nodes that contribute significantly to route continuity, similarly to the previous network configuration.

The topological metrics were calculated using the unweighted version of the network too. This allows the structural characteristics of the system to be examined independently of the risk-based weights assigned to nodes and edges.

Funded by the European Union
Grant Agreement: 101136257

The updated network remains structurally sparse, as reflected by its low-density value of 0.078. This indicates that only a small number of all possible connections between nodes actually exists in the network. The network diameter is equal to 8, meaning that the longest shortest path between any two nodes requires eight steps. The average path length is 3.95, indicating that, despite the sparse structure, most nodes remain reachable through a moderate number of intermediate edges. However, the complete absence of clustering, with an average clustering coefficient of 0, once again shows that the network does not contain triangular or locally redundant structures which also occurs in the original graph. This means that neighbouring nodes are generally not interconnected with each other, limiting the availability of alternative local routes.

Overall, the revised AUTOFLEX network displays a corridor-based and hub-oriented structure. It connects a wide set of inland and port locations through a limited number of route segments. However, from a resilience perspective, this structure remains fragile, because many shortest paths rely on a small number of central nodes. Rotterdam remains the most critical node from a purely structural perspective, while Moerdijk, Utrecht, Amsterdam, Oosterhout, Bergen op Zoom, Dordrecht, 's-Hertogenbosch, Leiden, and Gouda also emerge as important intermediary nodes.

The following Table 4-18 presents the differences between the original and revised network configurations, both in terms of their structural graph properties and their percolation thresholds. This comparison allows the impact of the added nodes and route segments on the overall resilience and fragmentation behaviour of the AUTOFLEX network to be assessed.

Table 4-18: Comparison between original and revised AUTOFLEX IWTS

Characteristics	Original AUTOFLEX IWTS	Revised AUTOFLEX IWTS	Difference
Nodes	16	30	+14
Edges	34	68	+34
Average Path Length	3.62	3.95	+0.33
Network Diameter	9	8	-1
Average Clustering Coefficient	0	0	0
Network Density	0.142	0.078	-0.064
Random Deletion p_c	0.25	0.3	+0.05
Weighted Degree p_c	0.125	0.167	+0.042
Node Weight p_c	0.125	0.233	+0.108
Edge Weight p_c	0.176	0.206	+0.03
Weighted Betweenness Centrality p_c	0.125	0.3	+0.175

The comparison between the Original and the Revised AUTOFLEX IWTS graph shows that the revised network represents a larger and more extended inland waterway transport system. The number of nodes increased from 16 to 30, while the number of directed edges doubled from 34 to 68. However, the network density decreased from 0.142 to 0.078. This is expected, since graph density expresses the ratio between existing edges and all theoretically

Funded by the European Union
Grant Agreement: 101136257

possible edges. Therefore, when the number of nodes increases faster than the number of interconnections, the resulting network becomes sparser.

The average path length increased from 3.62 to 3.95, showing that, on average, more intermediate nodes are required to connect two locations in the revised graph. Since average path length is based on the shortest paths between all node pairs, this increase suggests that the additional locations mainly extend the spatial coverage of the network rather than creating many direct shortcut connections between existing corridors. At the same time, the network diameter decreased from 9 to 8, meaning that the longest shortest-path distance in the system was slightly reduced. Therefore, although average accessibility became slightly longer due to the inclusion of more nodes, the worst-case separation between the most distant locations improved.

The clustering coefficient remains equal to 0 in both graph versions. This indicates the absence of local triangular connectivity patterns, where neighbouring nodes are also directly connected to each other. For the AUTOFLEX IWTS, this result reflects a corridor-based inland waterway structure, where locations are mainly connected along route segments rather than through local loops. From a resilience perspective, the absence of clustering indicates limited local redundancy, meaning that if a node or route segment fails, the network may depend on longer rerouting paths rather than nearby alternative connections.

The percolation results show an improvement in all disruption scenarios. Assuming that the percolation threshold p_c represents the fraction of removed nodes or edges required to significantly fragment the network, higher values indicate that the revised graph can tolerate a larger proportion of disruptions before reaching critical connectivity loss. Percolation theory is widely used in network reliability analysis because node or edge failures can be modelled as removals, while the critical percolation threshold can be used as a failure criterion for the overall network [40].

Under random deletion, p_c increased from 0.25 to 0.30. This suggests that the revised IWTS has become more robust to non-targeted failures. In absolute terms, the original graph reaches the critical point after the removal of approximately 4 out of 16 nodes, while the revised graph reaches it after approximately 9 out of 30 nodes. This improvement is consistent with the larger size of the revised network and the presence of additional route elements that can absorb random disruptions. Previous research on complex networks has shown that many networks can be relatively tolerant to random failures, especially when failures are not concentrated on structurally important nodes [41].

The targeted percolation scenarios provide a more risk-sensitive view of network resilience The weighted degree threshold increased from 0.125 to 0.167, the node weight threshold from 0.125 to 0.233, the edge weight threshold from 0.176 to 0.206, and the weighted betweenness threshold from 0.125 to 0.3. These increases show that the revised IWTS is more resilient not only to random failures, but also to disruptions affecting structurally or operationally important components.

The largest improvement is observed in the weighted betweenness scenario. This indicates that the revised network is substantially more robust against the targeted removal of nodes with high structural and risk-related importance. The node weight scenario also shows a considerable increase of 0.108, suggesting that operational and risk exposure is more effectively distributed across the expanded network. More moderate improvements are

Funded by the European Union
Grant Agreement: 101136257

observed for random deletion and weighted degree, with increases of 0.050 (20%) and 0.042 (33.6%), respectively. The edge weight scenario presents the smallest improvement, increasing by only 0.030, which indicates that certain high-risk or high-importance route segments may still play a critical role in maintaining network connectivity. Overall, the higher percolation thresholds demonstrate the enhanced resilience of the revised AUTOFLEX IWTS, as a larger fraction of nodes or edges must be removed before critical network fragmentation occurs. This is consistent with resilience studies in which lower thresholds indicate greater vulnerability, whereas higher thresholds indicate stronger resilience [42].

Overall, the revised AUTOFLEX IWTS demonstrates improved resilience across all percolation scenarios, especially when disruptions are assessed through edge weights and node weights. Nevertheless, the graph metrics reveal that this improvement is achieved mainly through network expansion rather than through dense local interconnection. The revised system remains sparse, corridor-based, and weakly clustered, which means that its resilience still depends on the protection of key nodes and route segments. Therefore, future risk mitigation should focus on reinforcing high-weight nodes, high-weight edges, and nodes with high weighted degree or weighted betweenness, as these components are most likely to act as critical points of failure within the inland waterway transport system.

4.5.2. RISK MINIMIZED GRAPH

Another risk mitigation strategy involves reducing the risk levels of the nodes in the IWTS graph by lowering the probability scores in the 5×5 risk matrix. During the workshops, it was discussed that certain optimisation measures could be implemented immediately in order to reduce the risk level and, consequently, the weight assigned to each node. By reapplying percolation theory using these reduced node weights, the response of the graph can be evaluated, and the extent to which the percolation threshold of the minimised graph differs from that of the original graph can be assessed.

All the hazardous events referred in the paragraphs below are thoroughly listed in tables Table A-1 to Table A-5 of the Appendix.

During the meetings, the hazardous events P_HE1, MDC_HE1 and MDC_HE2 were identified as having the highest average risk levels. In addition, the hazardous events T_T2, T_T3, MDC_HE3 and MDC_HE4 were identified as events that could be directly optimised at this stage, based on the building blocks and characteristics of the ports.

To mitigate supply chain delays associated with MDC-related hazards, the proposed measures should focus on prevention, early detection and rapid recovery. For MDC_HE1 and MDC_HE2, which refer to incorrect cargo loading/unloading and the delivery of an MDC to the wrong TPT or port, the main mitigation measures include cargo–MDC–booking–destination verification, standardised labelling, barcode or QR-based traceability and seal inspection [43]. These measures aim to reduce documentation errors, wrong unit selection, booking discrepancies and cargo rerouting. For MDC_HE3 , where improper use of the access-control system may lead to temporary malfunction or failure to execute commands, mitigation should include role-based access permissions, clear user instructions, backup access procedures and manual override protocols [44]. For MDC_HE4, which concerns inadequate physical security leading to fire, explosion, vandalism, theft, tampering or cargo loss, mitigation should focus on strengthened physical security at MDC storage and handover points, including CCTV, fencing, lighting, access logs and restricted access zones.

Funded by the European Union
Grant Agreement: 101136257

For terminal-related loading and unloading delays, particularly T_T2 and T_T3, mitigation should focus on operational flexibility, resource redundancy and dynamic rescheduling. For T_T2, where the planned pier is unavailable for the vessel's berthing operation due to occupation, blockage or being out of service, a predefined alternative berth or pier in another TPT or Port allocation plan should be prepared[45]. This should be supported by real-time berth-status monitoring and limited time buffers for congested or high-risk operations, so that the vessel can be reassigned before the disruption creates cascading delays. For T_T3, where malfunction or breakdown of lifting equipment, such as cranes, reach stackers or forklifts, may interrupt cargo handling, preventive maintenance, condition-based inspections, backup equipment availability, critical spare parts and rapid repair protocols should be implemented. If a breakdown occurs during cargo handling, remaining equipment and operators should be dynamically reallocated to priority tasks, so that the loading/unloading process can continue with reduced but not fully interrupted capacity [46].

For labour-related disruptions, particularly P_HE1 where strikes and labour protests result in the absence of workforce required to perform port or terminal operations, the mitigation strategy should combine preventive labour-relations management with contingency planning and early warning mechanisms. Based on the literature, labour strikes are recognised as one of the main causes of port disruption in East and South Asia. Port conflict shows that labour disputes can reduce port calls, alter port choice and affect container-handling performance. Since the absence of workforce can directly affect loading and unloading operations, ports and TPTs should establish and maintain strong and structured communication mechanisms with workforce representatives and labour unions, including regular dialogue, transparent communication of operational changes and early identification of unresolved labour concerns [47]. Moreover, where technically and operationally feasible, automated or semi-automated solutions could be considered as contingency support for selected critical terminal functions during periods of temporary workforce unavailability. Evidence from automated container terminals indicates that automation can contribute to more stable and flexible port operations under labour-shortage and wider disruption conditions [48].

Table 4-19 - Table 4-21 present the revised weights of the minimised graph and compare the resulting outcomes with those of the original graph. The edge weight removal scenario was evaluated to confirm the expected equivalence, as the edge risk levels were not reduced. However, its results are not presented separately because they are equal to those of the original network.

Table 4-19: Differences between the weights of original and risk minimized graphs

Category	Previous Weight	New Weight
TPT	111	106
MDC	87	68
Port	80	74

Table 4-20: Final Weights for the nodes of the AUTOFLEX IWTS risk minimized original graph

Funded by the European Union
Grant Agreement: 101136257

Nodes	Innovation	Previous Weight	New Weight
Leiden	TPT	25	22
Katwijk	TPT	25	22
Haarlem	TPT	8	7
Den Haag	TPT	12	11
Delft	TPT	8	7
Eindhoven 1	TPT	17	15
Eindhoven 2	TPT	4	3
Breda 1	TPT	6	5
Breda 2	TPT	4	3
Roosendaal	TPT	11	10
's-Hertogenbosch	TPT, S&C Hub	22	20
Amsterdam	Port, S&C Hub	20	18
Alphen a/d Rijn	TPT, S&C Hub	15	13
Rotterdam	Port, S&C Hub	30	26
Moerdijk	TPT, S&C Hub	33	30
Utrecht	TPT, S&C Hub	66	60

Table 4-21: Comparison between original and risk minimized AUTOFLEX IWTS

Characteristics.	Original AUTOFLEX IWTS	Minimized AUTOFLEX IWTS	Difference
Weighted Degree p_c	0.125	0.125	0
Node Weight p_c	0.125	0.125	0
Weighted Betweenness Centrality p_c	0.125	0.125	0

The invariance of the percolation thresholds after the revision of node weights can be justified on both theoretical and methodological grounds. First, the percolation threshold p_c is primarily associated with the connectivity structure of the network and is commonly expressed as the critical fraction of removed nodes at which the giant component disintegrates. Therefore, in its classical formulation, p_c depends on the topology of the network rather than on the absolute magnitude of node weights [49]. Since the revision of weights does not modify the number of nodes, the number of edges, or the degree distribution of the AUTOFLEX IWTS network, the underlying topological conditions that determine fragmentation remain unchanged.

Second, in targeted attack or intentional removal scenarios, the fragmentation process is governed mainly by the order in which nodes are removed according to a selected attack criterion, such as weighted degree, node weight, or weighted betweenness centrality, rather than by the absolute values of the metric [50]. In the revised dataset, the reduction of node weights lowers the absolute risk values assigned to the nodes, but it preserves the relative

Funded by the European Union
Grant Agreement: 101136257

hierarchy of the most critical nodes. For example, Utrecht, Moerdijk, Rotterdam, Leiden, Katwijk, 's-Hertogenbosch, and Amsterdam remain among the dominant nodes before and after the revision. As a result, the node removal sequence under the examined attack strategies remains unchanged. Since the same nodes are removed in the same order, the degradation trajectory of the giant component is identical, leading to unchanged percolation thresholds.

Finally, the stability of the percolation thresholds can be interpreted as an implicit sensitivity analysis of the model. The fact that p_c remains unchanged despite the recalibration of input weights suggests that the conclusions of the percolation analysis are robust to moderate uncertainty in the estimated node weights. Rather than weakening the analysis, this invariance strengthens the reliability of the results, as it demonstrates that the identified critical fractions are not artifacts of a specific weight calibration. Instead, they reflect stable structural properties of the AUTOFLEX IWTS network and the persistence of the same critical node removal sequence, in line with previous findings on attack vulnerability and weighted-network resilience [51].

4.5.3. COMBINATION OF THE TWO PREVIOUS METHODOLOGIES

The third mitigation approach combines the two previous methodologies in order to evaluate the simultaneous effect of improved network cohesion and reduced risk exposure on the resilience of the AUTOFLEX inland waterway transport system. In this combined scenario, the revised cohesive graph presented in Section 4.5.1 is used as the baseline network configuration, while the reduced node weights derived from the risk minimisation process in Section 4.5.2 are applied to the same expanded topology.

The purpose of this combined analysis is to examine whether the integration of additional nodes and route segments, together with the reduction of risk-related node weights, produces further improvements in the percolation behaviour of the network. In other words, this scenario assesses whether structural reinforcement and risk-level optimisation can jointly increase the resilience of the IWTS against targeted disruptions. The combined graph therefore represents a more comprehensive mitigation strategy, as it accounts for both topological resilience through improved connectivity and operational risk reduction through lower node vulnerability.

Table 4-22 presents the minimised node weights assigned to the cohesive AUTOFLEX IWTS graph, while Table 4-23 compares the percolation thresholds of the Original, Revised, and Combined network configurations. This comparison allows the added value of applying both mitigation strategies together to be evaluated.

Table 4-22: Minimized weights for the nodes of the revised version of the AUTOFLEX IWTS graph

Node	Innovation	Previous Weight	New Weight
Leiden	TPT	25	22
Katwijk	TPT	25	22
Haarlem	TPT	8	7
Den Haag	TPT	12	11
Delft	TPT	8	7
Eindhoven 1	TPT	17	15

Funded by the European Union
Grant Agreement: 101136257

Eindhoven 2	TPT	4	3
Breda 1	TPT	6	5
Breda 2	TPT	4	3
Roosendaal	TPT	11	10
's-Hertogenbosch	TPT, S&C Hub	22	20
Amsterdam	Port, S&C Hub	20	18
Alphen a/d Rijn	TPT, S&C Hub	15	13
Rotterdam	Port, S&C Hub	30	26
Moerdijk	TPT, S&C Hub	33	30
Utrecht	TPT, S&C Hub	66	60
Bergen op Zoom	TPT, S&C Hub	266	242
Tilburg	TPT, S&C Hub	266	242
Dordrecht	TPT, S&C Hub	133	121
Alkmaar	TPT	7	6
IJmuiden	TPT	12	11
Veghel	TPT	33	29
Gouda	TPT	198	174
Arnhem	TPT	8	7
Tiel	TPT	11	10
Nijmegen	TPT	25	22
Schiphol	TPT	99	87
Antwerp	TPT	12	11
Oosterhout	TPT	66	58
Dintelmond	TPT	12	11

Table 4-23: Comparison between the three cases of the AUTOFLEX IWTS graph

Characteristics	Original AUTOFLEX IWTS	Revised AUTOFLEX IWTS	Combined AUTOFLEX IWTS
Weighted Degree p_c	0.125	0.167	0.167
Node Weight p_c	0.125	0.233	0.233
Weighted Betweenness p_c	0.125	0.3	0.3

A notable finding of the analysis is that the Revised and Combined AUTOFLEX IWTS scenarios produce identical percolation thresholds for all three targeted-attack strategies. Specifically, the weighted degree threshold remains equal to $p_c = 0.167$, while the node weight and weighted betweenness thresholds remain equal to $p_c = 0.233$ and $p_c = 0.3$. This outcome is directly related to the fact that the two scenarios have the same network topology, consisting of the same 30 nodes and the same edge structure, and differ only in the absolute magnitude of the assigned node weights. In the Combined scenario, the node weights are reduced by an approximately uniform factor, but this reduction does not modify the structural configuration of the network.

Since the Revised and Combined AUTOFLEX IWTS scenarios are topologically identical, no additional change in the percolation threshold is expected from the network structure itself.

Funded by the European Union
Grant Agreement: 101136257

Second, in targeted attack simulations, node weights can affect the fragmentation process only if they change the order in which nodes are removed. The collapse trajectory of the giant component is governed by the ranking of nodes according to the selected attack metric, such as weighted degree, node weight, or weighted betweenness centrality, rather than by the absolute magnitude of the metric values alone. In the Combined scenario, the reduction of node weights is monotonic and rank-preserving. The same nodes remain dominant in the hierarchy: Bergen op Zoom and Tilburg remain the highest weighted nodes, followed by Gouda, Dordrecht, Schiphol, Utrecht, and the remaining nodes in the same relative order. As a result, the node removal sequences under the weighted degree, node weight, and weighted betweenness strategies remain identical to those of the Revised scenario.

Because the Revised and Combined scenarios share both the same topology and the same node removal sequences, they necessarily produce the same giant component degradation curves and, consequently, the same percolation thresholds. Therefore, a uniform or near uniform rescaling of node weights does not affect attack outcomes when it does not alter the ranking of critical nodes.

In other words, the model is sensitive to genuine structural changes, as demonstrated by the increase in p_c from the Original to the Revised scenario, but remains stable under a rank-preserving recalibration of node weights. This strengthens the reliability of the analysis, as it indicates that the identified thresholds are not artifacts of a specific weight assignment, but reflect robust structural properties of the AUTOFLEX IWTS network.

Funded by the European Union
Grant Agreement: 101136257

5 DISCUSSION

5.1 EVALUATION OF RESULTS

The results of the analysis demonstrate that the AUTOFLEX inland waterway transport system should be understood as a network, where operational vulnerability is determined not only by the presence of hazards at individual nodes or routes, but also by the way these elements are structurally connected. Combining HAZID-based hazard identification with graph theory and percolation analysis provided a systematic way to move from individual hazardous events to a system-level resilience assessment. The three pillars of the methodology presented in Figure 3-1 proved to be mutually reinforcing. The hazard identification stage supplied the risk-informed weights that made the network analysis operationally relevant, while the network analysis translated hazardous events into system level indicators of resilience and criticality that could subsequently guide mitigation.

At the level of Hazard identification, the HAZID process, supported by a targeted literature review and three dedicated workshops with ISE, DFDS, and DST, produced a structured list of hazardous events for all parts of the AUTOFLEX transport system, including ports, vessel routes, TPTs, S&C hubs, and MDCs. These hazards are not limited to conventional navigational or infrastructure risks, but also include operational, technical, human, environmental, energy related, and cyber related events that may lead to supply chain delays. Evaluating these events through the 5×5 risk matrix, refined by specific characteristics, namely Building Blocks, and route specific characteristics, namely traffic, CEMT class, and route length, yielded a consistent set of risk levels that could be directly translated into node and edge weights. This step, demonstrates that qualitative, expert-based hazard knowledge can be systematically converted into quantitative network attributes, addressing a gap identified in the literature, where purely topological approaches often fail to capture the heterogeneous hazard characteristics and operational attributes of real logistics systems.

The graph theoretical results revealed that the original AUTOFLEX network was relatively sparse and highly centralised. It connects a wide range of inland and port locations through relatively short topological paths. The absence of clustering shows that neighbouring nodes are not connected through alternative local paths, meaning that disruption at a central point can affect wider parts of the network. This type of graph is characteristic of sparse infrastructure networks, which tolerate random failures relatively well but fragment rapidly under the targeted loss of their most important components.

A key finding of the topological analysis is Rotterdam's dominant role. In the original network, Rotterdam confirmed its role as the primary intermediary node. This means that a large share of shortest path connectivity depends on Rotterdam, making it a critical element for maintaining network cohesion and supporting cargo flows. However, the risk weighted analysis also showed that criticality cannot be explained by topology alone. Nodes such as Utrecht, Moerdijk and Leiden, become highly important when node weights are incorporated, showing that the combination of structural position and risk exposure provides a more realistic picture of vulnerability. From a purely structural standpoint, Rotterdam is clearly the dominant node, yet under the weighted degree and node weight criteria, Utrecht emerges

Funded by the European Union
Grant Agreement: 101136257

as the first node whose removal triggers fragmentation, owing to the combination of its connectivity and high assigned risk weight. This contrast confirms the central methodological premise of Task 3.6. Node importance cannot be inferred from topological prominence alone but must incorporate node-specific risk profiles. A vulnerability assessment based exclusively on unweighted metrics would have systematically misidentified the system's most critical elements.

The percolation analysis further confirmed this interpretation. Under random node removal, the original network remains relatively robust, reaching its critical threshold after the removal of approximately 25% of its nodes, i.e., p_c=0.250. This suggests that the system can tolerate a moderate level of non-targeted failures. However, the targeted removal scenarios reveal a much higher level of vulnerability. The weighted degree and node weight scenarios both lead to network collapse after the removal of only 12.5% of nodes, $p_c = 0.125$, while the weighted betweenness strategy also produces a threshold of 0.125. These results show that the AUTOFLEX network is resilient against random failures but fragile against the loss of highly connected, high-risk, or highly intermediary nodes. The edge based removal scenario indicates a considerable degree of redundancy among connections. Highly important edges can, to some extent, be bypassed by alternative paths, although such rerouting is likely to introduce delays and reduced operational efficiency rather than preserve nominal performance.

The impact analysis following the removal of Utrecht offered additional insight into the redistribution of criticality after the loss of a major hub. Utrecht's removal does not result in an even redistribution of network responsibility. Instead, the additional betweenness burden is transferred mainly to Moerdijk, Rotterdam, Den Haag, Leiden, Delft, and Eindhoven 2. Moerdijk records the highest absolute increase in node-weighted betweenness centrality, while Den Haag records the highest relative increase. By contrast, Haarlem, Eindhoven 1, 's-Hertogenbosch, and Amsterdam lose intermediary relevance after the disruption, with the node-weighted betweenness of 's-Hertogenbosch and Amsterdam falling to zero. This means that the disruption of the primary hub does not merely degrade the system; it creates a new set of potential bottlenecks. This confirms that resilience planning should not focus only on protecting the most critical node itself but also on strengthening the secondary nodes that become critical under disrupted conditions. Otherwise, the system may simply transfer vulnerability from one hub to another.

The mitigation analysis showed that improving the cohesion of the graph has a clear positive effect on network resilience The revised AUTOFLEX configuration expands the system from 16 to 30 nodes and from 34 to 68 directed edges. Although the average path length increases slightly from 3.62 to 3.95, the network diameter decreases from 9 to 8. This is an important result, because it shows that the revised configuration becomes larger while also improving worst-case accessibility. The reduction in diameter indicates that additional route alternatives or bypass possibilities reduce the maximum separation between nodes. This suggests that the added routes act as effective bypasses that improve worst-case accessibility while preserving the sparse infrastructure character of the system.

The revised network also performs better in most of the percolation scenarios. The revised thresholds indicate that the extended configuration does not alter the network's fragmentation point under this specific removal criterion. These results indicate that the revised configuration distributes risk and connectivity more effectively across the network

Funded by the European Union
Grant Agreement: 101136257

under most removal strategies, reducing the dependence on a very small number of critical elements.

At the same time, the results also show that mitigation based only on reducing risk levels does not necessarily change the network's fragmentation behaviour. In the minimized risk level scenario, the absolute node weights are reduced, but the percolation thresholds remain unchanged. This occurs because the network topology remains the same and the ranking of the critical nodes is preserved. Therefore, the same nodes are removed in the same order during targeted removals leading to the same degradation trajectory. This invariance is theoretically expected, as the percolation threshold is a dimensionless structural quantity governed by network topology and by the ranking of nodes under the removal scenario. Since the applied weight reduction constitutes a monotonic, rank-preserving rescaling, it alters neither the topology nor the node-removal sequence.

The combined scenario further supports this observation. Although a uniformity factor reduces the node weights, the percolation thresholds remain identical to those of the revised network.. This indicates that the decisive factor is not the absolute magnitude of the weights, but whether the mitigation action changes the topology of the network or the relative hierarchy of critical nodes. Far from indicating that risk level reduction is ineffective, this result clarifies the complementary roles of the two mitigation strategies. Structural interventions, such as new nodes, edges, and alternative routes can shift the fragmentation thresholds when they alter the topology or the corresponding removal sequence, thereby influencing whether and when the network breaks apart. By contrast, risk-level interventions reduce the probability and severity of the disruptive events themselves and therefore govern how often the system is stressed toward those thresholds. Moreover, the invariance of the thresholds under weight recalibration functions as an implicit sensitivity analysis, demonstrating that the identified critical fractions and critical node sequences are robust to moderate uncertainty in the expert-derived weights and are structural properties of the AUTOFLEX network rather than artifacts of a particular calibration.

Overall, the results indicate that the AUTOFLEX inland waterway transport system could benefit from the introduction of additional routes and nodes, but it would still remain structurally sparse and dependent on key intermediary locations. The revised network is more resilient than the original network under most of the evaluated disruption scenarios, but its absence of clustering and low density indicate that local redundancy remains limited. Therefore, future improvements should focus on strengthening bypass routes, increasing alternative connectivity around high-betweenness nodes, and ensuring that secondary nodes have sufficient capacity to absorb rerouted flows during disruptions. Taken together, the results deliver the outputs required by Task 3.6, a prioritised set of critical nodes, namely Utrecht, Rotterdam, Moerdijk, Leiden, and, after disruption, Den Haag, Delft, and Eindhoven 2, a prioritised set of critical edges, notably the Rotterdam–Utrecht and Utrecht–'s-Hertogenbosch corridors, a quantified comparison of mitigation strategies, and a demonstration that resilience by design measures, including redundant routing and additional TPT and S&C locations, yield measurable improvements in network resilience.

5.2 LIMITATIONS AND AREAS FOR IMPROVEMENT

Although the proposed methodology provides a structured and quantitative basis for assessing the safety, security, and resilience of the AUTOFLEX inland waterway transport

Funded by the European Union
Grant Agreement: 101136257

system, several limitations should be acknowledged. These limitations define the boundaries within which the findings should be interpreted and indicate directions for methodological refinement.

First, the analysis is based on relatively small networks. Percolation theory is formally developed for large-scale networks, whereas the AUTOFLEX graphs comprise only 16 and 30 nodes respectively. At this scale, finite-size effects are significant, the removal of a single additional node can shift the computed threshold appreciably, and the phase transition is not sharply defined. Therefore, the reported p_c values should be interpreted as comparative indicators, valid for ranking scenarios and configurations against one another, rather than as absolute safety limits for the real transport system.

Second, the analysis equates network functionality mainly with the size of the giant connected component. While this is a standard and informative proxy, it does not capture service-oriented dimensions of performance such as travel times, schedule adherence, cargo volumes, berth and charging capacity, or the operational cost of rerouting. A network may remain connected after a failure, but the alternative route may be longer, slower, more expensive, or operationally constrained. Therefore, future work should complement connectivity-based indicators with performance-based indicators such as additional travel distance, expected delay, capacity loss, energy availability, and rerouting cost.

Third, the assigned weights depend on information from the HAZID process, the literature review, partner workshops, and the project-specific information available at the current stage of AUTOFLEX regarding node and route characteristics. Where detailed operational or configuration data were not yet fully defined, the parameterisation was based on the best available project knowledge and representative configurations consistent with the envisaged AUTOFLEX transport concepts. Thiss applies, in particular, to parameters concerning each vessel's round-trip route, ZES packs redundancy, backup power supplies for MDCs, alternative modes of goods transportation, cargo value, available capacity at each TPT, and the number of TPTs and S&C hubs. Although the workshop-based elicitation with ISE, DFDS, and DST and the subsequent internal review improve consistency, the weights inevitably retain a degree of subjectivity. In addition, the weights assigned to the newly introduced nodes of the extended network reflect the information and level of system definition available at this stage of the project, rather than fully specified and assessed final operational configurations. Nevertheless, the observed stability of the percolation thresholds under rank-preserving weight changes provides some confidence that the main structural findings are not overly sensitive to moderate variations in these input values..

Fourth, penetration testing is introduced conceptually through the edge-weight removal scenario in percolation theory, but it is not yet fully developed using empirical cyber vulnerability data. Cyber risk scores for vessel-route edges have been defined conceptually, but no empirical penetration tests of the actual AUTOFLEX digital systems, including vessel IT management, remote control interfaces, and communication edges, have yet been performed. The cyber-disruption scenarios therefore illustrate the approach rather than assess the deployed systems, and empirical validation remains an essential next step.

Overall, none of these limitations undermines the comparative conclusions of the analysis. Rather, they delineate a clear agenda for future work refinement, which is taken up in the recommendations of Section 6.

Funded by the European Union
Grant Agreement: 101136257

6 CONCLUSIONS AND NEXT STEPS

This section presents the principal conclusions resulting from the safety, security, and resilience assessment of the AUTOFLEX IWTS. It first summarises the key outputs of Task 3.6, including the integration of HAZID, graph theory, percolation theory, and risk mitigation into a unified assessment framework. It then outlines the main directions for future work, taking into account the limitations identified during the study and the necessity for further methodological validation, operational data integration, network optimisation, and cybersecurity assessment. Together, these conclusions and recommendations form the basis for advancing the AUTOFLEX network, moving towards a safer, more reliable, and more resilient operational configuration.

6.1 SUMMARY OF MAIN ACHIEVEMENTS

This deliverable developed and applied a risk-based methodology for assessing the safety, security, and resilience of the AUTOFLEX inland waterway transport system. The methodology combines three main components: hazard identification through a HAZID-based process, risk assessment through graph theory and percolation analysis, and risk mitigation through the evaluation of alternative resilience enhancing strategies. The work carried out within Task 3.6 integrates hazard identification, network-based risk assessment, and risk mitigation into a single, coherent workflow tailored to the AUTOFLEX innovations and to the consequence dimension of supply chain delay. By integrating these components, the work provides a structured approach for translating hazardous events into quantitative network indicators and for assessing how disruptions may affect the continuity of cargo flows.

The first main achievement of the work is the systematic identification and classification of hazards relevant to the AUTOFLEX transport system and its innovations. The analysis considered ports, TPTs, S&C hubs, MDCs, vessel routes, and the AUTOFLEX vessel. The HAZID process, supported by partner workshops and literature review, enabled the identification of hazardous events that may cause delays or disruptions in the supply chain. Building on a targeted literature review and three dedicated workshops with project partners, namely ISE, DFDS, and DST, a structured HAZID catalogue of hazards and hazardous events was produced, covering operational, infrastructural, environmental, technical, organisational, and cybersecurity-related disruption mechanisms. These hazards were then assessed through a 5×5 risk matrix, allowing each scenario to be ranked according to probability and impact. The resulting risk levels were further refined through node-specific TPT Building Block factors and route-specific factors, including traffic, CEMT class, and route length.

A second achievement is the conversion of hazard identification results into graph weights. Node weights and edge weights were derived from the risk levels associated with the corresponding locations and route segments (vessel routes). This step was essential because it allowed the AUTOFLEX transport system to be assessed not only as a topological network, but also as a risk-informed operational system. This constitutes one of the principal methodological contributions of the task, because it bridges conventional, expert-based

Funded by the European Union
Grant Agreement: 101136257

hazard analysis with quantitative network science, allowing heterogeneous hazard knowledge to be propagated into system-level vulnerability indicators.

A third achievement is the construction and evaluation of the AUTOFLEX inland waterway transport network as a graph. The analysis showed that the original network has a sparse, corridor-based, and hub-oriented structure, with Rotterdam playing a dominant intermediary role. The low density, absence of clustering, and relatively high diameter indicate limited redundancy and strong dependence on specific nodes. These results provide a clear structural explanation of why certain locations are critical for maintaining connectivity and continuity of operations.

A fourth achievement is the application of percolation theory to assess network resilience under different disruption scenarios. The analysis compared random node removal with targeted strategies based on weighted degree, node weight, weighted betweenness centrality, and edge weight. More specifically, the risk assessment combined graph-theoretic characterisation with percolation analysis under five removal scenarios: random, edge weight, weighted degree, node weight, and weighted betweenness. The results showed that the network is more tolerant to random failures than targeted disruptions. The analysis quantified the resilient yet fragile character of the network, tolerant to random failures, with $p_c = 0.250$, but highly vulnerable to targeted disruption of risk-critical elements, with p_c as low as 0.125. In particular, the removal of a small number of high-weight or high-centrality nodes is sufficient to fragment the network. The analysis identified Utrecht, Rotterdam, Moerdijk, and Leiden as the system's most critical nodes. Importantly, the results demonstrated that purely topological prominence is an insufficient criterion for criticality: risk-weighted rankings reordered the priority of nodes and revealed vulnerabilities that an unweighted analysis would have missed. The complementary impact analysis of Utrecht's removal further showed that criticality redistributes in a concentrated manner onto a small set of secondary nodes, namely Moerdijk, Rotterdam, Den Haag, Leiden, Delft, and Eindhoven 2, which should therefore be included in resilience planning.

A fifth achievement is the evaluation of mitigation scenarios. Three mitigation strategies were formulated and quantitatively evaluated. The revised network configuration, which increases the number of nodes and route connections, improves the percolation thresholds across all examined scenarios. The structurally enhanced, more cohesive network configuration, consisting of 30 nodes and 68 directed edges, improved the percolation thresholds in every scenario, while reducing the network diameter despite the near doubling of network size. This shows that additional connectivity and route alternatives can increase the resilience of the AUTOFLEX transport system. However, the minimization of risk levels alone does not change the percolation thresholds when the topology and node removal ranking remain unchanged. This outcome was theoretically justified and interpreted as an implicit sensitivity analysis confirming the resilience of the results to weight calibration uncertainty.

Overall, the deliverable demonstrates that the proposed methodology can support risk-informed decision-making for the development of safer and more resilient autonomous inland waterway transport systems. The approach provides a quantitative basis for identifying critical nodes and edges, assessing disruption thresholds, evaluating mitigation options, and prioritising interventions that can improve operational continuity. Finally, the task delivered actionable outputs to the wider work package: A prioritised list of critical nodes

Funded by the European Union
Grant Agreement: 101136257

and edges requiring protection, monitoring and redundancy, and quantitative evidence supporting resilience-by-design network extensions. The ultimate aim, to guide the development of autonomous inland waterway transport systems that are more resilient, safer, more reliable, and more sustainable, has been supported with quantitative, reproducible, and risk-informed evidence.

6.2 RECOMMENDATIONS FOR FUTURE WORK

Based on the findings and the limitations identified in Section 5, the following directions are recommended for future work in order to further improve the resilience, and operational applicability of the AUTOFLEX inland waterway transport system assessment.

First, future extensions of the methodology should integrate performance-based indicators such as additional travel distance, expected delay, schedule adherence, cargo-handling capacity loss, berth and charging capacity constraints, energy availability, and rerouting cost. This would allow the resilience of the AUTOFLEX IWTS to be evaluated not only on whether the network remains connected, but also on whether it can continue to provide an acceptable level of transport service after a disruption.

Second, a formal uncertainty and sensitivity analysis of the assigned node and edge weights could be conducted, as a complementary extension of the present analysis. Although the stability of the percolation thresholds under rank-preserving weight changes suggests that the main findings are not highly sensitive to these specific variations, a systematic sensitivity analysis would provide additional insight into their behaviour under a broader range of plausible input variations. This could be achieved through Monte Carlo simulations, controlled variations of probability and impact scores, or alternative weighting scenarios. Such analysis would help determine whether small changes in the input risk values could modify the ranking of critical nodes and edges, alter the node-removal sequence, or affect the resulting percolation thresholds. In this way, such an analysis could provide further support for the criticality results and the resulting mitigation priorities, while also enhancing the applicability of the methodology to future studies.

Third, future work should aim to improve the resilience targets of the AUTOFLEX IWTS graph. In the present results, the revised graph improves the percolation thresholds compared with the original configuration. However, further optimisation is still required. Future network designs should seek to increase these thresholds across the main disruption scenarios, enabling the network to tolerate the removal of a larger proportion of nodes or edges before critical fragmentation occurs. Therefore, future network design should focus not only on improving the current percolation thresholds but also on moving the system toward a more resilient configuration capable of maintaining connectivity under stronger failure conditions.

Fourth, future network improvements should address the limited local redundancy inherent to inland waterway topologies. In both the current and revised configurations, the clustering coefficient remains zero, indicating that the graph contains no triangular or locally redundant connectivity patterns. Although this result reflects the corridor-based structure of inland waterway transport networks, it also indicates that neighbouring nodes are generally not directly interconnected. As a result, the network has limited local rerouting capacity and remains dependent on a small number of central nodes and route segments. The physical

Funded by the European Union
Grant Agreement: 101136257

creation of alternative edges or direct cross-connections is strictly limited by geographical feasibility, economic viability, and infrastructure compatibility (e.g., CEMT class requirements). Future mitigation should focus on the broader investigation of feasible route redundancy and service substitutability under the above constraints. A non-zero clustering coefficient would indicate that the network contains local redundancy, improving its ability to absorb disruptions without relying exclusively on long-distance rerouting through central hubs.

Fifth, the revised AUTOFLEX IWTS graph could be re-analysed in future extensions of the present study, as further, more detailed and validated operational data become available. In the current mitigation analysis, several additional nodes, routes, attributes, and weights were introduced on the basis of the project-specific information available at this stage and representative configurations consistent with the planned AUTOFLEX transport concepts, in order to explore how a more cohesive network could affect resilience. However, future analysis could further refine and validate these network characteristics and input values using more detailed information, where available, from AUTOFLEX partners, demonstrations, operational records, or infrastructure datasets. Such data could include confirmed TPT configurations, S&C hub characteristics, vessel traffic levels, route utilisation, waterway capacity, validated CEMT classes, travel times, terminal handling capacity, berth availability, charging availability, and recorded delay events. This would allow the revised graph to evolve from a scenario-based mitigation model into a more operationally grounded network model supported by increasingly detailed and validated data.

Sixth, future work should further develop risk control options for hazardous events associated with edges, and not only those related to nodes. Since edges represent vessel routes and inland waterway segments, edge-related hazardous events may directly affect route availability, travel time, and supply chain continuity. This would make the mitigation framework more complete by addressing both node-related and route-related vulnerabilities.

Seventh, future work could explore the integration of real penetration testing results into the proposed methodology as the relevant AUTOFLEX digital systems mature. These results could be used to revise and expand the cybersecurity hazard list and update the risk scores assigned to the affected nodes and edges. The graph model could then be used to assess the broader impact of the identified vulnerabilities on the connectivity and resilience of the transport network. The penetration testing scope could include vessel IT management systems, remote monitoring and control interfaces, communication links, data-exchange platforms, route-management systems, and systems supporting autonomous or semi-autonomous vessel operations.

Eighth, future work should include a cost-benefit analysis of the risk control options and risk-reducing measures examined in the mitigation analysis in Section 4.5. The findings and analytical outputs of the present study, including the identified critical nodes and edges, the percolation-based resilience indicators, and the evaluated mitigation scenarios, could provide a useful basis for a more detailed future assessment incorporating economic considerations. This assessment should compare the implementation, operation, and maintenance costs of each measure with its expected benefits, including the reduction of risk exposure and potential supply chain delays. Combining risk-reduction effectiveness with economic feasibility would support the selection of the most appropriate mitigation measures among those examined in Sections 4.5.1–4.5.3, while also enabling the identification of the options

Funded by the European Union
Grant Agreement: 101136257

that offer the greatest overall net benefit. Such an extended assessment would build upon the conclusions of the present work and help determine whether the expected improvements in safety and resilience justify the associated investment.

Collectively, these steps would evolve the framework presented in this deliverable from a comparative, design-stage assessment into a comprehensive, data-driven risk and resilience management capability supporting the safe, secure, and resilient operation of the AUTOFLEX inland waterway transport system throughout its deployment and scale-up.

Funded by the European Union
Grant Agreement: 101136257

7 REFERENCES

[1] T. Chen, S. Wu, J. Yang, and G. Cong, 'Risk Propagation Model and Its Simulation of Emergency Logistics Network Based on Material Reliability', IJERPH, vol. 16, no. 23, p. 4677, Nov. 2019.

[2] J. R. Feng, M. Zhao, and S. Lu, 'Accident spread and risk propagation mechanism in complex industrial system network', Reliability Engineering & System Safety, vol. 244, p. 109940, Apr. 2024, doi: 10.1016/j.ress.2024.109940.

[3] H. Liu, Z. Tian, A. Huang, and Z. Yang, 'Analysis of vulnerabilities in maritime supply chains', Reliability Engineering & System Safety, vol. 169, pp. 475–484, Jan. 2018, doi: 10.1016/j.ress.2017.09.018.

[4] T. Wen and Y. Deng, 'The vulnerability of communities in complex network: An entropy approach',Volume 196, 2020, 106782, ISSN 0951-8320, doi:10.1016/j.ress.2019.106782.

[5] C. S. Ongkowijoyo and H. Doloi, 'Understanding of Impact and Propagation of Risk based on Social Network Analysis', Procedia Engineering, vol. 212, pp. 1123–1130, 2018, doi: 10.1016/j.proeng.2018.01.145.

[6] H. Hamedmoghadam, M. Jalili, H. L. Vu, and L. Stone, 'Percolation of heterogeneous flows uncovers the bottlenecks of infrastructure networks', Nat Commun, vol. 12, no. 1, p. 1254, Feb. 2021, doi: 10.1038/s41467-021-21483-y.

[7] S. LaRocca and S. Guikema, 'A Survey of Network Theoretic Approaches for Risk Analysis of Complex Infrastructure Systems', in Vulnerability, Uncertainty, and Risk, Hyattsville, Maryland, United States: American Society of Civil Engineers, Apr. 2011, pp. 155–162. doi: 10.1061/41170(400)19.

[8] I. Eusgeld, W. Kröger, G. Sansavini, M. Schläpfer, and E. Zio, 'The role of network theory and object-oriented modeling within a framework for the vulnerability analysis of critical infrastructures', Reliability Engineering & System Safety, vol. 94, no. 5, pp. 954–963, May 2009, doi: 10.1016/j.ress.2008.10.011.

[9] L. Meng, X. Yao, Q. Chen, and C. Han, 'Vulnerability cloud: A novel approach to assess the vulnerability of critical infrastructure systems', Concurrency and Computation, vol. 34, no. 21, p. e7131, Sep. 2022, doi: 10.1002/cpe.7131.

[10] X. Zhang, S. Mahadevan, S. Sankararaman, and K. Goebel, 'Resilience-based network design under uncertainty', Reliability Engineering & System Safety, vol. 169, pp. 364–379, Jan. 2018, doi: 10.1016/j.ress.2017.09.009.

[11] X. Li, P. Oh, Y. Zhou, and K. F. Yuen, 'Operational risk identification of maritime surface autonomous ship: A network analysis approach', Transport Policy, vol. 130, pp. 1–14, Jan. 2023, doi: 10.1016/j.tranpol.2022.10.012.

[12] Y, Kurt. B., Akyuz, E., & O Arslan. A quantitative HAZOP risk analysis under extended CREAM approach for Maritime Autonomous Surface Ship (MASS) operation. Marine Technology Society Journal, 56(4), 59–73. 2022, https://doi.org/10.4031/MTSJ.56.4.11

[13] M. Chaal, O. Banda, J. Glomsrud, S. Basnet, S. Hirdaris, P. Kujala,A framework to model the STPA hierarchical control structure of an autonomous ship, Safety Science, Volume 132, 2020, 104939, ISSN 0925-7535, https://doi.org/10.1016/j.ssci.2020.104939.

[14]E. Spachtholz, M. Glomsda, M. S. K. Illuri, T. Kerkmann, I. Bačkalov, and F. E. Kracht, "Risk Assessment for Inland Vessels with Various Levels of Automation: A Hazard

Funded by the European Union
Grant Agreement: 101136257

Identification Study," Journal of Physics: Conference Series, vol. 2867, no. 1, article 012037, 2024. https://doi.org/10.1088/1742-6596/2867/1/012037

[15] R. Wehrle, M. Wiens, and F. Schultmann, 'A framework to evaluate systemic risks of inland waterway infrastructure', Progress in Disaster Science, vol. 16, p. 100258, Dec. 2022, doi: 10.1016/j.pdisas.2022.100258.

[16] A. Dunant, M. Bebbington, T. Davies, and P. Horton, 'Multihazards Scenario Generator: A Network-Based Simulation of Natural Disasters', Risk Analysis, vol. 41, no. 11, pp. 2154–2176, Nov. 2021, doi: 10.1111/risa.13723.

[17] L. G. Brunner, R. A. M. Peer, C. Zorn, R. Paulik, and T. M. Logan, 'Understanding cascading risks through real-world interdependent urban infrastructure', Reliability Engineering & System Safety, vol. 241, p. 109653, Jan. 2024, doi: 10.1016/j.ress.2023.109653.

[18] S. Gbako, D. Paraskevadakis, J. Ren, J. Wang, and Z. Radmilovic, 'A systematic literature review of technological developments and challenges for inland waterways freight transport in intermodal supply chain management', BIJ, vol. 32, no. 1, pp. 398–431, Jan. 2025, doi: 10.1108/BIJ-03-2023-0164.

[19] B. R. Totakura, N. Narasinganallur, S. A. Jalil, and A. Pj, 'Factors Affecting Container Shipping Through Inland Waterways', JEMS, vol. 10, no. 3, pp. 156–167, Sep. 2022, doi: 10.4274/jems.2022.86094.

[20] Y. Chen et al., 'Research on Response Strategies for Inland Waterway Vessel Traffic Risk Based on Cost-Effect Trade-Offs', JMSE, vol. 12, no. 9, p. 1659, Sep. 2024, doi: 10.3390/jmse12091659.

[21] L. T. Pham and L. V. Hoang, 'A navigational risk evaluation of ferry transport: Continuous risk management matrix based on fuzzy Best-Worst Method', PLoS ONE, vol. 19, no. 9, p. e0309667, Sep. 2024, doi: 10.1371/journal.pone.0309667.

[22] K. Moses, 'Development of Risk Assessment Matrix for NASA Engineering and Safety Center'. Engineering, Environmental Science, 2004.

[23] M. Hagaseth, 'Kloch, Kristoffer, Alias, Cyril, Budde, Marvin, Kerkmann Thomas, Nordahl, Håvard, Mateienko, Dennis, Krause, Stefan; "AUTOFLEX Deliverable D3.1 Transport Concepts"; Revision 1.0; February 2026'.

[24] A. Majeed and I. Rauf, 'Graph Theory: A Comprehensive Survey about Graph Theory Applications in Computer Science and Social Networks', Inventions, vol. 5, no. 1, p. 10, Feb. 2020, doi: 10.3390/inventions5010010.

[25] R. Żochowska and P. Soczówka, 'ANALYSIS OF SELECTED TRANSPORTATION NETWORK STRUCTURES BASED ON GRAPH MEASURES', SJSUT.ST, vol. 98, pp. 223–233, Mar. 2018, doi: 10.20858/sjsutst.2018.98.21.

[26] D. Han, Z. Sui, C. Xiao, and Y. Wen, 'Reliability of Inland Water Transportation Complex Network Based on Percolation Theory: An Empirical Analysis in the Yangtze River', JMSE, vol. 12, no. 12, p. 2361, Dec. 2024, doi: 10.3390/jmse12122361.

[27] K. Louzis, M. Koimtzoglou, L. Serafeim, A. Koimtzoglou, and N. P. Ventikos, 'Risk and Resilience Assessment of Inland Waterway Transport Networks'.Proc. of the European Safety and Reliability Conference (ESREL 2026) Edited by José C. Matos, Paulo B. Lourenço, Michael Beer, Daniel Oliveira, Edoardo Patelli, Hélder S. Sousa, Rui A. Silva, Monica Santamaria and Chiara Turco © 2026 ESREL 2026 Organizers. Published by Research Publishing, Singapore. ISBN: 978-981-94-6718-1 | doi: 10.3850/ESREL2026061419_esrel26-p26506-cd.

Funded by the European Union
Grant Agreement: 101136257

[28] M. Alhamed and M. M. H. Rahman, 'A Systematic Literature Review on Penetration Testing in Networks: Future Research Directions', Applied Sciences, vol. 13, no. 12, p. 6986, Jun. 2023, doi: 10.3390/app13126986.
[29] G. Kavallieratos and S. Katsikas, 'Managing Cyber Security Risks of the Cyber-Enabled Ship', JMSE, vol. 8, no. 10, p. 768, Sep. 2020, doi: 10.3390/jmse8100768.
[30] V. Bolbot, G. Theotokatos, E. Boulougouris, and D. Vassalos, 'A novel cyber-risk assessment method for ship systems', Safety Science, vol. 131, p. 104908, Nov. 2020, doi: 10.1016/j.ssci.2020.104908.
[31] L.-G. Mattsson and E. Jenelius, 'Vulnerability and resilience of transport systems – A discussion of recent research', Transportation Research Part A: Policy and Practice, vol. 81, pp. 16–34, Nov. 2015, doi: 10.1016/j.tra.2015.06.002.
[32] H. Baroud, K. Barker, J. E. Ramirez-Marquez, and C. M. Rocco S., 'Importance measures for inland waterway network resilience', Transportation Research Part E: Logistics and Transportation Review, vol. 62, pp. 55–67, Feb. 2014, doi: 10.1016/j.tre.2013.11.010.
[33] 'Mateienko, Dennis (ISE) et al.: "AUTOFLEX Deliverable D4.2 – Uncrewed Vessel concept"; Revision 1.0; April 2024'.
[34] K. Kloch, C. Alias, H. Nordahl, S. Krause, T. Kerkmann, and M. Budde, 'Enabling an AUTOnomous and FLEXible hinterland transport ecosystem: Main modal shift issues and potential transport solutions', J. Phys.: Conf. Ser., vol. 3123, no. 1, p. 012045, Oct. 2025, doi: 10.1088/1742-6596/3123/1/012045.
[35] M. Shiokari et al., 'Structure model-based hazard identification method for autonomous ships', Reliability Engineering & System Safety, vol. 247, p. 110046, Jul. 2024, doi: 10.1016/j.ress.2024.110046.
[36] D. S. Callaway, M. E. J. Newman, S. H. Strogatz, and D. J. Watts, 'Network Robustness and Fragility: Percolation on Random Graphs', , vol. 85, no. 25, 2000.
[37] V. L. Aguirre and J. Hackl, 'Applying Computational Network Analysis Methods for Critical Infrastructure Ro- bustness: Integrating Centrality Metrics and Model Simplification for Efficient Failure Simulations'.Proc. of the European Safety and Reliability Conference (ESREL 2026), Edited by José C. Matos, Paulo B. Lourenço, Michael Beer, Daniel Oliveira, Edoardo Patelli, Hélder S. Sousa, Rui A. Silva, Monica Santamaria and Chiara Turco, © 2026 ESREL 2026 Organizers. Published by Research Publishing, Singapore., ISBN: 978-981-94-6718-1 | doi: 10.3850/ESREL2026061419_esrel26-p26393-cd.
[38] Thun, Kristian; Nordahl, Håvard; Rørvik, Ella-Lovise Hammervold 'AUTOFLEX Deliverable D3.2– Transport System'; Revision 1.0; September 2026.
[39] P. Crucitti, V. Latora, and M. Marchiori, 'Model for cascading failures in complex networks', Phys. Rev. E, vol. 69, no. 4, p. 045104, Apr. 2004, doi: 10.1103/PhysRevE.69.045104.
[40] D. Li, Q. Zhang, E. Zio, S. Havlin, and R. Kang, 'Network reliability analysis based on percolation theory', Reliability Engineering & System Safety, vol. 142, pp. 556–562, Oct. 2015, doi: 10.1016/j.ress.2015.05.021.
[41] R. Albert, H. Jeong, and A.-L. Barabasi, 'Error and attack tolerance of complex networks', Nature, vol. 406, no. 6794, pp. 378–382, Jul. 2000, doi: 10.1038/35019019.
[42] M. Bellingeri et al., 'Forecasting real-world complex networks' robustness to node attack using network structure indexes', Front. Phys., vol. 11, p. 1245564, Oct. 2023, doi: 10.3389/fphy.2023.1245564.

Funded by the European Union
Grant Agreement: 101136257

[43] U. Jüttner, H. Peck, and M. Christopher, 'Supply chain risk management: outlining an agenda for future research', International Journal of Logistics Research and Applications, vol. 6, no. 4, pp. 197–210, Dec. 2003, doi: 10.1080/1367556031000162701 6.
[44] M. Christopher and H. Peck, 'Building the Resilient Supply Chain', The International Journal of Logistics Management, vol. 15, no. 2, pp. 1–14, Jul. 2004, doi: 10.1108/09574090410700275.
[45] X. Xiang and C. Liu, 'An expanded robust optimisation approach for the berth allocation problem considering uncertain operation time', Omega, vol. 103, p. 102444, Sep. 2021, doi: 10.1016/j.omega.2021.102444.
[46] H. Zheng, Z. Wang, and H. Liu, 'The Integrated Rescheduling Problem of Berth Allocation and Quay Crane Assignment with Uncertainty', Processes, vol. 11, no. 2, p. 522, Feb. 2023, doi: 10.3390/pr11020522.
[47] J. S. L. Lam and S. Su, 'Disruption risks and mitigation strategies: an analysis of Asian ports', Maritime Policy & Management, vol. 42, no. 5, pp. 415–435, Jul. 2015, doi: 10.1080/03088839.2015.1016560.
[48] P. Holme, B. J. Kim, C. N. Yoon, and S. K. Han, 'Attack vulnerability of complex networks', Phys. Rev. E, vol. 65, no. 5, p. 056109, May 2002, doi: 10.1103/PhysRevE.65.056109.
[49] M. Molloy, 'A critical point for random graphs with given degree sequence'.Random Struct. Alg., 6: 161-180. https://doi.org/10.1002/rsa.3240060204.
[50] L. Dall'Asta, A. Barrat, M. Barthelemy, and A. Vespignani, 'Vulnerability of weighted networks', J. Stat. Mech., vol. 2006, no. 04, pp. P04006–P04006, Apr. 2006, doi: 10.1088/1742-5468/2006/04/P04006.
[51] B. Kim, G. S. Kim, and M. H. Kang, "Study on Comparing the Performance of Fully Automated Container Terminals during the COVID-19 Pandemic," Sustainability, vol. 14, no. 15, article 9415, 2022. https://doi.org/10.3390/su14159415.

Funded by the European Union
Grant Agreement: 101136257

A. APPENDIX

Table A-1 to Table A-5 present the hazardous events identified during the workshops through the HAZID analysis described in Section 4.1.2. The events are grouped according to the main system-level hazards. For each hazardous event, the tables provide its category, potential causes and consequences, final risk level calculated as the average of all expert assessments in the workshops, and corresponding risk ranking based on the 5 × 5 risk matrix. The final risk levels of the hazardous events associated with each node or edge are then summed to determine their respective weights in the original AUTOFLEX IWTS graph.

Funded by the European Union
Grant Agreement: 101136257

Table A-1: HAZID Process for the Ports of the AUTOFLEX IWTS.

No.	ID	Hazard (System Level)	Hazardous Event	Category	Causes	Consequences	Final Risk Level	Risk Ranking
1	P_P1	Port	Unavailability to repair technical failure of the vessel	Operational	Insufficient port & repair facilities	Port Waiting	6.5	Medium
	P_P2		The planned pier is unavailable for the vessel's berthing operation as scheduled		Occupied pier, out of service, or blocked, preventing berthing as scheduled	Loading/Unloading Delay	3.5	Low
	P_P3		Malfunction or breakdown of lifting equipment (cranes, reach stackers, forklifts, etc.)		Preventive maintenance not performed / overdue inspections	Loading/Unloading Delay	6	Medium
	P_P4		Obstructed fairway near port (grounded vessel, construction works, floating objects etc.)		Incorrect handling of the incident	Loading/Unloading Delay	4	Medium
2	P_WC1	Weather Conditions	Collision with other vessel/Infrastructure due to heavy weather conditions (fog, floods, ice, storms, tidal and currents etc.)	Environmental	Reduced visibility	Damage to vessel	9	Medium
	P_WC2		Stagnation at/near the port due to heavy			Late arrival at the terminal	6.5	Medium

Funded by the European Union
Grant Agreement: 101136257

			weather conditions (fog, floods, ice, storms, tidal and currents etc.)		Insufficient information to avoid the route in a specific time frame	Inability to departure from the terminal	6.5	Medium
3	P_HE1	Human Element	Strikes and labour protests	Operational	There is no workforce to perform the operations	Loading/Unloading Delay	10	High
4	P_V1	Vessel	Grounding/collision with other vessel/infrastructure	Technical	Poor RCC/vessel coordination on speed restrictions, Excessive speed and mechanical failures	Damage to vessel	9	Medium
	P_V2		Loss of propulsion/steering due to mechanical failure		Mechanical failure	Inability to depart from the terminal	7.5	Medium
	P_V3		Fire or explosion		Electrical fault, leakage, dangerous cargo	Damage to vessel	7.5	Medium
	P_V4		Loss of power/blackout due to battery failure		Battery failure (Internal fault, mechanical damage or incorrect charging/handling)	Inability to depart from the terminal	4	Medium

Funded by the European Union
Grant Agreement: 101136257

Table A-2: HAZID Process for the S&C Hubs of the AUTOFLEX IWTS.

No.	ID	Hazard (System Level)	Hazardous Events	Category	Causes	Consequence	Final Risk Level	Risk Ranking
1	SC_SC1	Charging Station	Disruption of access control operations caused by IT management system malfunction, cyberattack, or loss of network connectivity	Operational	Software & network connection failure, cyberattack	Unavailability of charging station	3	Low
	SC_SC2		Congestion at the charging station due to simultaneous battery-swapping demand from multiple AUTOFLEX vessels		Peak demand not took into considered	Inability to depart for the next terminal	3	Low
	SC_SC3		Fire or explosion in the charging station structure due to battery leakage or electrical fault	Technical	Leakage of batteries, electrical fault	Inability to depart for the next terminal	6.5	Medium
	SC_SC4		Charging station outage due to failure of critical components such as the charger module, cooling fans, contactors, or sensors		Component failure (charger module, cooling fans, contactors, sensors)		7	Medium
2	SC_HE1	Human Element	Improper use of charging station equipment, including forced	Operational	Wrong connection sequence, use of damaged cables/adapters,	Damage to ZES packs	2.5	Very Low

Funded by the European Union
Grant Agreement: 101136257

			connection/disconnection and overcharging		bypassing safety instructions			
	SC_HE2		Incidents of fire or explosion and acts of vandalism resulting from inadequate physical security measures		Inadequate physical security (fencing, CCTV coverage, human resources)	Broken /Out of order	4	Medium
3	SC_B1	Battery	Fire or explosion due to battery ignition caused by internal fault, mechanical damage, or improper charging/handling	Technical	Internal fault, mechanical damage or incorrect charging/handling	Damage to infrastructure	6.5	Medium
						Damage to charging station	6.5	Medium
	SC_B2		Battery leakage due to improper storage, overcharging, deep discharging, exposure to heat or mechanical damage, and undetected cracks resulting from insufficient inspections		Lack of inspections leading to undetected cracks	Damage to ZES packs	4	Medium
	SC_B3		Insufficient battery capacity during operation due to progressive battery degradation, ageing, high cycle count, unmonitored capacity fade, or repeated reuse of the same ZES packs		Ageing and high cycle count,capacity fade not monitored, reusage of the same zes packs	Reduced vessel range leading to route interruption and unscheduled battery replacement or charging	4.5	Medium

Funded by the European Union
Grant Agreement: 101136257

	SC_B4		Damage to ZES Packs due to heavy weather conditions	Environmental	Bad insulation of the structure	ZES Packs replacement	4	Medium
4	SC_RE1	Renewable energy	Insufficient renewable energy source for charging	Operational	Low solar irradiance, low wind availability,seasonal variation	Inability to depart from the terminal	4	Medium
5	SC_RS1	Reach Stacker	Zes packs falls from the reach stacker during lifting, transfer, or stacking	Technical	Mechanical failure, overload, improper spreader/locking, uneven ground, poor visibility, or unsafe maneuvering	Damage to infrastructure	4.5	Medium
						Damage to ZES packs	7.5	Medium

Funded by the European Union
Grant Agreement: 101136257

Table A-3: HAZID Process for the TPTs of the AUTOFLEX IWTS.

No.	ID	Hazard (System Level)	Hazardous Event	Category	Causes	Consequences	Final Risk Level	Risk Ranking
1	T_T1	TPT	Unavailability to repair technical failure of the vessel	Operational	Insufficient port & repair facilities	Port Waiting	7.5	Medium
	T_T2		The planned pier is unavailable for the vessel's berthing operation as scheduled		Occupied pier, out of service, or blocked, preventing berthing as scheduled	Loading/Unloading Delay	3.5	Low
	T_T3		Malfunction or breakdown of lifting equipment (cranes,reach stackers, forklifts, etc.)		Preventive maintenance not performed / overdue inspections	Loading/Unloading Delay	6	Medium
	T_T4		Obstructed fairway near port (grounded vessel, construction works, floating objects etc.)		Incorrect handling of the incident	Loading/Unloading Delay	6	Medium
2	T_WC1	Weather Conditions	Collision with other vessel/Infrastructure due to heavy weather conditions (fog, floods, ice,	Environmental	Reduced visibility	Damage to vessel	6.5	Medium

Funded by the European Union
Grant Agreement: 101136257

			storms, tidal and currents etc.)					
	T_WC2		Grounding due to heavy weather conditions (fog, floods, ice, storms, tidal and currents etc.)		Insufficient information to avoid the route in a specific time frame	Damage to vessel	6	Medium
	T_WC3		Stagnation at/near the port due to heavy weather conditions (fog, floods, ice, storms, tidal and currents etc.)		Insufficient information to avoid the route in a specific time frame	Late arrival at the terminal	9	Medium
						Inability to depart from the terminal	8	Medium
3	T_HE1	Human Element	Strikes and labour protests	Operational	There is no workforce to perform the operations	Loading/Unloading Delay	8.5	Medium
4	T_V1	Vessel	Grounding/collision with other vessel/infrastructure	Technical	Poor RCC/vessel coordination on speed restrictions, Excessive speed and mechanical failures	Damage to vessel	9	Medium
	T_V2		Loss of propulsion/steering due to mechanical failure		Mechanical failure	Inability to depart from the terminal	6.5	Medium
	T_V3		Fire or explosion		Electrical fault, leakage, dangerous cargo	Damage to vessel	7.5	Medium

Funded by the European Union
Grant Agreement: 101136257

5	T_V4	Complex Navigational Passages/Low Level Waters	Loss of power/blackout due to battery failure	Geographical	Battery failure (Internal fault, mechanical damage or incorrect charging/handling)	Inability to depart from the terminal	4	Medium
						Grounding	6	Medium
	T_NV1		Low river levels can reduce available water depth, creating excessive loading constraints by limiting vessel draft and cargo capacity		Seasonal low river levels and channel bathymetry changes	Operational delays and rescheduling	5	Medium
	T_NV2		Increased vessel density in narrow fairways can reduce maneuvering space and vessel maneuverability		Narrow channel and limited passing distances restricting turn radius	Damage to vessel	6	Medium
	T_NV3		Insufficient water depth caused by low river levels can increase transport disruptions, especially under high traffic conditions		Peak-time traffic concentration/scheduling conflicts, limited traffic management capacity	Damage to infrastructure	2	Very Low
						Damage to vessel	4	Medium

Funded by the European Union
Grant Agreement: 101136257

Table A-4: HAZID Process for the Vessel Routes of the AUTOFLEX IWTS.

No.	ID	Hazard (System Level)	Hazardous Event	Category	Causes	Consequences	Final Risk Level	Risk Ranking
1	VR_WC1	Weather Conditions	Collision with other vessel/infrastructure due to adverse weather conditions (fog, floods, ice, storms, tidal and currents etc.)	Enviromental	Reduced visibility	Damage to infrastructure	8	Medium
						Sinking	10	High
	VR_WC2		Grounding due to adverse weather conditions (fog, floods, ice, storms, tidal and currents etc.)			Damage to vessel	6	Medium
	VR_WC3		High/Low level waters due to adverse weather conditions (fog, floods, ice, storms, tidal and currents etc.)		Insufficient information to avoid the route in a specific time frame	Inability to arrive at the next terminal	5	Medium
	VR_WC4		Destroyed or damaged locks/ Bridges due to adverse weather conditions (fog, floods, ice, storms, tidal and currents etc.)		Insufficient information to avoid the route in a specific time frame	Inability to arrive at the next terminal	8	Medium
	VR_WC5		Stagnation due to adverse weather conditions (fog, floods, ice, storms, tidal and currents etc.)		Insufficient information to avoid the route in a specific time frame	Late arrival at the terminal	4.5	Medium
2	VR_ITS1		Failure of the vessel IT management systems may	Technical	Network outage/instability,	Damage to vessel	5	Medium

Funded by the European Union
Grant Agreement: 101136257

			result from software or network connection problems, causing malfunction or loss of connectivity and affecting the correct and continuous operation of the access control system		failed software update/patch causing incompatibility or downtime, power interruption without adequate UPS/redundancy	Damage to infrastructure	3	Low
						Incorrect data	5	Medium
						Out of Order	5	Medium
		IT Vessel Management Systems	The vessel IT management systems may also be compromised by cyberattacks, including attacks on the IT management system, data breaches, or denial-of-service (DoS) incidents			Incorrect data	5	Medium
	VR_ITS2			Cybersecurity	Vulnerable systems, inadequate security controls	Out of Order	6	Medium
						Damage to vessel	5	Medium
						Damage to infrastructure	3	Low
3	VR_EE1	Energy Efficiency	Insufficient renewable energy available to complete the route may result from energy consumption being higher than expected		Low solar irradiance,low wind availability,seasonal variation	Inability to arrive at the next terminal	12.5	Very High
						Grounding	7.5	Medium
	VR_HE1		Insufficient water depth may lead to unsafe vessel loading conditions or incorrect cargo load distribution		Low river levels may reduce limit cargo capacity	Sinking	5	Medium
						Operational delays and rescheduling	6	Medium
4		Human Element		Operational		Collision with other vessel	6.5	Medium
	VR_HE2		Incorrect navigation assessment may occur when Remote Control Center personnel incorrectly assess		Remote Control Center personnel incorrectly assess traffic, waterway	Collision with infrastructure	3.5	Low

Funded by the European Union
Grant Agreement: 101136257

			traffic, waterway conditions, or vessel status		conditions or vessel status	Grounding	6.5	Medium
						Sinking	5	Medium
5	VR_NP1	Complex Navigational Passages	Complex navigational passages may reduce vessel maneuverability due to increased vessel density in narrow fairways and the resulting reduction in maneuvering space	Geographical	Narrow channel and limited passing distances restricting turn radius	Damage to vessel	6	Medium
						Damage to infrastructure	3	Low
	VR_NP2		Complex navigational passages lead to channel blockage due to damaged vessels or fallen trees, making passage impossible until the obstruction is removed		Collision with infrastructure/ Mechanical failure	Inability to arrive at the next terminal	8	Medium
	VR_NP3		Under complex navigational conditions, high traffic combined with insufficient water depth caused by low river levels may increase transport disruptions		Peak-time traffic concentration / scheduling conflicts, limited traffic management capacity	Damage to vessel	9	Medium
						Damage to infrastructure	3	Low
6	VR_V1	Vessel	Grounding/collision with other vessel/infrastructure	Technical	Poor RCC/vessel coordination on speed restrictions, Excessive speed and mechanical failures	Damage to vessel	6	Medium
	VR_V2		Loss of propulsion/steering due to mechanical failure		Mechanical failure	Inability to depart from the terminal	6.5	Medium

Funded by the European Union
Grant Agreement: 101136257

	VR_V3		Fire or explosion		Electrical fault, leakage, dangerous cargo	Damage to vessel	10	High
	VR_V4		Loss of power/blackout due to battery failure		Battery failure (Internal fault, mechanical damage or incorrect charging/handling)	Inability to depart from the terminal	5	Medium

Funded by the European Union
Grant Agreement: 101136257

Table A-5: HAZID Process for the MDCs of the AUTOFLEX IWTS.

No.	ID	Hazard (System Level)	Hazardous Event	Category	Causes	Consequences	Final Risk Level	Risk Ranking
1	MDC_HE1	Human Element	Incorrect cargo is loaded/unloaded into the MDC, resulting in the customer receiving cargo that does not correspond to the planned shipment	Operational	Mismatch with documentation or booking/ Identification and documentation error (wrong unit selection, label mismatch, booking discrepancy)	Reduction of available space	6	Medium
						Cargo rerouting	12	High
	MDC_HE2		The MDC is delivered to the wrong TPT or port, leading to incorrect cargo being loaded or positioned on board the vessel		Wrong container, mismatch with documentation or booking/ Identification and documentation error (wrong unit selection, label mismatch, booking discrepancy)	Reduction of available space	7.5	Medium
						Cargo rerouting	10.5	High
	MDC_HE3		Improper use of the access control system leads to temporary malfunction or failure to execute commands, as access control procedures are not followed correctly		Clients' non-compliance with access control manual	Cargo delay	1.5	Very Low

Funded by the European Union
Grant Agreement: 101136257

	MDC_HE4		Inadequate physical security measures lead to fire, explosion, vandalism, or cargo theft, tampering, or loss during storage, handling, or transportation within the terminal		Inadequate physical security (fencing, CCTV coverage, human resources)	Cargo replacement	7.5	Medium
	MDC_HE5		Improper use of the reach stacker leads to incorrect lifting or positioning, unsafe manoeuvring, or execution of the wrong handling sequence		Insufficient training or non-compliance with safe operating procedures (speed, approach angle, sequence	Cargo Delay	6.5	Medium
	MDC_HE6		Structural failure of the MDC occurs due to cargo overload, resulting in internal damage or collapse of the structure		Load limit exceeded	Cargo rerouting	6.5	Medium
2	MDC_C1	MDC's Cargo	Dangerous cargo causes fire or explosion, leading to damage or destruction of the MDC during storage or handling	Technical	Leakage of hazardous material, electrical fault	Cargo replacement	5	Medium
	MDC_C2		Severe weather conditions, particularly snow and ice, may freeze MDC doors or otherwise restrict access	Environmental	Bad insulation of the structure	Inability to get/deliver the cargo	4	Medium
3	MDC_ACS1	Access Control System	Failure or loss of connectivity of the IT management and access control system renders the MDC out of order and	Technical	Software & Network connection failure,	Inability to get/deliver the cargo	5	Medium

Funded by the European Union
Grant Agreement: 101136257

			disrupts its correct and continuous operation		cyberattack (e.g. data breach, DoS)			
4	MDC_RS1	Reach Stacker	Container or cargo falls from the reach stacker during lifting, transfer, or stacking, causing damage to the cargo, MDC, or surrounding equipment	Technical	Mechanical failure, overload, improper spreader/locking, uneven ground, poor visibility, or unsafe maneuvering	Cargo replacement	7.5	Medium
5	MDC_MDC1	MDC	Failure of critical MDC components, such as the cooling system, power supply, renders the unit partially or fully inoperative during its operation	Technical	Electrical fault, wear and tear, inadequate maintenance, power failure, sensor/control malfunction	Inability to get/deliver the cargo	7.5	Medium

Funded by the European Union
Grant Agreement: 101136257

Funded by the European Union

Grant Agreement: 101136257

Funded by the European Union

Grant Agreement: 101136257